# NOVEL METERING SYSTEM FOR THE THREE PHASE FLOW IN HORIZONTAL OIL PIPES UNDER STEADY FLOW

BY

## MUHAMMAD SAJID IQBAL

A Thesis Presented to the

DEANSHIP OF GRADUATE STUDIES

**KING FAHD UNIVERSITY OF PETROLEUM & MINERALS**

DHAHRAN, SAUDI ARABIA

In Partial Fulfillment of the
Requirements for the Degree of

# MASTER OF SCIENCE

In

## ELECTRICAL ENGINEERING

**May 2015**

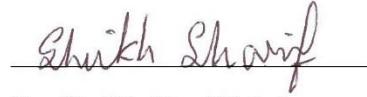KING FAHD UNIVERSITY OF PETROLEUM & MINERALS

DHAHRAN- 31261, SAUDI ARABIA

**DEANSHIP OF GRADUATE STUDIES**

This thesis, written by **MUHAMMAD SAJID IQBAL** under the direction his thesis

advisor and approved by his thesis committee, has been presented and accepted by the

Dean of Graduate Studies, in partial fulfillment of the requirements for the degree of

**MASTER OF SCIENCE IN ELECTRICAL ENGINEERING.**

Dr. Essam El Hassan
(Advisor)

Dr. Sheikh Sharif Iqbal
(Member)

Dr. Khurram Karim Qureshi
(Member)

Dr. Al-Shaikhi, Ali Ahmad

Department Chairman

Dr. Salam A. Zummo
Dean of Graduate Studies

20/5/15

Date

*Every challenging work needs self-efforts as well as guidance and prayers of elders, especially those who are very close to our heart*

*My humble efforts are dedicated to*

*My parents, brother, sisters and teachers*
*Without them, none of my success would be possible*

# ACKNOWLEDGMENTS

# TABLE OF CONTENTS

# LIST OF TABLES

# LIST OF FIGURES

xvii

# THESIS ABSTRACT

**NAME:**                   Muhammad Sajid Iqbal

**TITLE OF STUDY:**         Novel Metering System for the Three Phase Flow in
                           Horizontal Oil Pipes under Steady Flow

**MAJOR FIELD:**           Electrical Engineering (Electromagnetic)

**DATE OF DEGREE:**        May 2015

In the oil industry, oil is pumped out of the producing wells into pipelines to
different destinations. Estimation of the volume of the oil flowing in the pipes is a very
important element in the determination of the size of production. The problem is quite
difficult because the fluid is normally composed of three different elements consisting of
saline water, oil and gas. In this work we have developed a technique to solve this problem
by externally measuring the capacitance of liquids in the pipe line and then relating the
capacitance to the liquid height. So a metering system for oil industry to calculate the
amount of each component is designed based on the solution of static electric field solution
for longitudinally partially filled circular waveguides. The problem of determination of the
capacitance of a partially filled circular waveguide with a substance having a dielectric
constant $\varepsilon_r$ is attempted. The problem is attempted both theoretically and numerically and
the interrelation between the measured capacitance and the volume of the liquid inside the
pipe is made. Theory is also formulated for empty and longitudinally partially filled

*circular waveguide. To solve the problem numerically the "Finite Difference Method (FDM)" is used and results generated by FDM are compared to the values of capacitance obtained from "inclined plate capacitance method". MatLAB is used for simulations and analysis. Finally experiments are carried out for different cases and the results obtained from numerical analysis are compared to experimental results.*

# ملخص الرسالة

| | |
|---|---|
| **الاسم الكامل:** | محمد ساجد اقبال |
| **عنوان الرسالة:** | نظام لقياس حجم تدفق الزيت في انابيب النفط الافقية في حالة التدفق ثلاثي الاطوار |
| **التخصص:** | الهندسة الكهربية |
| **تاريخ الدرجة العلمية:** | مايو 2015 |

في حقل صناعة الزيت يتم ضخ الزيت خارج ابار الانتاج الى اماكن التخزين او التصدير خلال الانابيب الافقية. التحديد الدقيق لهذا الحجم يتسم بكثير من الصعوبات التقنية. ان تدفق الزيت في هذه الانانيب يكون عادة مخلوطا بمياه مالحة وبكثير من الغازات فيما يسمى بالتدفق ثلاثي الاطوار, وبالتالي علينل تقدير حجم الزيت وسط هذه المكونات. تم في هذه الرسالة تطوير نظام لقياس سعة المكثف المكافئ للانبوب حامل المكونات الثلاثة ونسنته الى كمية الزيت المارة في الانبوب. هذه السعة قيست من الداخل ومن الخارج لتقييم حجم الزيت. في هذا العمل استخدمت عدة طرق لايجاد السعة المكافئة . استخدمت اولا الاثبات النظري لقيمة المكثف المكافئ, ثم استخدمت طريقة "الفارق المحدد " العددية. تم تأكيد النتائج باستخدام اسلوب " الالواح المائلة" وهو اسلوب استحدث في جامعة الملك فهد لاول مرة. تم تأكيد النتائج بالتجارب المعملية.

# CHAPTER 1

# INTRODUCTION

Multiphase flow refers to the flow of two or more physically distinct or mixed materials in a container or a pipeline. It can be widely found in many engineering applications, such as, power generation, chemical engineering and crude oil extraction and processing. Oil production and supply involves multiphase flow of liquids composed of oil, saline water and gas [1]. Oil retrieval process often involves the injection of water and gas into the well to maintain the pressure and viscosity of the extracted liquids. This process requires constant monitoring using multiphase flow sensors, to optimize the efficiency of the oil production line. And estimation of the volume of the oil flowing in the pipes is a very important element in the determination of the size of production with all its associated economical issues. This problem is quite difficult since the fluid is normally composed of three phases. When multiphase fluids flow in a pipe, the flow is generally turbulent and the different constituents may flow at different rates [5]. This is the case when there is a gas phase as part of the flowing compound.

A number of techniques are devised to estimate the relative volumes of each of the three components. Those techniques are either mechanical or electrical in nature. In the mechanical world different flow meters are designed such as turbometers, sampling tubes,

mean density method, vortex meter and vibrating densitometer [1-3]. These have the drawback of being dependent on the pressures and temperatures which fluctuate rapidly along the pipe. Further, they need penetration inside the pipe which may not be always feasible in addition to the fact that it is preferable that the measurement method be non-intrusive such that the sensors must be at the periphery of the pipe. On the other hand, electrical measurements have been used extensively in this field; the conductance measurement of the three phase compound in conjunction with correlative flow meter was employed [4]. Microwave measurements are attempted by placing crossed dipole antenna pairs at different locations inside the pipe, exciting a single element and recording the gain of all other elements. By correlating the results, the unknown volume may be estimated [5]. Another technique uses measurements of a bank of capacitances where the electrodes are placed in the axial direction of the pipe. Using the recorded values in an empirical formula, it is possible to relate the targeted oil volume to the recorded set of capacitance [6]. Quite recently, a technique involving patch antennas and measurements of different resonant frequencies as well as reflection parameters is attempted to estimate the unknown oil volume [7].

In this work we have developed a technique to solve this problem by externally measuring the capacitance of liquids in the pipe line and then relating the capacitance to the liquid height. So a metering system for oil industry to calculate the amount of each component is designed based on static electric field solution for longitudinally partially filled circular waveguides. The problem of determination of the capacitance of a partially filled circular waveguide with a substance having a dielectric constant $\varepsilon_r$ is attempted during this work. The problem is solved both theoretically and numerically and the

interrelation between the measured capacitance and the volume of the liquid inside the pipe is obtained. To solve the problem numerically the "Finite Difference Method (FDM)" is used and results generated by FDM are compared to the values of capacitance obtained from "inclined plate capacitance method". MatLAB is used for simulations and analysis. In results and discussion section some results are presented, by using them we can estimate the volume of oil in pipeline at a high degree of accuracy. An experimental setup is also constructed to verify the validity and accuracy of the developed metering system.

## 1.1    Research Problem

When the oil is pumped from production wells and sent to different destinations through pipelines, the pipelines do not contain only the oil. The fluid inside the pipeline consists of three different materials namely saline water, oil and gas and is termed as water-oil-gas three phases of fluid. It is important to calculate the volume of each fluid in order to identify the exact production of oil. Different concepts and devices are available for measuring the phase fractions of a multiphase flow within petroleum carrying pipelines. Some of these devices use microwave signals, and some of them are intrusive. So either they are expensive or create serious issues like pipeline leakage.  Some non-intrusive techniques are also proposed to calculate the rough amount of oil, but those techniques do not give the exact volume of oil flowing inside the pipeline. So a more accurate and reliable non-intrusive solution is needed. And a new technique based on the static solution of electric field inside a partially filled circular waveguide is presented in this work, which is capable of relating capacitance of waveguide to liquid heights with a high degree of accuracy.

## 1.2    Research Objectives

The objectives of current work can be summarized as follows.

1. Design a novel technique based on theoretical analysis to precisely measure the amount of oil flowing in the pipe lines in water-oil-gas three phases fluid.

2. To develop the equi-capacitance contours for the circular waveguide that is longitudinally partially filled with dielectric subtance, by placing the matellic strips in the azimuthal direction and perpendicular to azimuthal direction.

3. Test the validity of the devised technique through experimental setup and physical measurements to verify the developed theory.

I am glad to say that above listed objectives are successfully achieved with the help of my thesis adviser and committee members.

## 1.3    Thesis Methodology

The following steps are followed to solve the problem. The main objective was to find the capacitance of a longitudinally partially filled circular waveguide and to relate the capacitance with the height of individual substance (water, oil and gas), which is discussed in details in chapter 4. Here a very brief summary of whole methodology is discussed.

- Circular pipe is supposed to be filled horizontally with three different substances (water, oil and gas). Water is at the bottom, then oil and gas on top of these two. The height of water is supposed to be $d_1$, that of oil is $d_2$ and for gas it is $d_3$. These materials are separated by their respective dielectric coefficients $\varepsilon_{rw}$, $\varepsilon_{ro}$ and $\varepsilon_{rg}$ respectively. The summation $d_1+d_2+d_3$ is equal to the diameter of the pipe (D), as shown in figure 1.1.
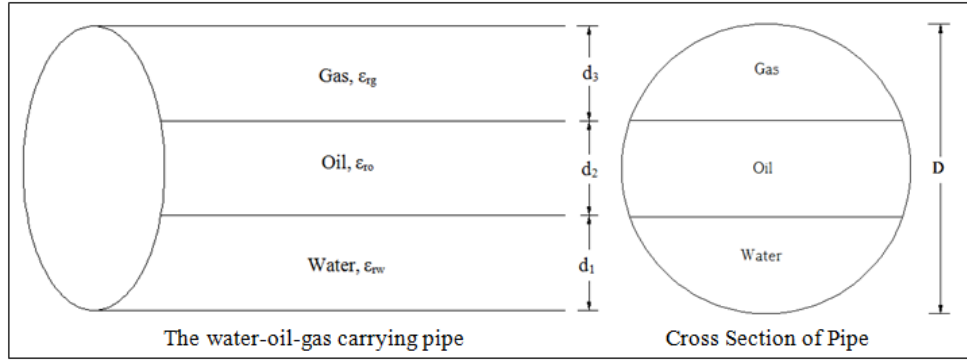
Figure 1.1: Schematic Diagram of Water-Oil-Gas three phases flow in pipelines

- Any dielectric when enclosed partially or fully by two separate conducting elements form a capacitance C. The value of C depends upon the shape of conducting elements, geometry of assembly and dielectric constant of the materials. The aim is to find the capacitance. That then can be related to the height of each material.

- The capacitance is calculated by placing two metallic strips of width W, on the cylinder's outer surface, perpendicular to the azimuthal direction and separated by an infinitesimal gap as shown figure 1.2. Capacitance is calculated by using three different methods namely; finite difference method, parallel plate capacitance method and inclined plate capacitance method which are discussed in details in chapter 4. By applying the voltage V on these plates, the capacitance is calculated. For each value of $d_1/d$ and $d_2/d$, there exists a corresponding value of C. The value of C is a function of $d_1$, $d_2$ and d. As $d_3$ is a function of $d_1$ and $d_2$, so it will not appear in the equation. The value of capacitance can be given as:

$$C_n = f_1\left(\frac{d_1}{d}, \frac{d_2}{d}\right)$$
(1.1)

5
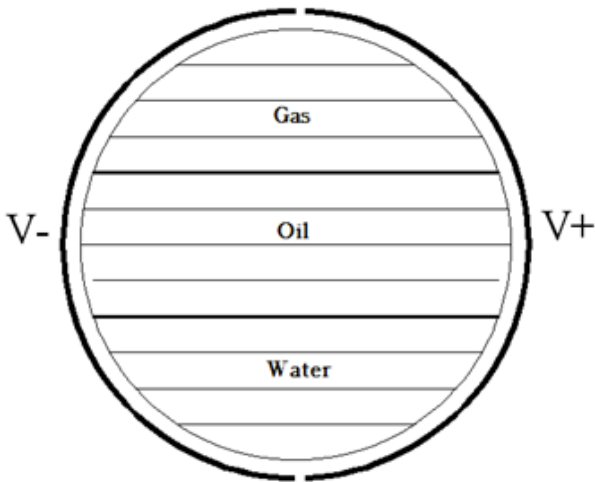
Figure 1.2: Metallic Strips around the circumference of the oil pipe

- The main part of the project is to calculate the values of $C_n$. Once the values are calculated, their equi-capacitance contours are plotted on the same graph. After constructing the graph, every value corresponding to the intersection of $C_n$ is denoting a unique point on that graph, which is determining the ratios $d_1/d$ and $d_2/d$. And the problem of the heights of each substance is solved.

- In addition to above numerical techniques theoretical formulation is made to check the special cases of work, which are discussed in chapter 5.

- Finally the values of capacitance were measured experimentally. The experiments were carried out by using a tube of plexiglass, closed from both ends, the oil was inserted inside the tube and capacitance was measured using capacitance meter. Different measurements were taken by varying the heights of water, oil and gas and compared to simulated results. The experiments along with their results are discussed in detail in chapter 6.

## 1.4    Organization of Thesis

The thesis is organized is follows. Chapter 2 consists of background needed to understand the further thesis. Chapter 3 consists of a literature survey related to thesis topic. The metering systems using low frequency and high frequency are described in this chapter. Chapter 4 is the heart of thesis, discussing the techniques used for calculating the capacitance of structure. Theoretical formulation for some selected cases is given in chapter 5. Experiments and results are listed in chapter 6. And finally thesis is concluded in chapter 7 providing main contribution, limitation and future work suggestions. References and vitae are also provided after chapter 7.

# CHAPTER 2

# BACKGROUND

This chapter provides the necessary background needed to navigate and understand the rest of this thesis. It covers four core knowledge areas: multiphase flow in pipe lines, finite difference method (FDM) and capacitance calculation between two inclined plates. These areas are discussed very briefly here; a reader interested in knowing more about a particular topic under these three areas is encouraged to consult the relevant reference used in this chapter.

## 2.1    Multiphase Flow in Pipelines

When a mixture of multiple substances (gases, liquids or solids) flows together as a mixture (without completely dissolving into each other) then this type of flow is referred as multiphase flow. Multiphase flow can be found everywhere, like in the atmosphere, in food industry, in cooling systems, in the process industry, in oil and gas reservoirs and in oil pipelines. In oil and gas production, multiphase flow often occurs in wells and pipelines because the wells produce gas and oil simultaneously. This is called two-phase flow. In addition to gas and oil, water is also often produced at the same time. This is called three-phase flow [8].

It is easy to understand that multiphase flow causes more problems as compared to single phase flow because; in multiphase flow the phases of different substances are neither completely mixed with each other nor separated completely. And the other most challenging task about multiphase flow is the fact that it may take one of several forms. Some commonly known forms in a gas-liquid flow are: Dispersed bubble flow, annular flow, slug flow, elongated bubble flow, stratified flow and stratified wavy flow and are shown in figure 2.1. The details about these regimes are discussed in [9] with details. Some techniques to deal with the multiphase flow are discussed in [9] but there exists no solid theory in open literature, which can determine the percentage of each substance in multiphase flow with a high degree of accuracy.
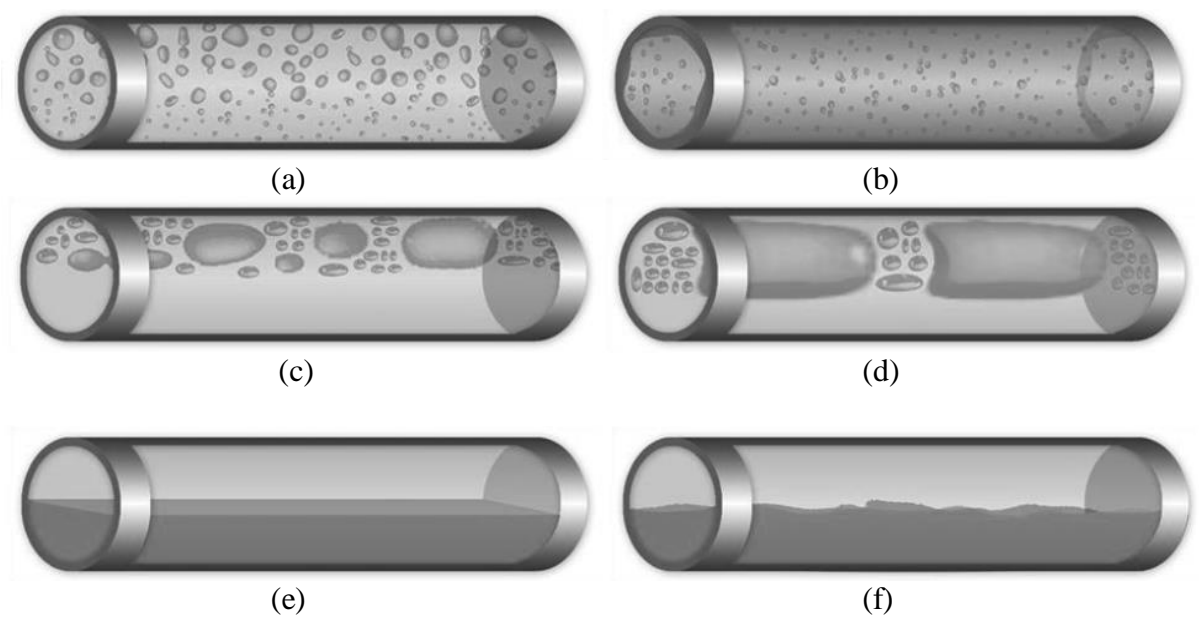


Fig 2.1: Flow regimes in gas-liquid flow in horizontal pipelines [9]

(a) Dispersed bubble flow (b) Annular flow (c) Elongated bubble flow

(d) Slug flow (e) Stratified flow (e) Stratified wavy flow

## 2.2   Finite Difference Method

Finite difference method (FDM) is a well-known numerical technique which is used to estimate the solution of problems that are defined by these conditions [10]:

1.  The problem is defined by differential equations

2.  A solution region is present for that particular problem

3.  Boundary conditions or initial conditions are known

In this thesis finite difference method is used to solve the Laplace equation in cylindrical coordinates. But before proceeding to cylindrical coordinates, knowledge of FDM in Cartesian coordinates is necessary. The Poisson or Laplace equation in Cartesian coordinate system can be solved by using FDM by following three steps, which are:

1.  Dividing the solution region into grids of nodes

2.  Approximating the differential equation and boundary conditions by a set of linear algebraic equations (called difference equations) on grid points within the solution region

3.  Solving this set of algebraic equations

Above steps are illustrated with the help of an example taken from [10]. Suppose we are trying to find the solution of Poisson equation for the region given by figure 2.2 [10]. For this particular example:

*Step 1:* The field region is divided into smaller grids called nodes as shown in figure 2.2. Any node at the boundary of the region where potential is always fixed is called a fixed node. Other nodes are free nodes, and we will calculate the voltage at each free node.

*Step 2*: Main objective is to find the approximate solution of Poisson equation. So in this step we will form a set of algebraic equations to achieve the objective by finding the voltage at all free nodes. As we know that the Poisson equation is given as [10]

$$\nabla^2 V = -\frac{\rho_v}{\varepsilon} \tag{2.1}$$

And $\nabla^2 V$ for Cartesian coordinate system is given as

$$\nabla^2 V = \frac{\partial^2 V}{\partial x^2} + \frac{\partial^2 V}{\partial y^2} + \frac{\partial^2 V}{\partial z^2} \tag{2.2}$$

For a 2 dimensional region as described by figure 2.1. $\rho_v$ Will be replaced by $\rho_s$ and $\frac{\partial^2 V}{\partial z}$ will be equal to zero. So equation 2.2 becomes [10]

$$\frac{\partial^2 V}{\partial x^2} + \frac{\partial^2 V}{\partial y^2} = -\frac{\rho_s}{\varepsilon} \tag{2.3}$$



(a)                                          (b)
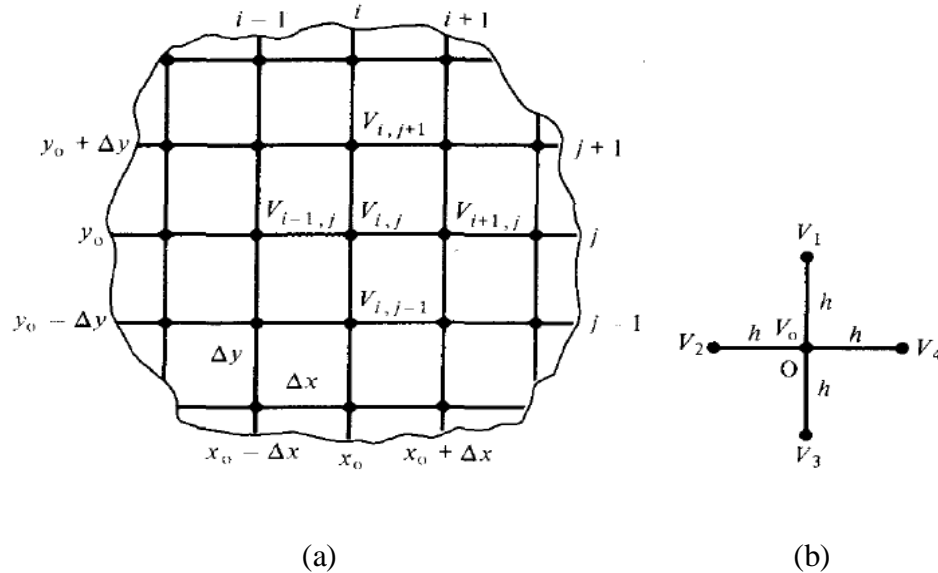
Figure 2.2: Solution pattern for finite difference method [10] (a) division of region in grids (b) five point molecule

11

By using the definition of partial derivative of V(x, y) at any given point (x₀, y₀), we can write

$$V' = \frac{\partial V}{\partial x}\bigg|_{x=x_0} \approx \frac{V(x_0 + \Delta x, y_0) - V(x_0 - \Delta x, y_0)}{2\Delta x} = \frac{V_{i+1,j} - V_{i-1,j}}{2\Delta x} \qquad (2.4)$$

Here $\Delta x$ is a very small distance along X axis. Similarly 2nd derivative will be calculated by using the same method. And 2nd derivative of V can be written as

$$V'' = \frac{\partial^2 V}{\partial x^2}\bigg|_{x=x_0} = \frac{\partial V'}{\partial x} \approx \frac{V'\left(x_0 + \frac{\Delta x}{2}, y_0\right) - V'(x_0 - \Delta x/2, y_0)}{\Delta x}$$

$$= \frac{V(x_0 + \Delta x, y_0) - 2V(x_0, y_0) + V(x_0 - \Delta x, y_0)}{(\Delta x)^2}$$

$$= \frac{V_{i+1,j} - 2V_{i,j} + V_{i-1,j}}{(\Delta x)^2} \qquad (2.5)$$

Equations (2.4) and (2.5) are the finite difference approximations for first and second order of derivative. The error in approximation given by equation (2.4) is proportional to $\Delta x$ and that of (2.5) is proportional to $(\Delta x)^2$. Similarly we can form the approximations along $Y$ direction and those are [10]:

$$V'' = \frac{\partial^2 V}{\partial y^2}\bigg|_{y=y_0} = \frac{\partial V'}{\partial y} \approx \frac{V'\left(x_0, y_0 + \frac{\Delta y}{2}\right) - V'(x_0, y_0 - \Delta y/2)}{\Delta y}$$

$$= \frac{V(x_0, y_0 + \Delta y) - 2V(x_0, y_0) + V(x_0, y_0 - \Delta y)}{(\Delta y)^2}$$

$$= \frac{V_{i,j+1} - 2V_{i,j} + V_{i,j-1}}{(\Delta y)^2} \qquad (2.6)$$

Now using equation (2.5) and (2.6) in equation (2.3), and considering that $\Delta x = \Delta y = h$ we get

$$V_{i+1,j} + V_{i-1,j} + V_{i,j+1} + V_{i,j-1} - 4V_{i,j} = \frac{h^2 \rho_s}{\varepsilon}$$

Here $h$ is the mesh size, if we consider the charge free region then $\rho_s = 0$ and equation can be rearranged as follows.

$$V_{i,j} = \frac{1}{4}\left(V_{i+1,j} + V_{i-1,j} + V_{i,j+1} + V_{i,j-1}\right) \qquad (2.7)$$

The equation (2.7) is the final form of approximation that is formed by using finite difference method when $x$ and $y$ grids are equal and region is charge free.

*Step 3:* There are two commonly known methods for solving the above approximation. One is the iteration method, and other one is band matrix method. In iteration method, the voltages are set to 0 initially at all free nodes, and then calculated and replaced after each number of iteration. In band matrix technique, a sparse matrix is formed based on the set of approximation equations the sparse matrix consists of all the unknown voltages [A], another column matrix is formed from fixed nodes [B]. As given in equation (2.8).

$$[A][V] = [B] \qquad (2.8)$$

And then the solution matrix [V] is obtained by inversing the sparse matrix and multiplying it with the matrix obtained by fixed nodes. It can be written in the form of equation (2.9). More details about these methods can be seen in [10].

$$[V] = [A]^{-1}[B] \qquad (2.9)$$

The thought of FDM can be extended to Poisson's, Laplace's, or wave equations in different coordinate systems. The accuracy of the strategy depends on the fineness of the grid and also the amount of time spent in purification of the potentials. We can cut back simulation time and increase the accuracy and convergence rate by the strategy of serial over relaxation, by creating affordable guesses at initial values, by taking advantage of symmetry if possible, by creating the mesh size as little as potential, and by victimization a lot of advanced finite difference molecules. One limitation of the finite difference method is that interpolation of some kind will not confirm solutions at points, those are not on the grid. One obvious way to overcome this is often to use a finer grid; however this might need a bigger range of computations and a bigger quantity of memory.

## 2.3    Capacitance Calculation between Two Inclined Plates

The electrical capacitor is a very important sort of electrical component used extensively in engineering. One common sort could be a parallel-plate electrical capacitor consisting of two conducting plates parallel to each other. If the area of plates is "$A$" and separation between plates is "$d$", then the capacitance of two parallel plates can be given by equation (2.10).

$$C = \frac{\varepsilon_r \varepsilon_0 A}{d} \qquad (2.10)$$

However due to manufacturing constraints and application requirements, the plates are not often parallel to each other, instead one plate is inclined at an angle to other as shown in figure 2.3. So it is necessary to determine the capacitance of two inclined plates

in general case for precise measurements and calculations. There are several methods available in literature to calculate the capacitance of two inclined plates. J.M. Bueno has suggested the use of mathematical expressions based on hyperbolic functions to evaluate the capacitance [11]. In [12] Y. Xiang has used finite element method to find the capacitance of two inclined plates. B. R. Patla has used the small angle approximation to approximate the capacitance of inclined plates in [13]. Similarly some other approximations can also be found in open literature.
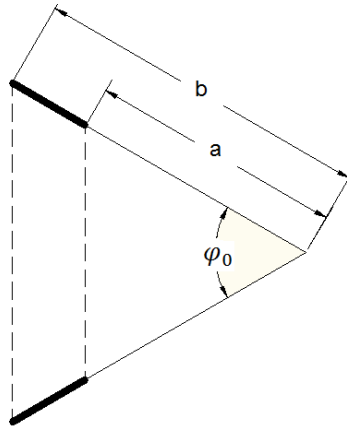


Figure 2.3: Inclined plate capacitor

There are several approximation techniques for inclined plate capacitance, during this work we have derived an approximate expression for the capacitance between two inclined plates (if plates are formed by arcs of a circular region) which is given below.

$$C = \frac{\epsilon_0 \varepsilon_r \, ln\left(\frac{b}{a}\right)}{\varphi_0} \tag{2.11}$$

Where $a$, $b$ and $\varphi_0$ are denoted in the figure 2.3 above. To apply the same formula for a circular waveguide, a, b and $\varphi_0$ will be calculated by using some trigonometric relations which is discussed in chapter 4.

15

# CHAPTER 3

# LITERATURE REVIEW

Details of the subject of measuring the three phase compound flow in the oil pipe is unfortunately a matter of industrial secrecy, where very little details are available in the open literature. Most of the available data are through patents of different companies, some are well known like Schlumberger and General electric and other less famous like Zhonyuan oil field. As mentioned earlier, the techniques used in these measurements are based on a variety of principles: some are mainly mechanical by measuring parameters like pressure and velocity which are generally either invasive or require sampling the flow through an external tube. Other techniques mix between electrical and mechanical. The third category is purely electrical and provides the estimate of oil by measuring the capacitance, which is a low frequency operation. So if we go through the literature, then we can find that radio frequency and microwave measurements are also attempted. So we can put radio frequency and microwave measurements in fourth category. In this section the focus will be on purely electrical techniques.

## 3.1    Low Frequency Electrical Techniques

In order to analyze the dielectric properties of the multiphase contents of a petroleum carrying pipeline, the pipeline is modeled as a circular waveguide. The equations governing the waveguide are then used to calculate the modal behavior of a dielectric loaded circular waveguide. In the literature, models exist for perfectly conducting waveguides loaded with the dielectric.

The use of capacitance tomography was suggested by Isaksen [6] in which 8 electrodes were placed axially on the surface of the pipe. Each electrode is excited one time and the capacitance $C_{ij}$ between the excitation electrode i and j is measured. Repeating the process eight times, the total number of measured capacitances was 28. With the help of these capacitances, a Linear Back Projection (LBP) algorithm is constructed to build an image of the level of darkness inside the pipe, from which an approximate volume of oil is calculated.

Another technique using capacitance measurement was reported by X. Chen and L. Chen [1]. In this technique the capacitance is measured at two different locations separated by a distance called S. These $C_1$ and $C_2$ represent two signals which when cross correlated and the time delay $T_m$ corresponding to the correlated signal. Maximum value is obtained and consequently the velocity of flow is obtained. The schematic of cross correlation analysis is shown in figure 3.1. Further the heights of water and oil are related to signal $C_1$. No information is presented about this function. Moreover the technique requires a by-pass tube for further data on the pressure drop to complete the measurements.
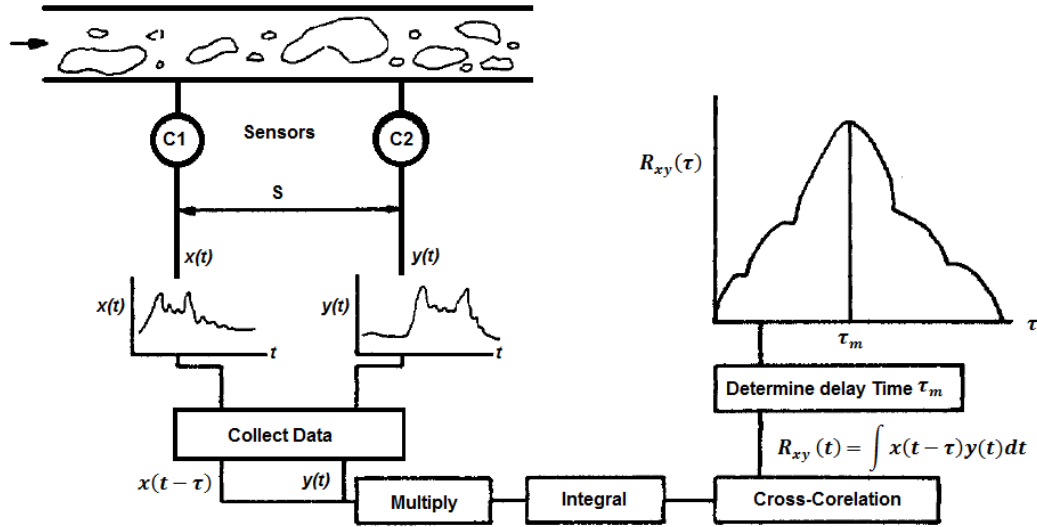
Figure 3.1: Block diagram for cross correlation analysis [1]

In [14] an impedance technique is presented by placing electrodes at the perimeter of a pipeline and measuring the impedance across the electrodes, there are many different possibilities to arrange a system of electrodes for void fraction measurement purposes. Two cases have been considered electrical conductivity and capacitance probes; depending on the type of instrumentation used and liquid material to be investigated. Commonly used radioactive sources of gamma radiation include isotopes of americium, cesium or cobalt. Radiation is generally detected by using a scintillator coupled to a photo detector. The scintillator absorbs radiation and emits visible light by fluorescence [15].

Another technique for multiphase measurements is multiphase flow imaging tomography and commonly called process tomography or industrial process tomography, finds many applications in the imaging and measurement of industrial processes. A tomographic image is a two-dimensional representation of a slice through an object. The use of various tomographic methods is widespread in diagnostic medicine [16] and several

imaging modalities originally developed for medical imaging are now being adapted to industrial process imaging. The use of tomographic imaging for the investigation of multiphase flows has been reported in a few exhaustive review papers [17-20] and books [21-23].

An application of one of the tomography types called Electric Resistance Tomography (ERT) has been done in [24]. The experiments for the ERT were carried out in an acrylic test pipe in the horizontal direction with 38 mm in diameter. The phase continuity and appearance of phase inversion were investigated using conductivity (wire and ring) probes and an Electrical Resistance Tomographic (ERT) system. In this technique the phase has been monitored to determine the flow and especially the process of phase inversion or continuity affected by interfacial tension of the materials by adding a small concentration of glycerol to water.

## 3.2    High Frequency Electrical Techniques

Unlike the techniques mentioned in above section, there are some other techniques in the literature for multiphase flow sensing in which the high frequency (Radio Frequency or Microwaves) are used for the same purpose. Some examples for such techniques are presented below.

A patent [5] registered at US describes a technique comprised of a series of antennas mounted inside the wall of the pipe with radiating faces flush with the inner surface. Each antenna is a crossed dipole cavity backed slot antenna is operating at a frequency range of 100 to 2000 MHz. Each antenna has one dipole along the pipe axis to couple with the TE modes of the cylindrical waveguide and another circumferential to

couple with the TM modes. The technique is to excite one dipole at a time and record the received signal at all other dipoles. The problem then turns to be inverse problem of determining the medium once the excitations and the fields at the boundaries are known. The medium is divided into cells and dielectric constants for each cell are supposed and a search sub-routine is then applied to find the most appropriate dielectric constant for the cells. In this way the flow and volume of each component of fluid is measured. The technique is very complicated and uncertain due to extensive numerical work. The inverse problems are also characterized by non-stable solutions.

In another US patent [7], a technique is proposed by using several patch antennas. The antennas are distributed around the circumference of the pipe. Single antenna radiates at a single time and received power is then measured across all other antennas. Unlike the previous technique the input signal is swept over the band of frequencies. The transmitted and received signals are measured and the resonance frequency is recorded. The baseline resonance frequency is obtained and then the shift from this line is used to estimate the composition of fluid. It is worth mentioning that this technique can be only used for two phase fluids and becomes inefficient when the proportion of water is high in the pipeline.

In [25], they apply the method based on dielectric spectroscopy to investigate two kinds of flow in the pipeline: the homogeneous flow of oil and water and the annular flow oil, water and gas. In this process, two different probes are inserted within the pipeline as shown in figure 3.2: one at high frequency (around 40 GHz) to determine the composition of the liquid phase, i.e. the oil—liquid ratio and the water-liquid ratio; a second one at low frequency (10-800 MHz) to calculate the gas ratio or gas hold-up. The reason for the two frequency bands are based on the signal penetration, which is inversely proportional to the

frequency. However, this intrusive design needs to insert probes within the pipeline, which requires drilling and that will cause leaking or cleaning related problems.
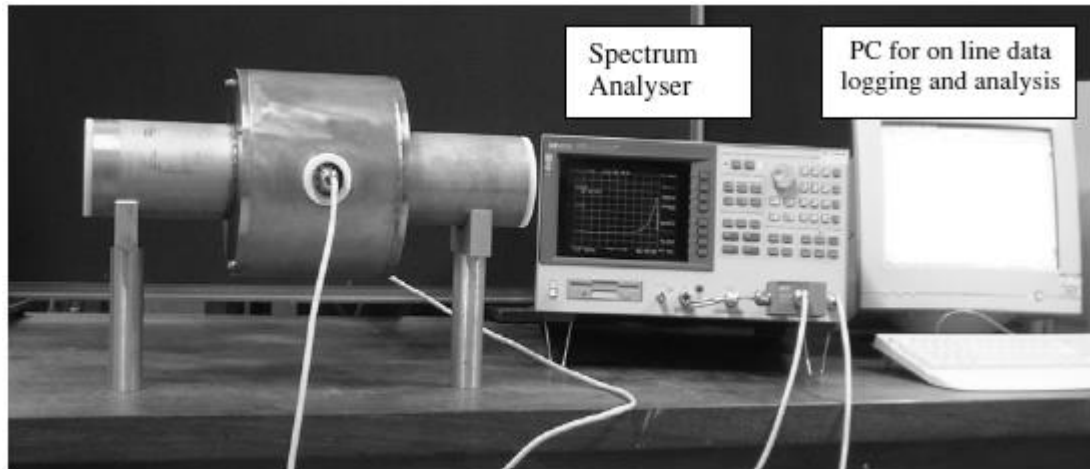


Figure 3.2: Laboratory setup for cavity resonator [25]

In reference [26], the authors introduce a capacitance wire-mesh sensor to measure the permittivity of the mixture. This sensor consists of two plates placed at a certain distance from each other and connected to two probes. Each plate is made of 16 wires, mounted in a rectangular acrylic frame that itself is part of a rectangular flow channel. The sensor can be used to measure transient phase fraction distributions in a flow cross-section. The drawback of this intrusive sensor was low mechanical rigidness and less protection of the probes from sandy component or solid particles of the fluid.

In [27] a non-intrusive electromagnetic cavity sensor is developed for detecting the content of an oil pipeline by transmitting a 10 mW signal in the range of 100 — 350 MHz, This sensor technique is based on measuring the dielectric constant of the combined oil, gas and water phases. The drawbacks of this design are the antenna dimension is big and the resolution is low and this is because the range of the frequency is in the MHz,

In reference [28] the microwave sensor consisted of two coaxial probes, separated by a certain distance. This sensor is used to determine the water holdup of the hydrocarbon mixture for a near horizontal oil carrying pipeline. It can be noticed from figure 3.3 that this design is intrusive and there is possibility for leakage due to high pressure within the pipeline.
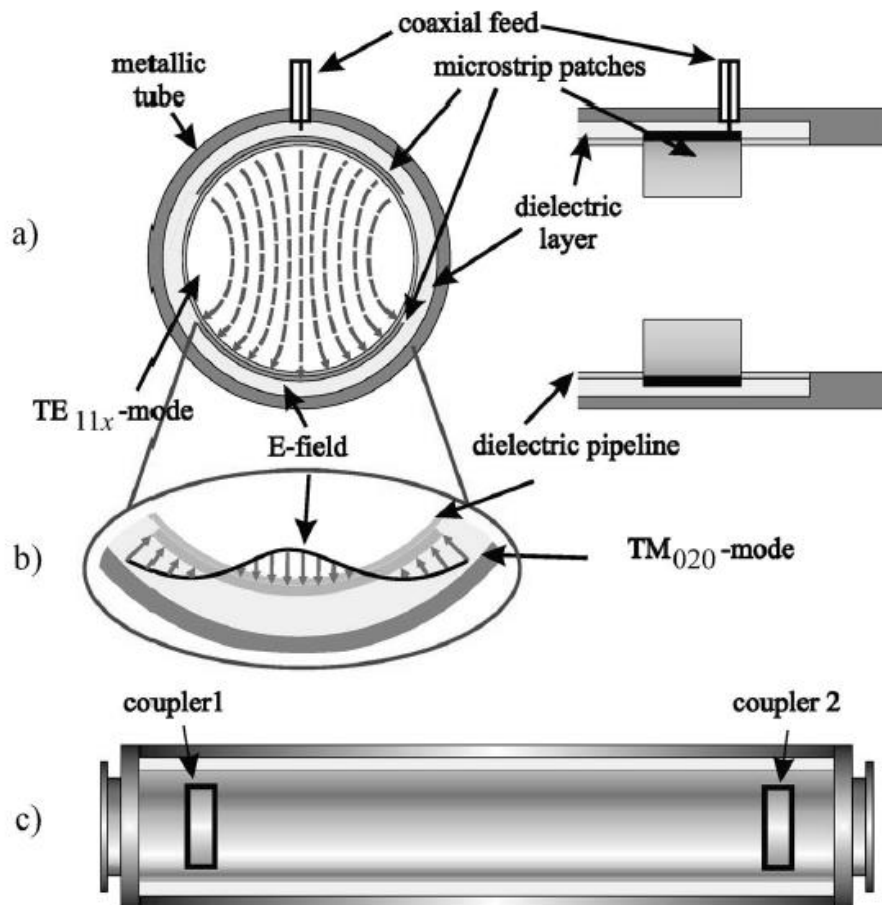


Figure 3.3: Micro-strip patch, mass flow detector [28] (a) coaxial line to circular cylindrical waveguide coupler (b) corresponding electric field distributions (c) Assembly of sensor with two integrated patch couplers.

Another intrusive technique was described in [29-32], and is based on two microstrip couplers connected in a Composite Right Left Handed (CRLH) manner. The dominant mode excited within the cylindrical waveguide using the coaxially feed microstrip patch and a parasitic patch. Two sets of the patches are connected using microwave couplers to measure reflection and transmission parameters in order to determine the content ratio.

In spite of huge contribution in the field of petroleum measurements, only 0.2% of current oil wells are instrumented with multiphase flow meters as estimated in [33]. Therefore there still exists the need of new research and innovation in this field of study. So we are proposing a non-intrusive technique to determine the percentage of oil, water and gas in multiphase flow with high degree of accuracy.

# CHAPTER 4

# NUMERICAL EVALUATION OF CAPACITANCE

As mentioned in chapter 1 that the heart of this thesis is to find the capacitance of a longitudinally partially filled circular waveguide. And we have applied three different methods to estimate the capacitance of structure namely, finite difference method, parallel plate capacitance method and inclined plate capacitance method. In this chapter all three techniques are discussed in details that how these methods are used to find the overall capacitance of a partially filled circular waveguide.

## 4.1    Calculation of Capacitance by Finite Difference Method

In this section the capacitance calculation with the finite difference method is described. The oil pipeline is considered as a circular waveguide and the finite difference approximations for Laplace equation are derived in cylindrical coordinate system and then these approximations are used to calculate the capacitance of empty waveguide, a partially filled waveguide with one dielectric and finally the approximations are modified to calculate the capacitance when waveguide is longitudinally partially filled with two dielectrics.

### 4.1.1  Finite Difference Method for Cylindrical Coordinates

In chapter 2 a brief introduction of finite difference method is given and approximations for Poisson's equation are made. As we are considering the pipeline as a circular waveguide, so the approximations given by equation (2.5) and (2.6) must be transformed to cylindrical coordinates. In the following steps the approximations for Laplace equation in cylindrical coordinates are made.

To apply FDM on circular pipeline we have considered the pipeline as a circular waveguide. Then the cross section of this waveguide is divided into several patches as shown in the figure 4.1. The voltage at each point is found by solving Laplace equation in cylindrical coordinates.
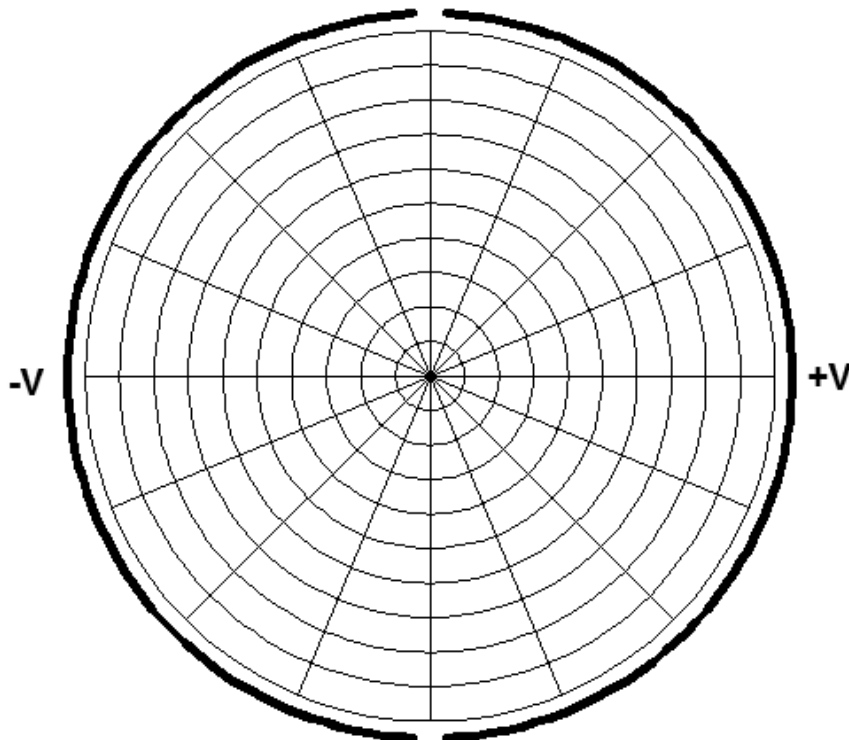
Fig.4.1: Cross Section of pipeline

As discussed in chapter 2 that Finite Difference Method finds the approximate solution at any particular point by accumulating the values at neighboring points. So the voltage at any particular point is found by deriving a relation between the point itself and four neighboring points. The derivation of formula for voltage is based on figure 4.2.
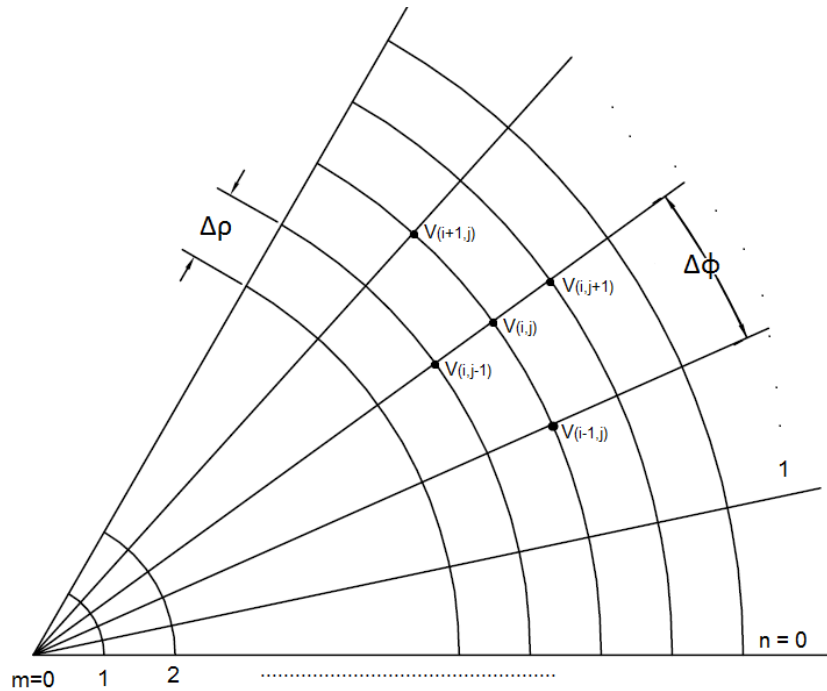


Fig.4.2: Illustration of neighboring points for using FDM in cylindrical coordinates

For cylindrical coordinates Laplace equation is given as

$$\nabla^2 V = \frac{1}{\rho}\frac{\partial}{\partial \rho}\left(\rho \frac{\partial V}{\partial \rho}\right) + \frac{1}{\rho^2}\left(\frac{\partial^2 V}{\partial \varphi^2}\right) + \left(\frac{\partial^2 V}{\partial z^2}\right)$$

As we are working in row ($\rho$) and phi ($\varphi$) plane so $\left(\frac{\partial^2 V}{\partial z^2}\right) = 0$.

Thus the equation becomes

26

$$\nabla^2 V = \frac{1}{\rho} \frac{\partial}{\partial \rho} \left( \rho \frac{\partial V}{\partial \rho} \right) + \frac{1}{\rho^2} \left( \frac{\partial^2 V}{\partial \varphi^2} \right)$$

After simplifying we get

$$\nabla^2 V = \frac{1}{\rho} \left( \frac{\partial V}{\partial \rho} \right) + \left( \frac{\partial^2 V}{\partial \rho^2} \right) + \frac{1}{\rho^2} \left( \frac{\partial^2 V}{\partial \varphi^2} \right) \qquad (4.1)$$

From figure 4.2 by using the definition of derivative we can say that

$$\frac{\partial V}{\partial \rho} = \frac{V_{(i+1,j)} - V_{(i-1,j)}}{2\Delta\rho} \qquad (4.2)$$

$$\frac{\partial^2 V}{\partial \rho^2} = \frac{V_{(i+1,j)} - 2V_{(i,j)} + V_{(i-1,j)}}{(\Delta\rho^2)} \qquad (4.3)$$

$$\frac{\partial^2 V}{\partial \varphi^2} = \frac{V_{(i,j+1)} - 2V_{(i,j)} + V_{(i,j-1)}}{(\Delta\varphi^2)} \qquad (4.4)$$

By using equation (4.2), (4.3) and (4.4) in equation (4.1), and then putting $\nabla^2 V = 0$ for free nodes we can find the value of $V_{(i,j)}$ for a charge free region. After doing above steps and simplifying we get the final expression for $V_{(i,j)}$ that is given by equation (4.5).

$$V_{(i,j)=} \frac{m(\Delta\varphi)^2(2m + 1)V_{(i+1,j)} + m(\Delta\varphi)^2(2m - 1)V_{(i-1,j)} + V_{(i,j+1)} + V_{(i,j-1)}}{4m(\Delta\varphi)^2 + 2} \qquad (4.5)$$

Where $m = \rho/\Delta\rho$

    Equation (4.5) gives the finite difference approximation for Laplace equation in cylindrical coordinates when the solution region is charge free. And this equation will be used to calculate the voltage at each free node in further scenarios.

### 4.1.2 Finite Difference Method for Air Filled Waveguide and Plates are Put inside The Tube

As it is mentioned earlier that oil carrying pipelines have a three phase water-oil-gas flow. To calculate the capacitance of pipeline, we have modeled the pipeline as a partially filled circular waveguide and water, oil and gas are considered as dielectrics. The method of capacitance calculation by using finite difference method is divided into three steps. In first step only air filled waveguide is considered, that means pipeline is filled with only one substance (water, oil or gas). In $2^{nd}$ step it is supposed that the waveguide is partially filled with one dielectric, that means only oil and gas are present in the pipeline. And in third and last step waveguide partially filled with two dielectrics is considered, which means that pipeline is carrying water, oil and gas.

In the first step a circular waveguide is considered that is completely filled with one substance (air for example); the radius of waveguide is set to 4.4 and two metal plates are placed perpendicular to azimuthal direction and a voltage of +100 V and -100 V is applied on these plates to calculate the capacitance as shown in figure 4.3. As the waveguide is completely filled with only one substance so there are no discontinuities of Electric filed. Thus there is no need to modify the approximation given by equation (4.5). Finite difference method is applied with the specifications given in table 4.1; the set of approximation equations are solved by iteration method.

| Radius (ρ) | Δ ρ | Δ φ | m | No. of iterations | Fixed node voltage |
|---|---|---|---|---|---|
| 4.4 cm | 0.01 cm | $1^0$ (0.01745 rad) | 440 | 12000 | +100 and -100 Volts |

Table 4.1: Specifications for applying FDM on air filled circular waveguide
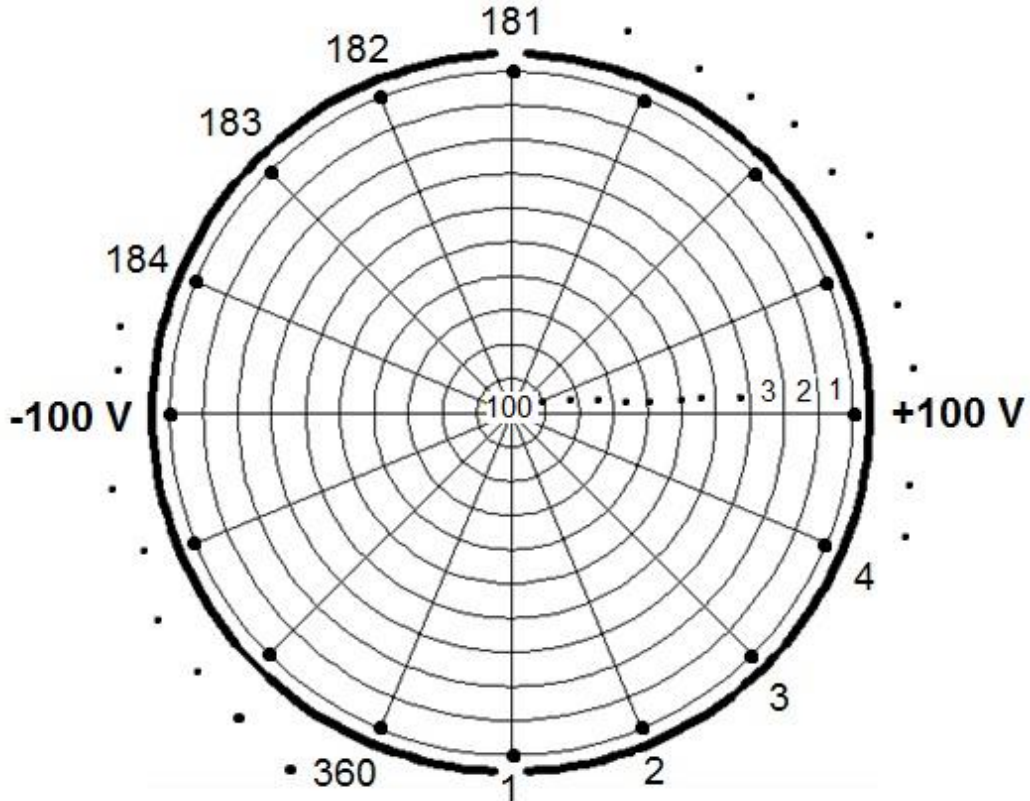


Figure 4.3: Illustration of fixed and free nodes for air filled circular waveguide

As radius of waveguide is 4.4 and we have Δ ρ and Δ φ equals to 0.01 and $1^0$ respectively so there will be 360 points along φ direction and 440 points along ρ direction as denoted in figure 4.3 above. So there will be a total of 36000 nodes. 360 nodes which are on the circumference of the waveguide are fixed nodes and all other are free nodes. Each node is denoted by an order pair (Δ ρ, Δ φ). The voltage at nodes (1, 1) to (101, 1) and (1, 181) to (101, 181) is set to zero to create an infinitesimal gap between two plates.

The voltage at nodes (1, 2) to (1, 180) is fixed to +100 volts and that on nodes (1, 182) to (1, 360) is -100 volts. Then approximation equations are obtained for all free nodes and solved by using iteration method with number of iterations fixed to 12000. The values of $\Delta\rho$, $\Delta\varphi$ and number of iterations are chosen by examining the results at different values. By decreasing the values of $\Delta\rho$ and $\Delta\varphi$ and by increasing the number of iterations the percentage of error reduces and finite difference method produce more accurate results. But when the values of $\Delta\rho$ and $\Delta\varphi$ decreased further then the voltage at free nodes was oscillating, so these values are selected because at these particular values the results are quite stable.

Once the voltage at each free node is found by solving the set of approximation equations, the electric field in $\rho$ direction can be found by using following equation.

$$E = \frac{\varepsilon_r V_1 - \varepsilon_r V_2}{\Delta\rho}(\rho\Delta\varphi) \tag{4.6}$$

Once the electric field is found, the total charge enclosed by that waveguide can be found by adding E-filed at all point. From that total charge the capacitance of structure can be found by using following relation.

$$C = \frac{\varepsilon_r \varepsilon_0 (Q)}{2V} \tag{4.7}$$

The capacitance of structure that is completely filled with gas is calculated by using above method and satisfactory results are found. The detailed results are discussed in results section of chapter 6.

### 4.1.3 Finite Difference Method When Waveguide is filled with two Dielectrics and Plates Are Put Inside

In second case the pipeline is considered to be having only oil and gas flowing through it, so it will be modeled as a longitudinally partially filled circular waveguide with two dielectrics. The dimensions of waveguide are kept same as previous case; the structure of waveguide is shown in figure 4.4 where two metallic plates are placed perpendicular to azimuthal direction and a voltage of +100 V and -100 V is applied on these plates. The plates are placed perpendicular to azimuthal direction in order to utilize the symmetry of structure. Finite difference method is applied with the same specifications. As it can be seen from figure 4.4 that there is a boundary inside the structure and it will cause the discontinuity in electric field. Thus the approximation equation must be modified according to boundary conditions.
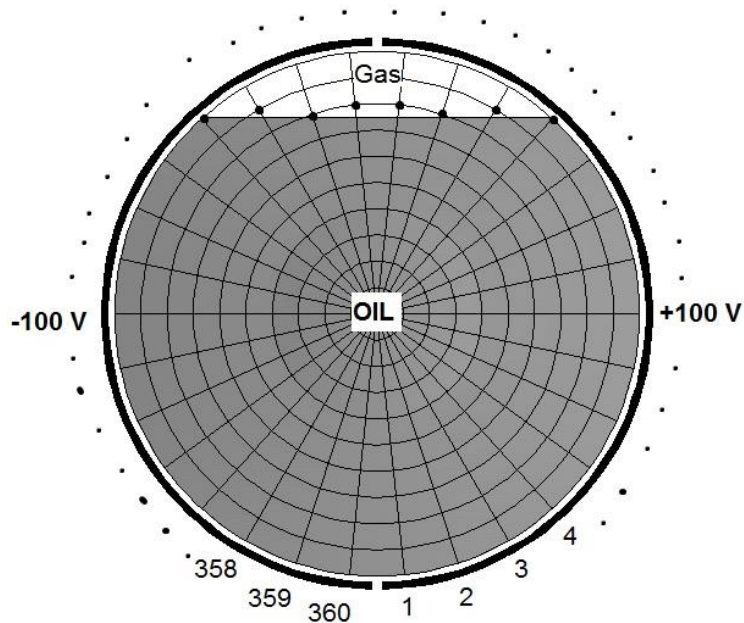


Figure 4.4: Illustration of fixed nodes, free nodes and boundary points when waveguide is partially filled with two dielectrics

The general rules that apply on neighboring points when applying finite difference method on partially filled structures are given as:

1. To apply boundary conditions the point must be taken on the boundary

2. Out of four neighboring points, two must be on the boundary, one should be in upper region and one should be in lower region, as shown in figure 4.5.

3. If the node is on the boundary then the value of voltage of that particular node will be divided by average of dielectric constants of two regions.

4. The voltage of each region's node will be multiplied by its dielectric constant.

5. If voltage is calculated at a node existing on a boundary, the true voltage will be obtained by dividing it with the average of dielectric constants of two regions. For example the voltage $V_0$ from figure 4.5 will be given as (Cartesian coordinates):

$$\left(\frac{\varepsilon_{r1} + \varepsilon_{r2}}{2}\right) V_0 = \frac{1}{4}\left(\left(\frac{\varepsilon_{r1} + \varepsilon_{r2}}{2}\right) V_1 + \left(\frac{\varepsilon_{r1} + \varepsilon_{r2}}{2}\right) V_3 + \varepsilon_{r1} V_2 + \varepsilon_{r2} V_4\right) \qquad (4.8)$$
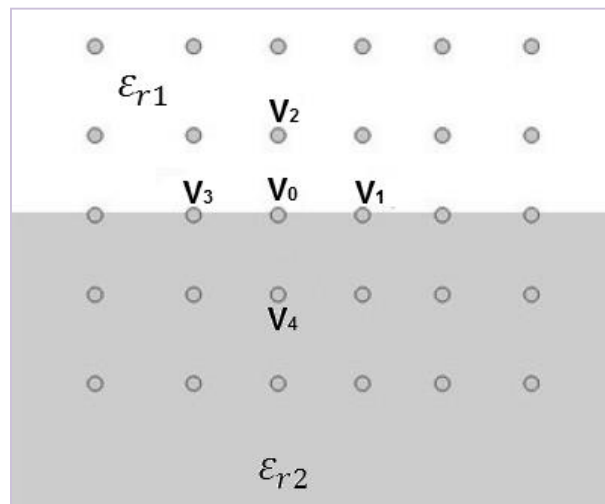


Figure 4.5: Finite difference approximation for dielectric boundary

Keeping above five steps in mind, the finite difference approximations are modified for figure 4.4. The points highlighted in figure 4.4 are strictly considered to be on the boundary, and for each point the distance $\Delta \rho$ is monitored precisely and adjusted accordingly in equation (4.5) to generate the modified approximations. Then the voltage at each free node is found and then electric field, total charge and capacitance are found by using equation (4.6) and (4.7) respectively. As the distance $\Delta \rho$ is very small and each point the distance is calculated separately, so due to these extensive calculations the total error for this case is much higher as compared to air filled waveguide. The detailed results are discussed in chapter 6.

## 4.1.4 Finite Difference Method When Waveguide is filled with Three Dielectrics and Plates are Put Inside

In third case the pipeline is considered to be having water, oil and gas flowing through it, so it is modeled as a longitudinally partially filled circular waveguide with three different dielectrics. The dimensions of waveguide are kept same as previous case; the structure of waveguide is shown in figure 4.6 where two metallic plates are placed perpendicular to azimuthal direction and a voltage of +100 V and -100 V is applied on these plates. The plates are placed perpendicular to azimuthal direction in order to utilize the symmetry of structure. Finite difference method is applied with the same number of iterations, $\Delta \rho$, $\Delta \varphi$ and fixed node voltage. As it can be seen from figure 4.6 that there are two boundaries inside the structure and those will cause the discontinuity in electric field. Thus the approximation equation must be modified according to boundary conditions for this case.
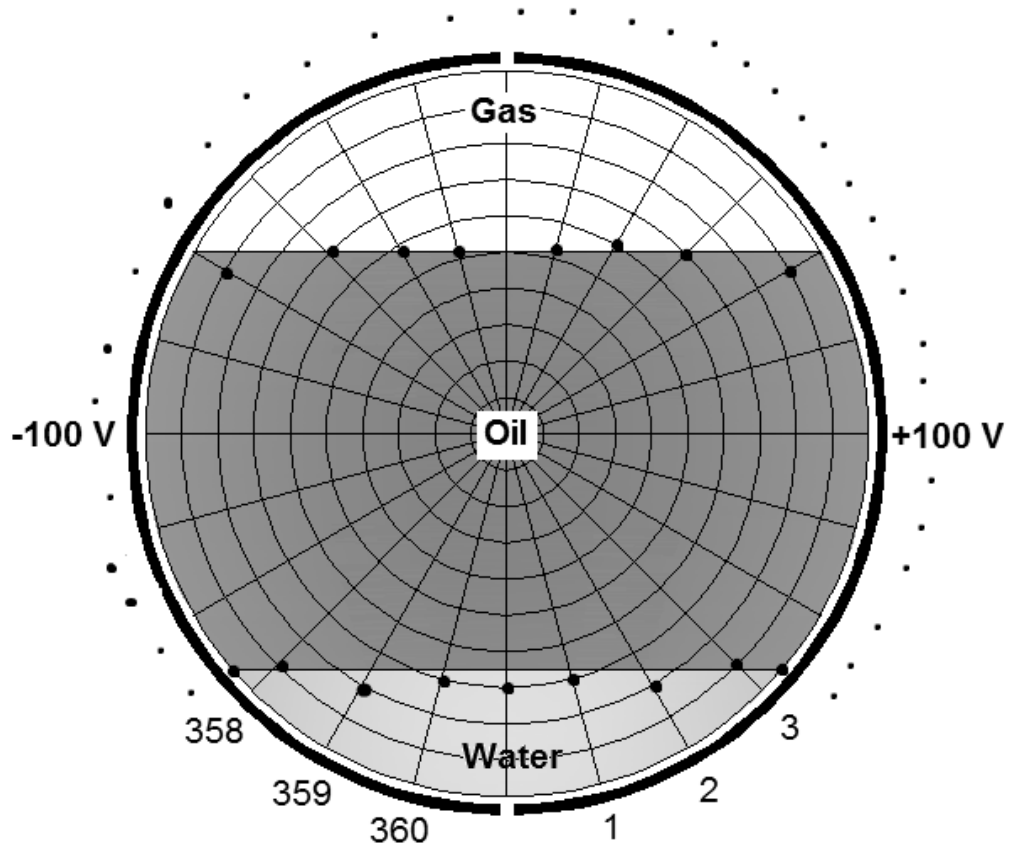
Figure 4.6: Illustration of fixed nodes, free nodes and boundary points when waveguide is partially filled with three dielectrics

The rules for applying boundary conditions in this case are same as previous. So highlighted points in figure 4.6 are strictly taken to be on the boundaries and distance for each point is calculated separately and approximation equations are solved. As we have seen in one dielectric case that the approximations of points introduce errors in the final results, here the dielectric constant of water is much higher than that of oil and gas, so in this case the error will be much higher, so when the waveguide is partially filled with two dielectrics, and one of them is water then finite difference method becomes less efficient. Thus a refinement is necessary for this case which is discussed in next paragraph.

A refinement technique for finite difference method is discussed in [34]. According to refining technique, the regions where high electric field exists as compared to low electric field region the grid must have small spacing. In this way the whole structure will have variable grid spacing and thus there is a need of remodeling the finite difference approximations for Laplace equation in terms of different size values of grid size. The remodeled approximation equation will take care of grid size for each point as given in equation (4.9).

$$\left(\frac{1}{h_1 h_3 + h_2 h_4}\right) V_0 = \frac{V_1}{h_1(h_1 + h_3)} + \frac{V_2}{h_2(h_2 + h_4)} + \frac{V_3}{h_3(h_1 + h_3)} + \frac{V_4}{h_4(h_2 + h_4)} \quad (4.9)$$

The distance $h_1$, $h_2$, $h_3$ and $h_4$ are shown in figure below. This above expression is for Cartesian coordinate system when there is no boundary inside the region. By applying the rules discussed previously, this expression can be used for any structure and any number of boundaries.
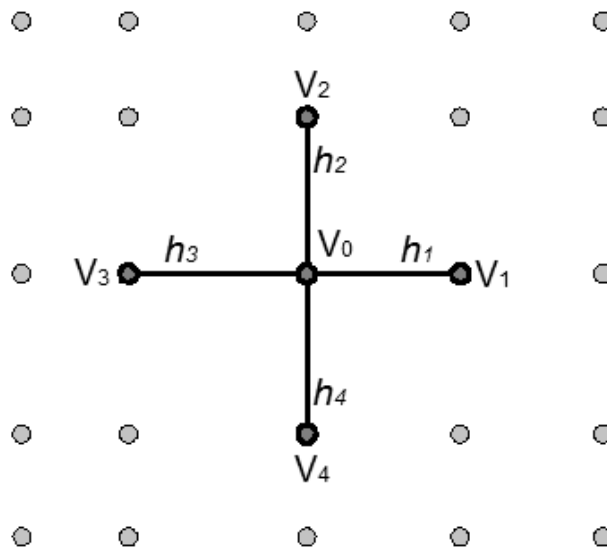


Figure 4.7: Refined grid for finite difference method

Using the modified approximation we can model the waveguide in Cartesian coordinates system instead of cylindrical as shown in figure 4.8. The nodes which are highlighted in figure 4.8 will be solved by equation (4.9) and remaining free nodes will be solved by using equation (2.7). The boundary condition rules will remain same discussed on page 32. The refined finite difference is applied by using the specifications given in table 4.2. And the improved results are obtained which are discussed in chapter 6.
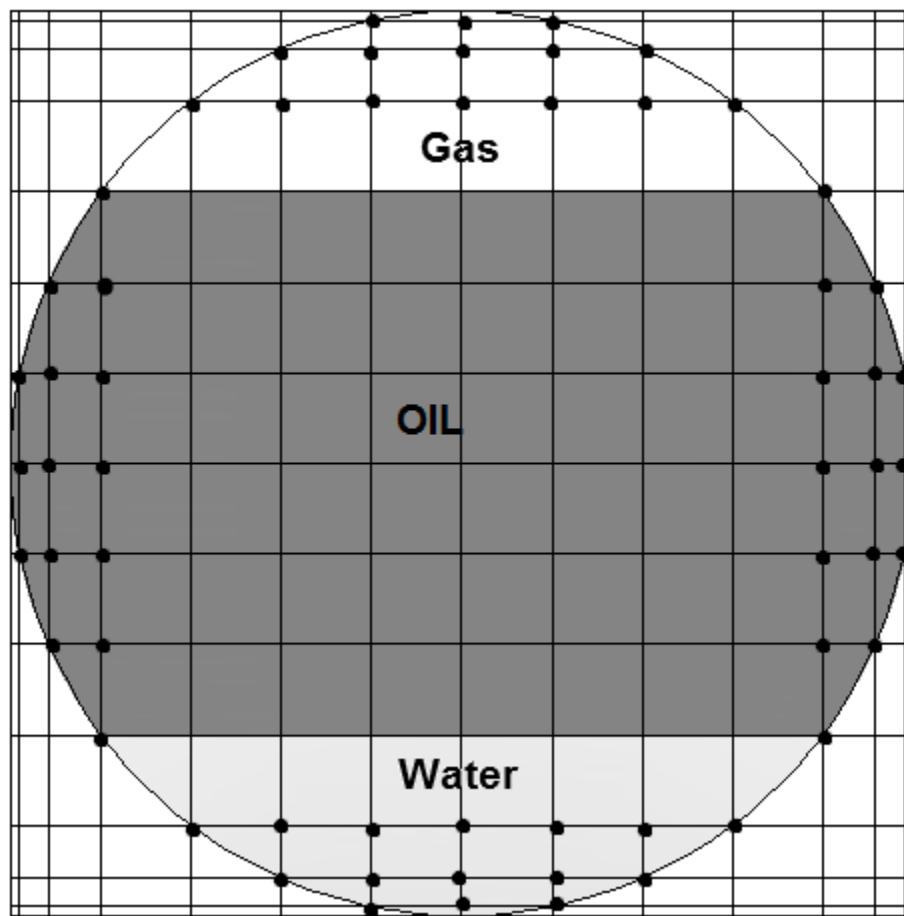


Figure 4.8: Illustration of free nodes, fixed nodes and boundary points for refined finite difference method when waveguide is filled with three dielectrics

| Radius (ρ) | Δ x | Δ y | No. of iterations | Fixed node voltage |
|------------|------|------|-------------------|--------------------|
| 4.4 cm | ≤ 0.01 | ≤ 0.01 | 12000 | +100 and -100 Volts |

Table 4.2: Specifications for applying refined finite difference method on partially filled

circular waveguide

### 4.1.5  Finite Difference Method When Plates are put outside the Tube

The second case is to find the capacitance by finite difference method when the

metal plates are considered outside the tube. A plexiglass tube is considered with an inner

radius of 4.4 cm and tube thickness of 0.5 cm. The method of applying FDM in this case

is same as previous one. The only difference is the inclusion of extra boundary points which

are formed due to plexglass-air interface. Such boundary points are shown in figure below.
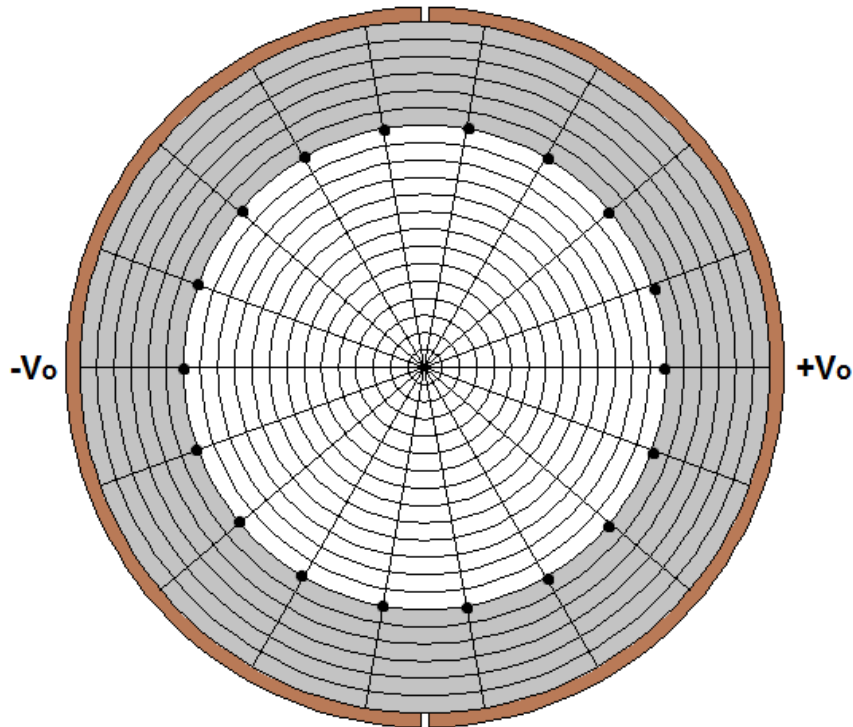


Figure 4.9: Boundary points formed at plexiglass-air interface

All these boundary points are evaluated according to rules mentioned in section 4.1.3. As the electric flux now is more concentrated inside the plexiglass tube so we need more points to evaluate the capacitance accurately. The specifications for applying the FDM in such a case are given in the table below.

| Radius (ρ) | Δ ρ | Δ φ | m | No. of iterations | Fixed node voltage |
|---|---|---|---|---|---|
| 4.4 cm | 0.005 cm | $0.25^0$ (0.00436 rad) | 880 | 12000 | +100 and -100 Volts |

Table 4.3: Specifications for applying FDM on air filled circular waveguide when plates are placed outside the tube

The approximation equations are formed by applying the rules discussed in section 4.1.3. Once the approximation equations are formed, then these equations are solved by iteration method. And finally the capacitance is calculated by using the equations (4.6) and (4.7). For other cases when tube is partially filled with two or three dielectrics, the same method is applied as discussed in sections 4.1.3 and 4.1.4. The only addition is another interface which is formed by plexiglass-air interface. So in case when tube is partially filled two dielectrics and plates are put outside, then there will be three interfaces. First one is the plexiglass-air interface, second is the plexiglass-water interface and third one will be water-air interface. Similarly for three dielectrics there will be four interfaces namely plexiglass-oil interface, plexiglass-air interface, plexiglass-water interfece, oil-water interface and oil-gas interface. Approximation equations in these cases are formed by applying rules discussed in section 4.1.3 and values of capacitance is obtained.

## 4.2    Calculation of Capacitance by Parallel Plate Capacitance Method

The capacitance of a cross section of a waveguide can be found by slicing the structure into N strips, and then finding the capacitance between each pair of slices. Finally the total capacitance will be addition of all these capacitances because all of these will appear in parallel. The slicing of structure is shown in figure below.
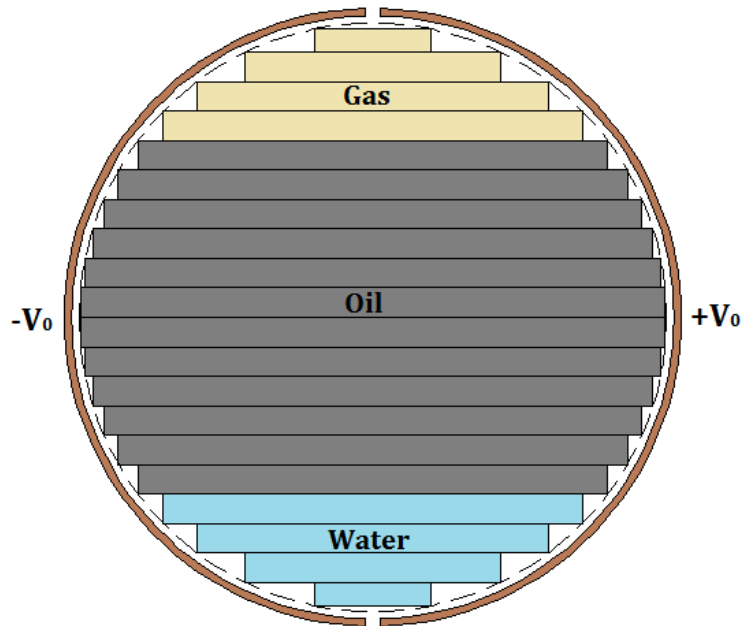


Fig.4.10: Slicing of waveguide to form parallel plate capacitors

Here the plates are of different lengths, so in order to find the capacitance, we need to take the average of both lengths and then find the capacitance. We calculated the capacitance by using this technique and it is found that the results were inaccurate. The reason of this inaccuracy is approximation of length of each slice. So if we are making a total of 100 slices, then the amount of error will be huge, and by make less slices the lengths of two adjacent slices will be much different and hence error will be large. The only positive of this method is that, we got the idea that instead of slicing it along the diameter;

we can make the chunks along the circumference of the waveguide and then considering the each pair of chunk as inclined plate capacitance. The method of inclined plate capacitance is discussed in next section.

## 4.3    Calculation of Capacitance by Using Inclined Plate Capacitance Method

In chapter 2 the general relation to find the capacitance between two inclined plates is given by equation (2.11). In this section it is discussed in details that how we can use inclined plate capacitance method to calculate the capacitance of a circular waveguide. The capacitance calculation for air filled waveguide, partially filled waveguide with one dielectric and partially filled waveguide with two dielectrics is discussed here. For all these cases we are dividing the waveguide along the circumference in small arcs, an arc formed by very smaller angle can be considered as a straight line, so by dividing the waveguide in smaller arcs each arc will act as a line with an angle. Each inclined section of waveguide in the upper half will have a corresponding inclined part at the lower half, as shown in figure below which will form an inclined capacitor and can be solved by equation (2.11).
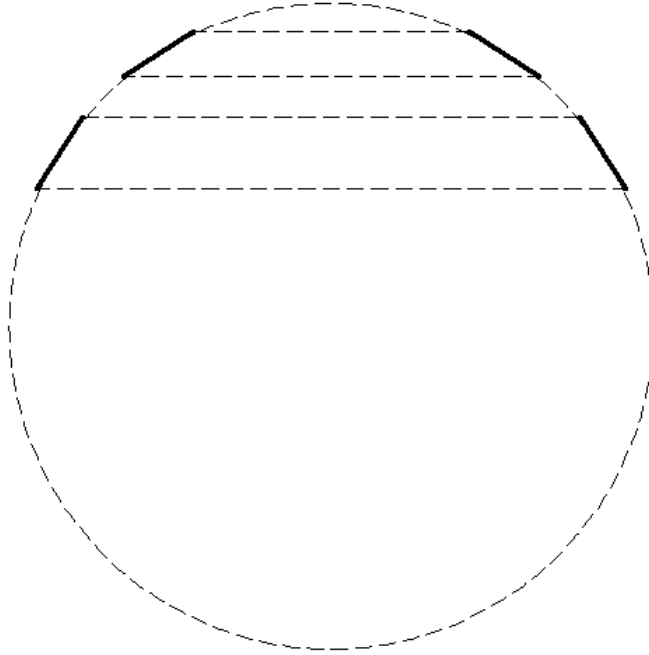
Figure 4.11: Inclined plate capacitors along the circumference of waveguide

A number of inclined plate capacitors will be formed along the circumference of the waveguide and the total capacitance can be found by adding all these capacitors, because all these inclined capacitors are parallel to each other. It can be noted from figure 4.10 that smaller the angle of arc, more accurate the results will be. Because when the angle decreases arcs become more like a straight line.

### 4.3.1 Inclined Plate Capacitance Method for Uniformly Filled Waveguide and considering the plates inside the tube

In this case the waveguide is considered to be completely filled with one dielectric (or completely empty). The pipeline is considered as a waveguide and several inclined plate capacitors are formed along the circumference of waveguide. To calculate the capacitance we need to know the expressions for lengths $a$, $b$ and angle $\varphi_0$. These lengths, angle and inclined capacitors are shown in figure below.
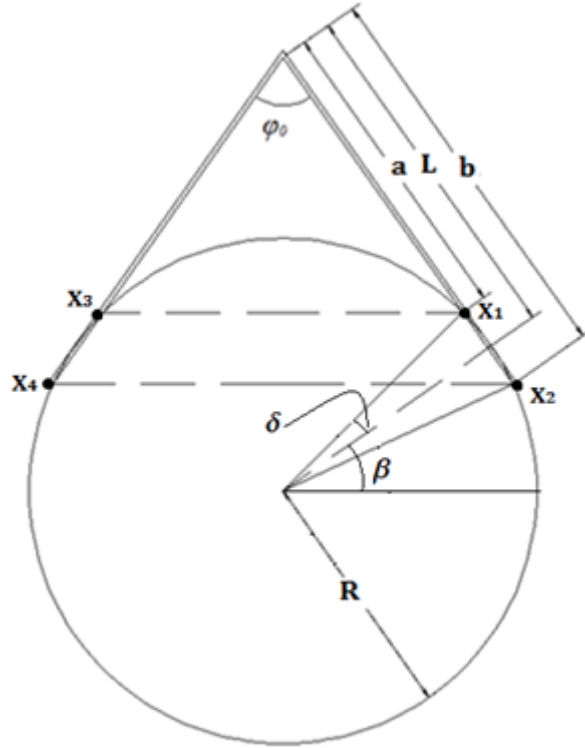
Figure 4.12: Illustration of inclined capacitors parameters for empty waveguide

The differential capacitance is shown with dotted lines with its two plates being $X_1X_2$ and $X_3X_4$. In figure 4.12, "*delta* ($\delta$)" is the angle subtended by half the chord, "*beta* ($\beta$)" is the angle from axis to center of the chord and "*R*" is the radius of waveguide as shown in figure 4.12. From above information we can estimate the value of "*L*" by solving the triangles ABC and DBC as shown in figure below.

By using figure 4.12 and 4.13, we can solve the triangles ABC and DBC by using trigonometric relations, and following equations can be formed.

$$\overline{AB} = \frac{R}{2}(1 + \cos(\delta))$$

$$\overline{BC} = \frac{R}{2}(1 + \cos(\delta))\sin(\beta)$$

$$\overline{BD} = L = \frac{\frac{R}{2}(1 + \cos(\delta))}{\tan\left(\frac{\varphi_0}{2}\right)} \qquad (4.10)$$

Here δ is fixed while β will change for each pair of inclined capacitors and can be given by expression:

$$\beta = \left(\frac{n}{2} - \delta\right); \quad n = 1,2,3, \dots \dots \dots ,179 \qquad (4.11)$$
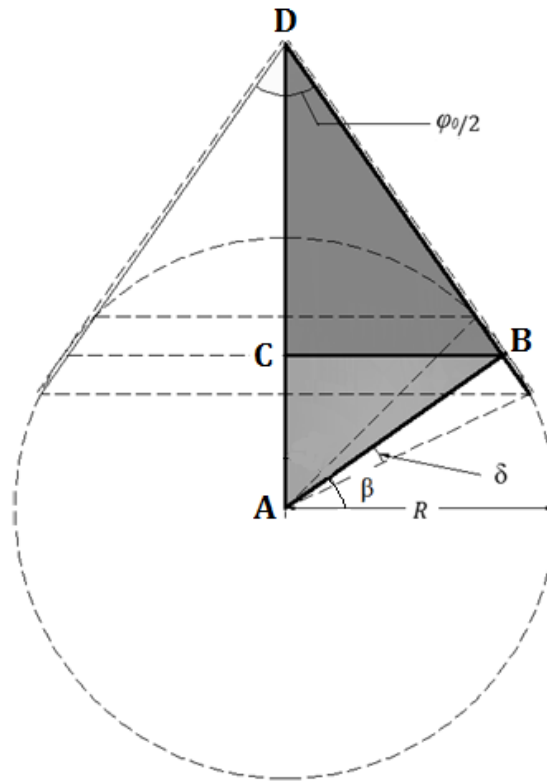


Figure 4.13: Triangles formed by inclined capacitors in empty waveguide

For this case the angle δ is taken to be $0.25^0$ and inclined capacitors are formed by taking the arc of $0.5^0$. Thus, in equation (4.11) δ is equal to $0.25^0$ and *n* can be any integer from 1 to 179. It can be easily seen from figure 4.12 that if length "*L*" is known, we can easily find the lengths "*a*" and "*b*". Lengths *a, b* and *L* are denoted in figure 4.12.

$$a = L - R\sin(\delta) \qquad (4.12)$$

$$b = L + R\sin(\delta) \qquad (4.13)$$

It can also be noted from figure 4.12 that $\varphi_0 = 2\beta$ , so

$$\varphi_0 = 2\left(\frac{n}{2} - \delta\right); \quad n = 1,2,3,\dots\dots\dots,179 \qquad (4.14)$$

Now all the parameters for equation (2.11) are known, so by using equations (4.10) to equation (4.14) in equation (2.11), the capacitance of all the inclined capacitors can be calculated. Then all individual capacitances are added to obtain the net capacitance of one half of the circular waveguide because all the inclined capacitors are in parallel. Finally this capacitance can be multiplied by 2 to obtain net capacitance of circular waveguide excited as shown in Fig.4.10, mathematically we can write the expression of net capacitance is given by equation (4.15).

$$C_{empty} = 2\sum_{n=1}^{179} \frac{\varepsilon_0 \, ln\left(\frac{b}{a}\right)}{\varphi_n} \qquad (4.15)$$

Equation (4.15) will give the total capacitance of a dielectric filled waveguide. The same procedure is used for partially filled waveguides with some modification, which is discussed in the upcoming subsection.

44

### 4.3.2 Inclined Plate Capacitance Method When Waveguide is filled with Two Dielectrics and Plates are considered inside the Tube

In this case it is supposed that the pipeline is carrying only two phase flow. So pipeline is modeled as a longitudinally partially filled circular waveguide with one dielectric and rest is air as shown in figure below. The inclined capacitors are formed like the previous cases, but here the portion of the capacitance of inclined capacitors inside the dielectric is multiplied by the dielectric constant of that material as shown in figure below. It can be seen from the figure that the two regions are separated by angle $\alpha$, region I has a dielectric constant $\varepsilon_{r1}$ and region II has dielectric constant $\varepsilon_{r2}$.
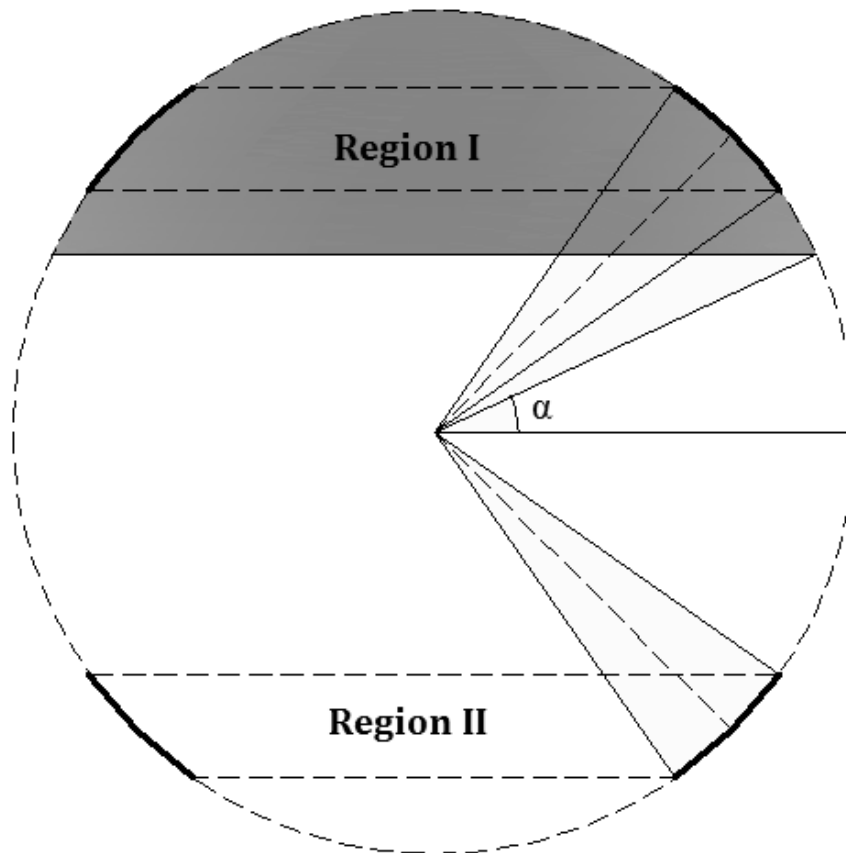
Figure 4.14: Inclined capacitors when waveguide is partially filled with one dielectric

To find the inclined plate capacitance, the unknown parameters are found by applying the same procedure as done in section 4.3.1. The angles $\varphi_0$, $\alpha$, $\beta$, $\delta$ and lengths $a$, $b$ and $L$ are shown in figure below. By applying trigonometric relations the above mentioned parameters are found and summarized in table below.
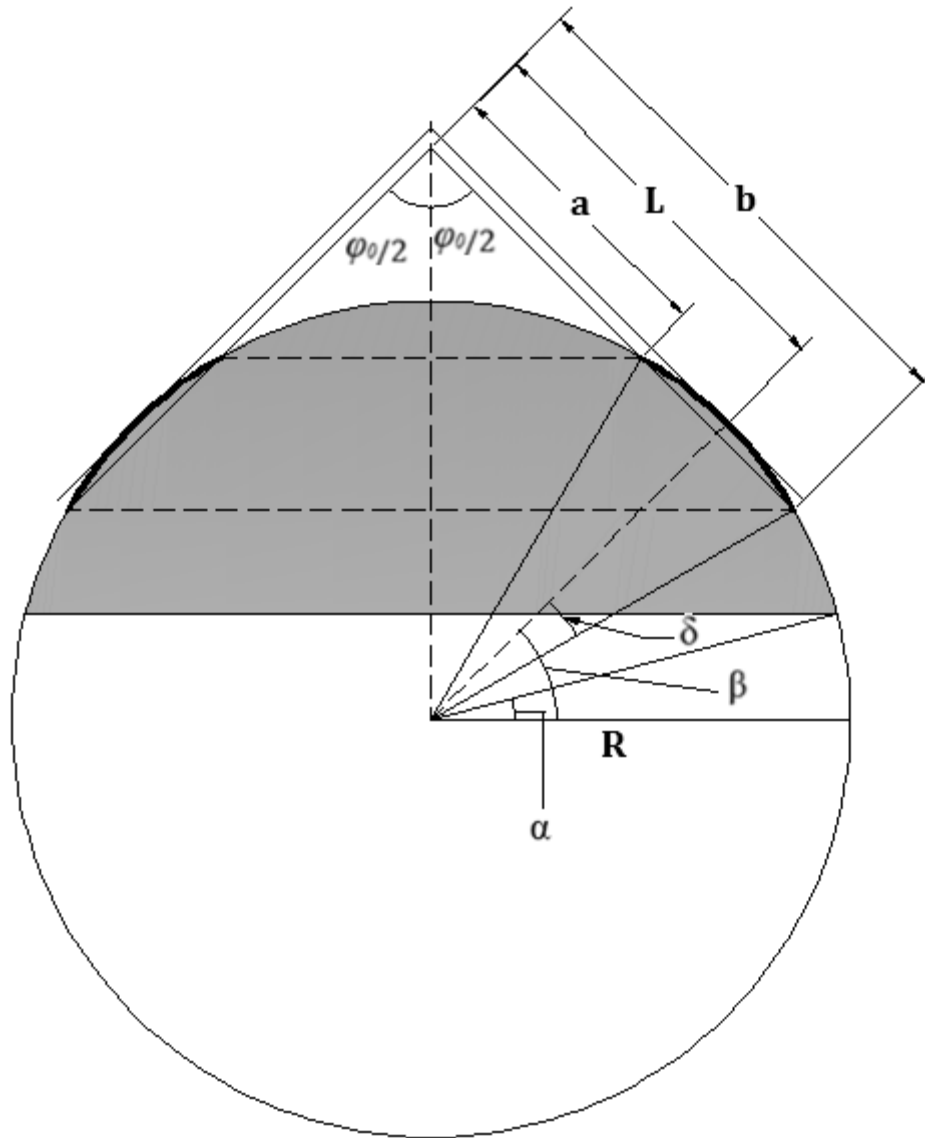


Figure 4.15: Inclined capacitor parameter when circular waveguide is partially filled with two dielectrics

| Parameters | Region I | Region II |
|---|---|---|
| β | $(3\delta)$ to $(\frac{\pi}{2} - \delta)$ And $3\delta$ to $(\alpha - \delta)$ | $(\alpha + \delta)$ to $(\frac{\pi}{2} - \delta)$ |
| $\varphi_o$ | 2 β | 2 β |
| L | $\dfrac{\frac{R}{2}(1 + \cos(\delta))}{\tan\left(\frac{\varphi_0}{2}\right)}$ | $\dfrac{\frac{R}{2}(1 + \cos(\delta))}{\tan\left(\frac{\varphi_0}{2}\right)}$ |
| a | $L - R\sin(\delta)$ | $L - R\sin(\delta)$ |
| b | $L + R\sin(\delta)$ | $L + R\sin(\delta)$ |
| δ | $0.25^0$ | $0.25^0$ |

Table 4.4: Inclined capacitor parameter when circular waveguide is partially filled with

two dielectrics

For this case the angle δ is taken to be $0.25^0$ and inclined capacitors are formed by

taking the arc of $0.5^0$. Thus *n* can be any integer from 1 to 179. The capacitance is calculated

in both regions separately and then total capacitance is found by adding them. We can write

the mathematical expression for total capacitance in this case as given by equation (4.16).

$$C_{total} = \left( \sum_{n=2\alpha+1}^{179} \frac{\varepsilon_0 \varepsilon_{r1} \ln\left(\frac{b_1}{a_1}\right)}{\varphi_{01}} + \sum_{n=1}^{2\alpha} \frac{\varepsilon_0 \varepsilon_{r2} \ln\left(\frac{b_2}{a_2}\right)}{\varphi_{02}} + \frac{1}{2} C_{empty} \right) \quad (4.16)$$

Here $a_1$, $b_1$, $a_2$, $b_2$, $\varphi_{01}$ and $\varphi_{02}$ are the expressions for a, b and $\varphi_0$ for regions I and

II as given in table 4.3. $\varepsilon_{r1}$ and $\varepsilon_{r2}$ are respective dielectric constants for regions I and II

respectively. Using equation (4.16) the capacitance of a circular waveguide when it is partially filled with two dielectrics can be found.

### 4.3.3 Inclined Plate Capacitance Method When Waveguide is filled with Three Dielectrics and Plates are considered inside the Tube

In this case it is supposed that the pipeline is carrying three phase flow, which is the water-oil-gas flow. So pipeline is modeled as a partially filled circular waveguide with three dielectrics as shown in figure below. The inclined capacitors are formed similar to the previous cases, but with proper dielectric constants. It can be seen from the figure that the regions are separated by angle $\alpha_1$ and $\alpha_3$. Region I contains gas with dielectric constant $\varepsilon_{rgas}$, followed by oil in region II with dielectric constant $\varepsilon_{roil}$ and finally water is in region III with dielectric constant $\varepsilon_{rwater}$.
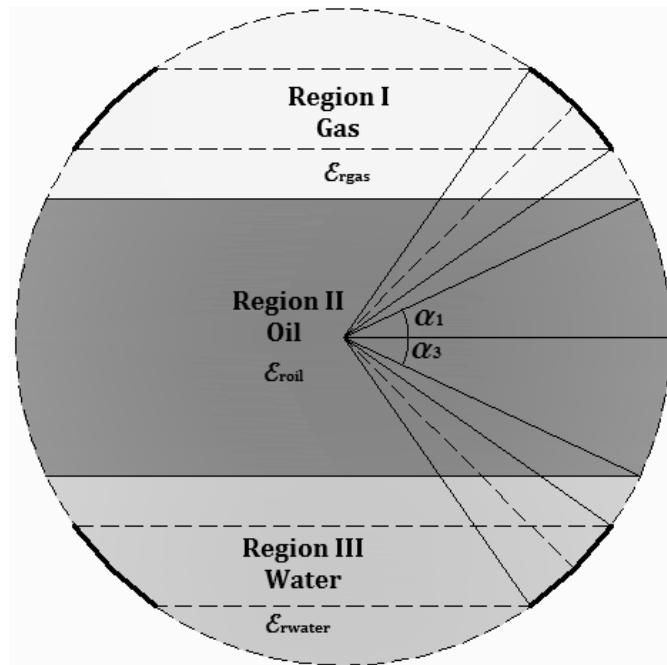


Figure 4.16: Inclined capacitors when waveguide is partially filled with three dielectrics

In this case the parameters needed to find the inclined capacitance are calculated by using the same technique discussed in section 4.3.1. The parameters for all three regions are listed in table below.

| Parameters | Region I | Region II | Region III |
|---|---|---|---|
| $\beta$ | $\left(\dfrac{n-1}{2+\delta}\right)$ | $\left(\dfrac{n}{2}-\delta\right)$ | $\left(\dfrac{n-1}{2+\delta}\right)$ |
| n | $2\alpha_1+1, 2\alpha_1+2, \ldots,179$ | $1, 2,\ldots,2\alpha_1$ <br> $1, 2,\ldots,2\alpha_3$ | $2\alpha_2+1, 2\alpha_2+2, \ldots,179$ |
| $\varphi_o$ | $2\beta$ | $2\beta$ | $2\beta$ |
| L | $\dfrac{\dfrac{R}{2}(1+\cos(\delta))}{tan\left(\dfrac{\varphi_0}{2}\right)}$ | $\dfrac{\dfrac{R}{2}(1+\cos(\delta))}{tan\left(\dfrac{\varphi_0}{2}\right)}$ | $\dfrac{\dfrac{R}{2}(1+\cos(\delta))}{tan\left(\dfrac{\varphi_0}{2}\right)}$ |
| a | $L-Rsin(\delta)$ | $L-Rsin(\delta)$ | $L-Rsin(\delta)$ |
| b | $L+Rsin(\delta)$ | $L+Rsin(\delta)$ | $L+Rsin(\delta)$ |
| $\delta$ | $0.25^0$ | $0.25^0$ | $0.25^0$ |

Table 4.5: Inclined capacitor parameters when circular waveguide is partially filled with three dielectrics

By using the above parameters the capacitance of each inclined pair is found and then all these capacitances are summed up to get the total capacitance. Mathematical form of total capacitance in this case is given by equation in which region II is divided in two parts, in one part the capacitance till $\alpha_1$ is calculated and in the other part the capacitance till $\alpha_3$ is calculated.

$$C_{total} = \left( \begin{array}{c} \sum\limits_{n=2\alpha_1+1}^{179} \dfrac{\varepsilon_0 \varepsilon_{rgas} \; ln\left(\dfrac{b_1}{a_1}\right)}{\varphi_{01}} + \sum\limits_{n=1}^{2\alpha_1} \dfrac{\varepsilon_0 \varepsilon_{roil} \; ln\left(\dfrac{b_2}{a_2}\right)}{\varphi_{02}} \\[3em] + \sum\limits_{n=1}^{2\alpha_3} \dfrac{\varepsilon_0 \varepsilon_{roil} \; ln\left(\dfrac{b_2}{a_2}\right)}{\varphi_{02}} + \sum\limits_{n=2\alpha_3+1}^{179} \dfrac{\varepsilon_0 \varepsilon_{rwater} \; ln\left(\dfrac{b_3}{a_3}\right)}{\varphi_{03}} \end{array} \right) \qquad (4.17)$$

Here $a_1$, $b_1$, $a_2$, $b_2$, $a_3$, $b_3$, $\varphi_{01}$, $\varphi_{02}$ and $\varphi_{03}$ are the expressions for a, b and $\varphi_0$ for region I, II and III respectively as given in table 4.4. $\varepsilon_{rgas}$, $\varepsilon_{roil}$ and $\varepsilon_{rwater}$ are respective dielectric constants for gas, oil and water. Thus by using equation (4.17) the capacitance of a circular waveguide when it is partially filled with three dielectrics is obtained.

### 4.3.4 Inclined Plate Capacitance Method When Plates are considered outside the Tube

Previously we were considering the metal plates inside the tube so the effect of tube thickness was ignored. Now the plates are considered outside the plexiglass tube and we need to consider the effect of tube thickness as well. If we put the metal plates perpendicular to azimuthal direction then the electric flux lines will start from positive end and will terminate at negative end. There will be some flux which is flowing through the tube itself. The concentration of flux lines in the upper and bottom ends of tube will be higher and a very small amount of flux will go through air. The electric flux lines in such a case are shown in figure below.
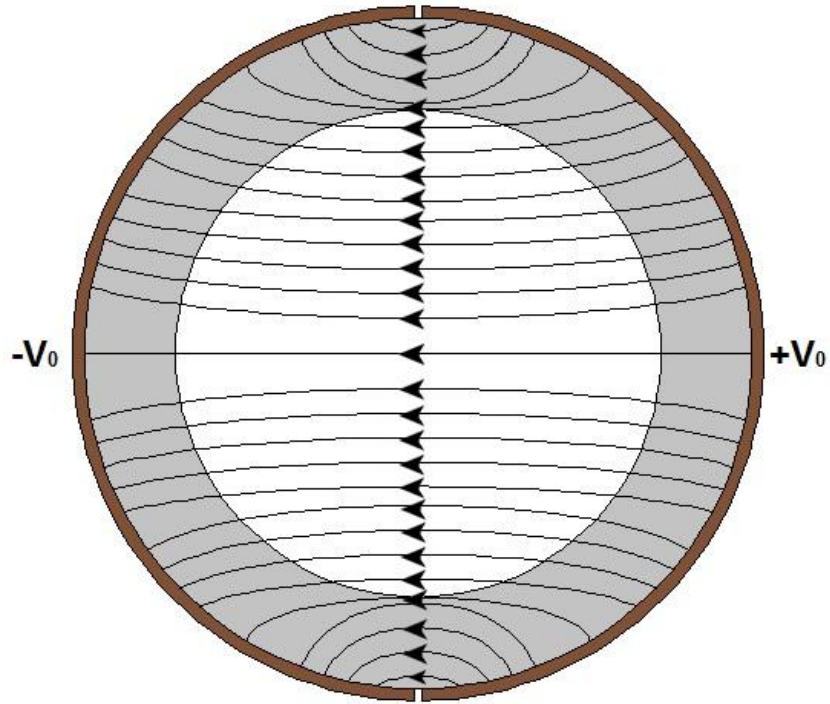
Figure 4.17: Illustration of Electric Flux lines when metal plates are placed outside the
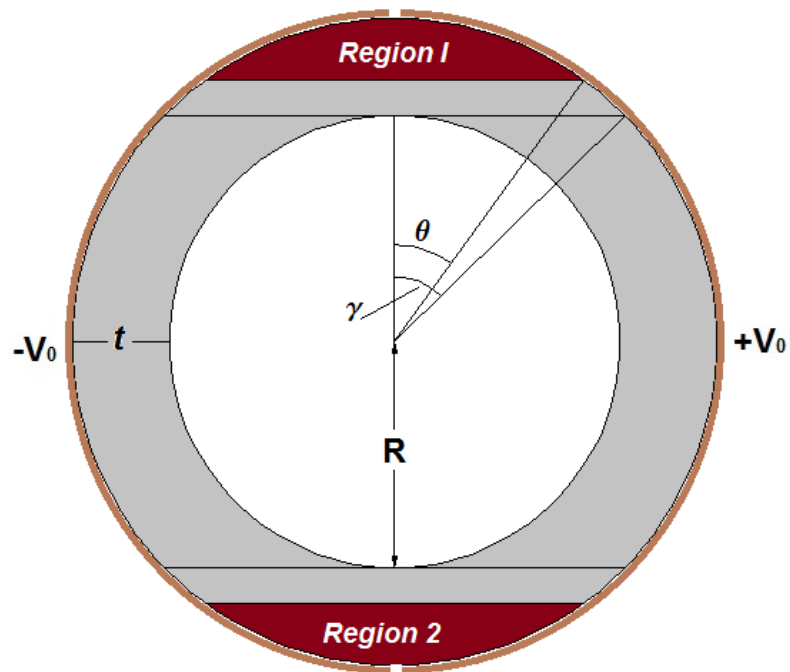
tube



Figure 4.18: Illustration of regions where all the flux is inside the plexiglass tube

It can be noticed from figure 4.17 and figure 4.18 that in region 1 and 2, all the flux is flowing through plexiglass and nothing is inside. Except region 1 and 2 the capacitance is calculated by forming the strips of plexiglass and empty tube as it is done in section 4.2.1. The capacitance due to plexiglass is in series with the capacitance of tube which is already calculated in section 4.2.1. So for each strip starting from angle $(\pi - \theta - \delta)$ to positive x axis, the capacitance is calculated for plexiglass and tube separately by using equations (4.10) to equation (4.16). Then these capacitances are combined in series multiplied by 2. Now to calculate the capacitance of region 1 and 2 we need to know the angles $\gamma$ and $\theta$. If tube has a radius $R$ and thickness $t$, then angle $\gamma$ can be given by following equation:

$$\gamma = cos^{-1}\left(\frac{R}{R+t}\right) \qquad (4.18)$$

There is no exact relation to find $\theta$. It can be given as $\theta = \gamma - (K \times \gamma)$, where $K$ is a constant and we have shown experimentally that $K$ is always 15-30% of $\gamma$. For an empty tube $K$ was measured to be around 20% of $\gamma$. The other cases when the tube is partially filled with two or three dielectrics the same procedure is followed. And capacitance of individual substance is calculated and then combined in series with the capacitance of plexiglass. We are glad to say that the results obtained by above mentioned technique were very close to numerical and experimental results. The detailed results are discussed in chapter 6.

# CHAPTER 5

# THEORATICAL FORMULATION

As mentioned in chapter 1 that there exists no solid theory in open literature that relates the height of individual liquids to overall capacitance of pipeline. So in this section a theoretical formulation is given which is able to relate the height of individual fluid (water, oil and gas) to the total capacitance of pipeline and also validate the numerical results. The inclusion of water in the pipeline will produce conductivity, so in this work the conductivity is also used to simplify the problem of finding the approximate amount of each liquid. Theoretical formulation of empty and partially filled waveguide is given in this section and at the end the method of relating the liquid height to net capacitance is discussed.

## 5.1    Theoretical Formulation for Capacitance of Air Filled Circular Waveguide when Plates are Considered Inside

In this section the pipeline is considered as an empty waveguide, it is supposed that from 0 to $\pi$ radians the voltage is $+V_0$ and from $-\pi$ to $2\pi$ the voltage is $-V_0$. The radius of waveguide is taken to be $\rho$ and we are interested to find the voltage at a point $P$ which is located at a distance $R$ from the center as shown in figure 5.1.
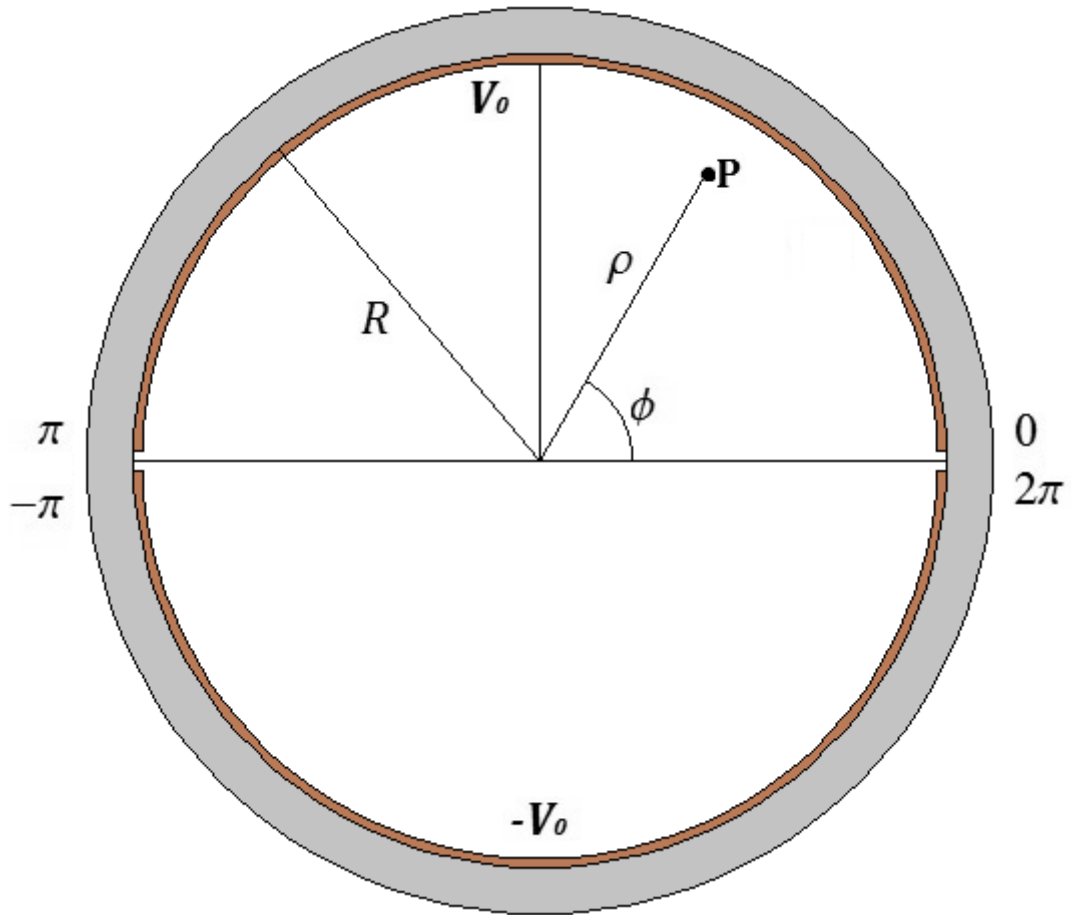
Figure 5.1: Model of an empty circular waveguide with metal plates inside for theoretical formulation

The general expression for finding the voltage at a distance $\rho$ inside a circular waveguide is given as:

$$V = \sum A_n \sin(n\varphi)\rho^n + A_0$$

At $\rho = R$, the expression becomes

$$V(R) = \sum A_n \sin(n\varphi)R^n$$

As

$$V = \begin{cases} +V_0, & 0 < \varphi < \pi \\ -V_0, & \pi < \varphi < 2\pi \end{cases}$$

So the expression of voltage can be written as:

$$\int \sum A_n \sin(n\varphi)\sin(\rho\varphi)R^n = \int_0^\pi V_0 \sin(\rho\varphi)d\varphi - \int_\pi^{2\pi} V_0 \sin(\rho\varphi)d\varphi$$

$$\int_0^{2\pi} \sum A_\rho \left(\frac{1 - \cos(2\rho\varphi)}{2}\right) R^\rho d\varphi = -V_0 \left|\left(\frac{\cos(\rho\varphi)}{\rho}\right)\right|_0^\pi + V_0 \left|\left(\frac{\cos(\rho\varphi)}{\rho}\right)\right|_\pi^{2\pi}$$

After solving we get:

$$A_\rho \pi R^\rho = \frac{V_0}{\rho}(2 - 2\cos(\rho\pi)) = \frac{2V_0}{\rho}(1 - \cos(\rho\pi))$$

Or generally we can write that

$$A_n = \frac{2V_0}{\pi R^n}\frac{1}{n}(1 - \cos(n\pi))$$

This expression will lead us to the expression of voltage inside a circular waveguide that is empty of completely filled with a specific dielectric.

$$V = \sum_{n=1}^{\infty} \frac{2V_0}{n\pi}(1 - \cos(n\pi).\sin(n\varphi))\left(\frac{\rho}{R}\right)^n \tag{5.1}$$

Equation (5.1) gives the exact expression for finding the voltage at any point inside an empty circular waveguide. If waveguide is completely filled with a dielectric the value of voltage will be multiplied by the dielectric constant of that particular substance.

55

It can be noted from equation (5.1) that.

$$\sum \frac{2}{n\pi}(1 - \cos(n\pi)\sin(n\varphi)) = \begin{cases} 1, & 0 < \varphi < \pi \\ -1, & \pi < \varphi < 2\pi \end{cases}$$

Once voltage inside the waveguide is found, we can find the electric field by using the relation $E = -\nabla V$. For cylindrical coordinate system the $\nabla V$ can be given as:

$$\nabla V = \frac{\partial V}{\partial \rho}\overrightarrow{a_\rho} + \frac{1}{\rho}\frac{\partial V}{\partial \varphi}\overrightarrow{a_\varphi} + \frac{\partial V}{\partial z}\overrightarrow{a_z}$$

As we are working only in $\rho$ and $\varphi$ plane, so above expression will reduce to:

$$\nabla V = \frac{\partial V}{\partial \rho}\overrightarrow{a_\rho} + \frac{1}{\rho}\frac{\partial V}{\partial \varphi}\overrightarrow{a_\varphi}$$

So

$$\overrightarrow{E} = -\nabla V = -\frac{\partial V}{\partial \rho}\overrightarrow{a_\rho} - \frac{1}{\rho}\frac{\partial V}{\partial \varphi}\overrightarrow{a_\varphi} \tag{5.2}$$

By using (5.2) we get:

$$E_\varphi\big|_{\rho=R} = \left[\frac{2V_0}{R\pi}\sum_{n=1}^{\infty}(\cos(n\pi - 1)\cos(n\varphi))\right]\overrightarrow{a_\varphi}$$

And

$$E_\rho\big|_{\rho=R} = \left[\frac{2V_0}{R\pi}\sum_{n=1}^{\infty}(1 - \cos(n\pi)\sin(n\varphi))\right]\overrightarrow{a_\rho}$$

Now total charge enclosed can be found by using following equation.

$$Q = \int\limits_{\varphi=0}^{\pi} D_n . R d\varphi \qquad (5.3)$$

Where "$D_n = \varepsilon_0 E_\rho$" Here only $\rho$ component of E field is used because, $E_\varphi$ at $\rho = R$ is always zero. Thus the expression for total charge enclose can be written as:

$$Q = \sum_{n=1}^{\infty} \varepsilon_0 \int_0^{\pi} \frac{2V_0}{\pi} (1 - \cos(n\pi) \sin(n\varphi)) d\varphi$$

After solving it will give:

$$Q = \sum_{n=1}^{\infty} \frac{2\varepsilon_0 V_0}{n\pi} (1 - \cos(n\pi))^2 \qquad (5.4)$$

Equation (5.4) is giving the total charge enclosed inside an empty circular waveguide. When waveguide is completely filled with any dielectric, the charge enclosed will be multiplied by dielectric constant of that particular material. From total charge we can easily find the capacitance of the waveguide by using the relation given by equation (5.5).

$$C = \frac{Q}{2V_0} \qquad (5.5)$$

Thus

$$C = \sum_{n=1}^{\infty} \frac{\varepsilon_0 \varepsilon_r}{n\pi} (1 - \cos(n\pi))^2 \qquad (5.6)$$

Equation (5.6) is the general expression for capacitance of an empty or completely filled (with one dielectric) circular waveguide.

## 5.2 Theoretical Formulation for Capacitance of Air Filled Circular Waveguide when Plates are Considered Outside

Consider a tube is made of plexiglass with a thickness "$t$" and having an inner radius "$a$" and outer radius "$b$". Voltage $+V_0$ and $-V_0$ is applied to metal plates and we want to find the voltage at a point "$P$" that is located at a distance "$r$" from origin and at an angle "$\varphi$" from positive x-axis as shown in figure below.
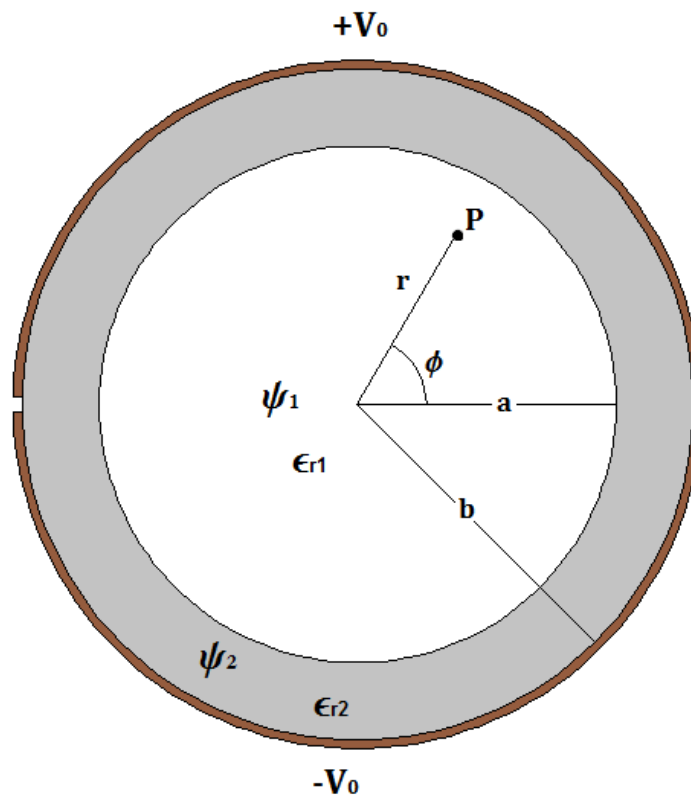


Figure 5.2: Model of an empty circular waveguide with metal plates outside for theoretical formulation

Suppose that the inside of tube having a voltage distribution of $\psi_1$ and dielectric constant of $\epsilon_{r1}$. Similarly the voltage distribution in plexiglass is $\psi_2$ and dielectric constant of $\epsilon_{r2}$. So we can write that:

$$\psi_1 = \sum_{n=1}^{\infty} C_n r^n \sin(n\varphi)$$

$$\psi_2 = \begin{cases} V_0, & 0 < \varphi < \pi \\ -V_0, & \pi < \varphi < 2\pi \end{cases} \qquad (a)$$

We can also write that:

$$\psi_2 = \sum_{n=1}^{\infty} (D_n r^n + E_n r^{-n}) \sin(n\varphi) \qquad (b)$$

Comparing above equations (a) and (b), we get:

$$\sum_{n=1}^{\infty} (D_n b^n + E_n b^{-n}) \sin(n\varphi) = \begin{cases} V_0, & \pi < \varphi < 0 \\ -V_0, & \pi < \varphi < 2\pi \end{cases}$$

$$\pi(D_n b^n + E_n b^{-n}) = \frac{2V_0}{n}(1 - \cos(n\pi)) \qquad (5.7)$$

As

$$E = -\nabla\psi = -\frac{\partial\psi}{\partial r}\overrightarrow{a_r} - \frac{1}{r}\frac{\partial\psi}{\partial\varphi}\overrightarrow{a_\varphi}$$

So

$$E_{2r} = -\frac{\partial\psi_2}{\partial r}\overrightarrow{a_r} = -\left(\sum_{n=1}^{\infty}(nD_n r^{n-1} - nE_n b^{-n-1})\sin(n\varphi)\right)\overrightarrow{a_r} \qquad (5.8)$$

$$E_{2\varphi} = -\frac{\partial\psi_2}{r\,\partial\varphi}\overrightarrow{a_\varphi} = -\frac{1}{r}\left(\sum_{n=1}^{\infty}(D_n r^n + E_n b^{-n})n.\cos(n\varphi)\right)\overrightarrow{a_\varphi} \qquad (5.9)$$

And similarly

$$E_{1r} = -\sum_{n=1}^{\infty} n. C_n r^{n-1} \sin(n\varphi)\overrightarrow{a_r} \qquad (5.10)$$

$$E_{1\varphi} = -\frac{1}{r}\sum_{n=1}^{\infty} n. C_n r^{n} \cos(n\varphi)\overrightarrow{a_\varphi} \qquad (5.11)$$

Now applying boundary conditions at $r=a$

$$E_{1\varphi} = E_{2\varphi}\big|_{r=a}$$

So we get

$$\sum_{n=1}^{\infty} -\frac{n}{a}D_n a^n \cos(n\varphi) - \sum_{n=1}^{\infty}\frac{n}{a}E_n a^{-n} \cos(n\varphi) = \sum_{n=1}^{\infty} -\frac{1}{a}nC_n a^n \cos(n\varphi)$$

Multiplying both sides by $\cos(m\varphi)$ and integrating from 0 to $\pi$

$$D_n a^{n-1} + E_n a^{-n-1} = C_n a^{n-1}$$

$$D_n + \frac{E_n}{a^{2n}} = C_n \quad ; \quad n = 1,2,3 \ldots\ldots \qquad (5.12)$$

Similarly by applying boundary conditions

$$\varepsilon_{r1}E_1 = \varepsilon_{r2}E_2$$

Multiplying both sides by $\cos(m\varphi)$ and integrating from 0 to $\pi$

$$\varepsilon_{r2}(D_n a^{n-1} - E_n a^{-n-1}) = \varepsilon_{r1}C_n a^{n-1}$$

Which gives

$$\left(D_n - \frac{E_n}{a^{2n}}\right) = \frac{\varepsilon_{r1}}{\varepsilon_{r2}} C_n \quad ; \quad n = 1,2,3 \ldots \ldots \tag{5.13}$$

From equation (5.7) we get:

$$D_n + \frac{E_n}{b^2} = \frac{2V_0}{n\pi} \frac{(1 - \cos(n\pi))}{b^n} \tag{5.14}$$

$$D_n + \frac{E_n}{a^{2n}} = C_n \tag{5.15}$$

$$\left(D_n - \frac{E_n}{a^{2n}}\right) = \frac{\varepsilon_{r1}}{\varepsilon_{r2}} C_n \tag{5.16}$$

Adding equations (5.15) and (5.16), we get

$$2D_n = \left(1 + \frac{\varepsilon_{r1}}{\varepsilon_{r2}}\right) C_n \tag{5.17}$$

Now solving equations (5.15) and (5.17), we get

$$E_n = (C_n - D_n)a^{2n}$$

$$E_n = \left[C_n - \frac{1}{2}\left(1 + \frac{\varepsilon_{r1}}{\varepsilon_{r2}}\right) C_n\right] a^{2n}$$

$$E_n = C_n \left[1 - \frac{1}{2}\left(1 + \frac{\varepsilon_{r1}}{\varepsilon_{r2}}\right)\right] a^{2n} \tag{5.18}$$

Now using the equations (5.17) and (5.18) in equations (5.14) we get:

$$\left[\frac{1}{2}\left(1 + \frac{\varepsilon_{r1}}{\varepsilon_{r2}}\right) + \frac{1}{b^{2n}}\left\{1 - \frac{1}{2}\left(1 + \frac{\varepsilon_{r1}}{\varepsilon_{r2}}\right)\right\}\right] C_n = \frac{2V_0}{n\pi} \frac{(1 - \cos(n\pi))}{b^n} \tag{5.19}$$

From equations (5.19), (5.18) and (5.17) we can find $C_n$, $E_n$ and $D_n$ respectively.

Finding the charge Q

As

$$Q = \varepsilon_{r2} \int_0^\pi E_{r2}.rd\varphi|_{r=b}$$

$$Q = \int_0^\pi \varepsilon_{r2} \sum_{n=1}^\infty (nD_n b^{n-1} - nE_n b^{-n-1}) \sin(n\varphi).bd\varphi$$

$$Q = \int_0^\pi \varepsilon_{r2} \sum_{n=1}^\infty (nD_n b^{n-1} - nE_n b^{-n-1}) \sin(n\varphi).b \frac{(1 - \cos(n\pi))}{n}$$

And finally capacitance can be calculated by using following relation:

$$C = \frac{Q}{2V_0}$$

## 5.3    Equi-Capacitance Contours Plotting

In chapter 4 numerical techniques to calculate the capacitance of waveguide are discussed and in first 2 sections of this chapter, theoretical formulation for capacitance of a partially filled circular waveguide is discussed. With this knowledge of capacitance we are able to draw the equi-capacitance contours that will relate the capacitance of waveguide to the height of individual liquid. The pipeline has a diameter D, and three substances (gas, oil and water) are having individual heights $d_1$, $d_2$, $d_3$ respectively. The voltage is applied on metal plates that are perpendicular to azimuthal direction as shown in figure 5.3.
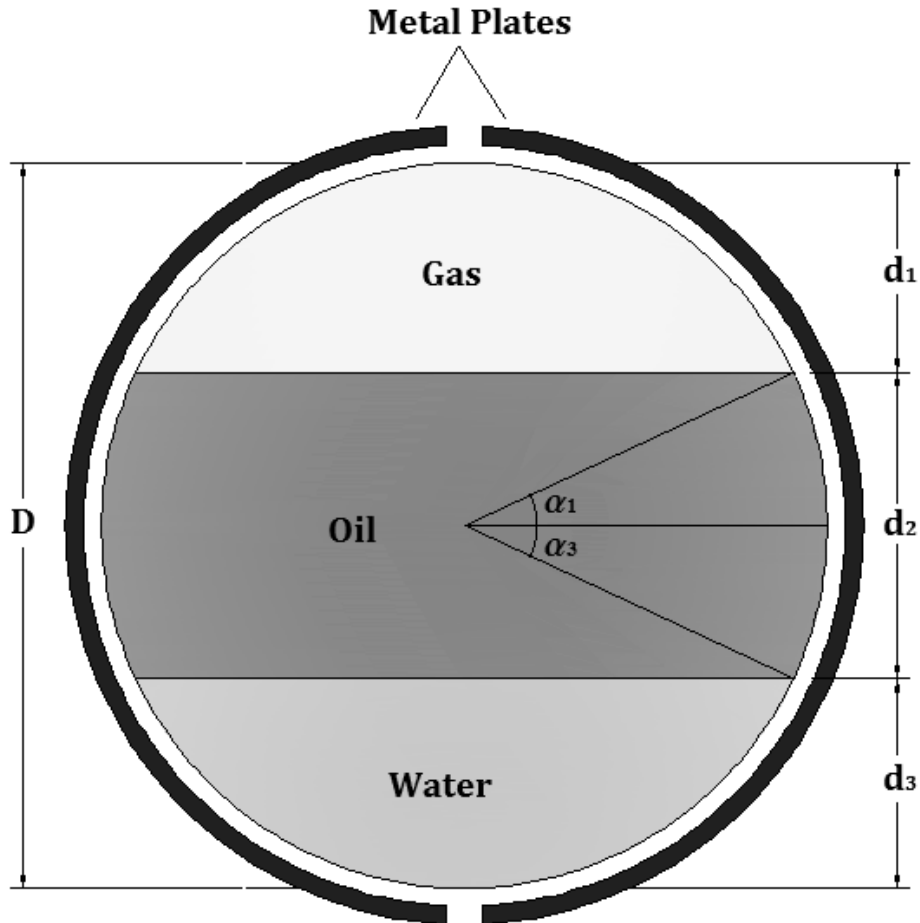
Figure 5.3: Oil carrying pipeline as a partially filled waveguide

It is supposed that the portion of waveguide that is containing gas has a capacitance $C_1$, the portion containing oil, has a capacitance $C_2$ and portion containing water has a capacitance of $C_3$. Due to inclusion of water, there will be some conductivity and that conductivity is taken as $R_3$. All these capacitances and conductance are in parallel. When a voltage V is applied on metal plates, then the currents $I_1$, $I_2$, $I_3$ and $I_4$ will flow from capacitances $C_1$, $C_2$, $C_3$ and $G_4$ respectively. The equivalent electrical circuit for this waveguide is shown in figure 5.4.
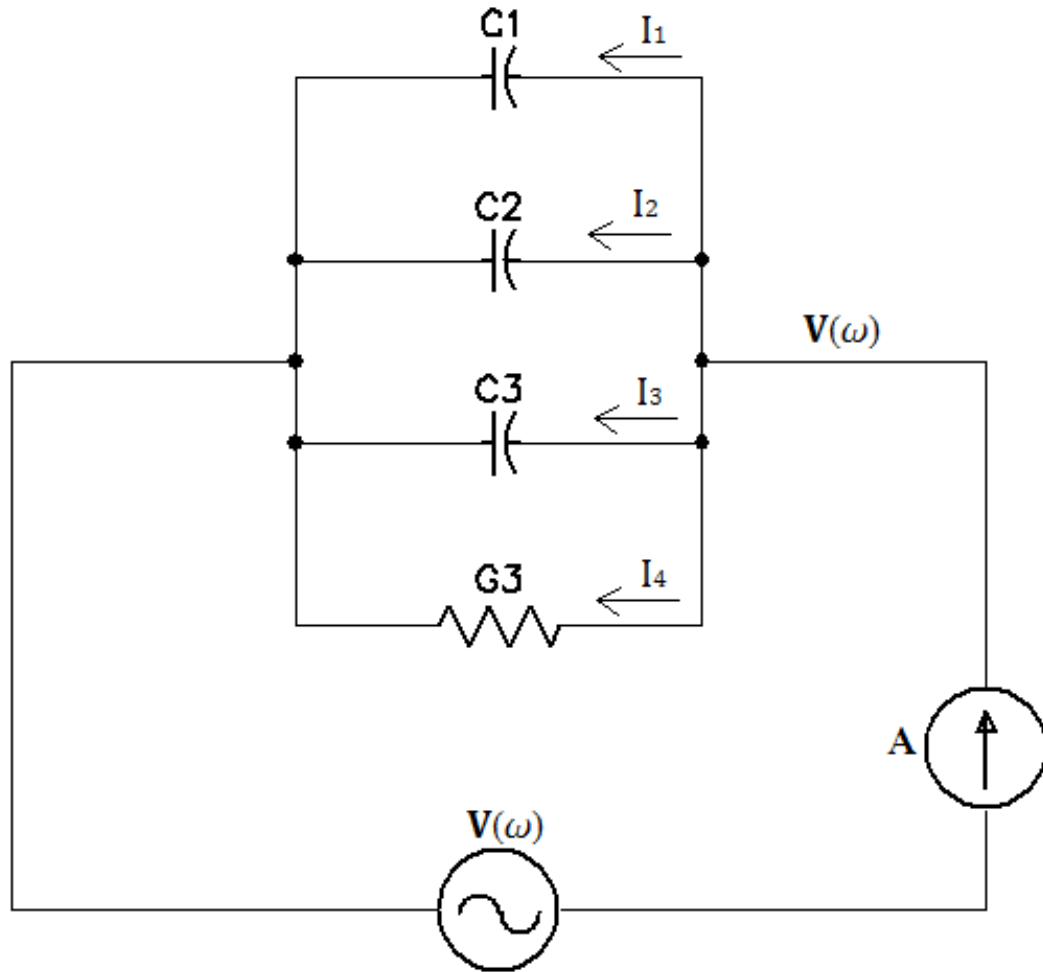
Figure 5.4: Electrical equivalent circuit of partially filled circular waveguide

After constructing the electrical model of partially filled circular waveguide, there are two different ways to relate the capacitance with the individual heights of substances. Both methods are described below.

*Method 1:* In this method the voltage of fixed frequency will be applied and magnitude and phase of the current will be measured to relate the capacitance with individual liquid height.

As $C_1$, $C_2$, $C_3$ and $G_3$ are already calculated numerically and theoretically and total current I is the summation of all currents flowing through circuit's components. We can write:

$$I = I_1 + I_2 + I_3 + I_4$$

$$I = V\left(j\omega C_1 + j\omega C_2 + j\omega C_3 + \frac{1}{R_3}\right) \qquad \therefore \left(G_3 = \frac{1}{R_3}\right)$$

$$I = V\left\{\frac{1}{R_3} + j\omega(C_1 + C_2 + C_3)\right\}$$

$$I = V\left\{\frac{1}{R_3} + j\omega(C_{eq})\right\} = \|I\| \, \llcorner\theta$$

Where

$$\|I\| = V_0\sqrt{\omega^2 C_{eq}^2 + \frac{1}{R_3^2}}$$

And $$\theta = \tan^{-1}\left(\omega C_{eq} R_3\right)$$

Thus, measuring $\|I\|$ and $\theta$ enable us to obtain $C_{eq}$ and $R_3$.

This method requires measuring magnitude and phase of current at the same time, which will affect the accuracy of the solution, so an alternative method can be produced in which we can obtain $C_{eq}$ and $R_3$ by just measuring the magnitude of current. The second method is described below.

Method 2: In this method the magnitude of current is measured by applying the voltage of two different frequencies, while the magnitude of voltage kept same for both

cases. Then a relation can be formed between $C_{eq}$ and $R_3$ and the magnitudes of current flowing through waveguide at two different frequencies.

For $\omega_1$:
$$\|I_1\| = V_0 \sqrt{\omega_1{}^2 C_{eq1}{}^2 + \frac{1}{R_3{}^2}}$$

For $\omega_2$:
$$\|I_2\| = V_0 \sqrt{\omega_2{}^2 C_{eq2}{}^2 + \frac{1}{R_3{}^2}}$$

Solving for $C_{eq}$ and $1/R_3$ we get

$$(\omega_1{}^2 - \omega_2{}^2)C_{eq}{}^2 = \frac{1}{V_0{}^2}(\|I_1\|^2 - \|I_2\|^2)$$

After rearranging

$$C_{eq} = \sqrt{\frac{\|I_1\|^2 - \|I_2\|^2}{V_0{}^2(\omega_1{}^2 - \omega_2{}^2)}}$$

And Hence

$$G_{eq} = \frac{1}{R_3} = \frac{C_{eq}\sigma}{\varepsilon_0 \varepsilon_r}$$

In above equation $\sigma$ is the conductivity of water. So a relationship between $G_3$ and $d_3$ can be plotted, because by increasing the amount of water in the waveguide, the conductivity will increase, so the plot of $G_3$ against $d_3$ will look like figure 5.5.
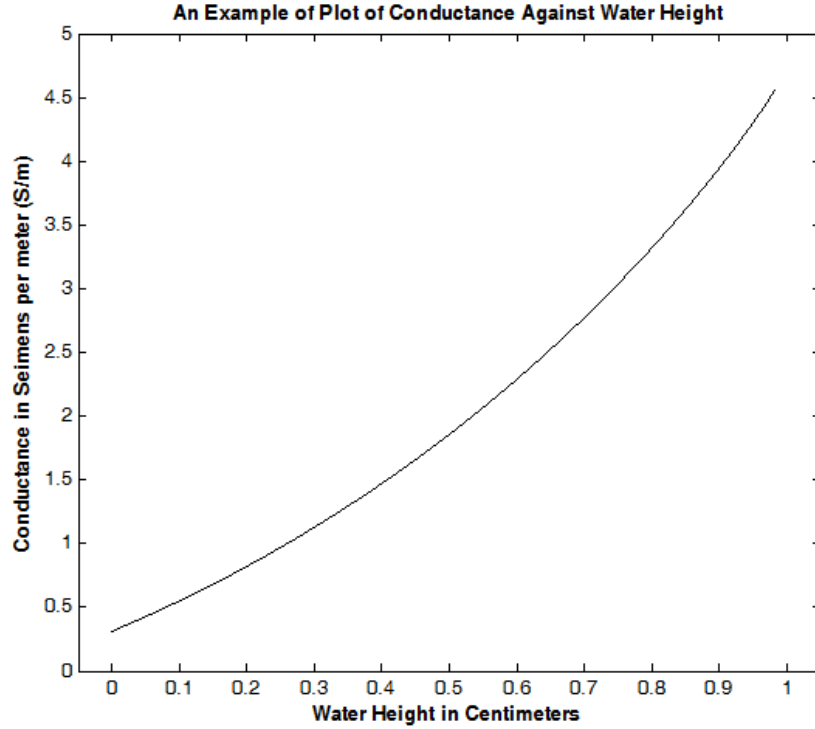
Figure 5.5: An example of plot of conductance against water height

The above plot will relate the water height ($d_3$) with conductance of waveguide and after plotting the conductance curve, it is possible with one experiment to obtain $d_2$ and $d_3$ as follows.

From $G_3$, we can estimate $C_3$ via the relation:

$$C_3 = \frac{\varepsilon_0 \varepsilon_r}{\sigma} G_3$$

From $C_{eq} = C_1 + C_2 + C_3$ we can obtain $(C_1 + C_2)$.

Now for a fixed $d_1$, the relation between $d_2$ and $(C_1 + C_2)$ can be plotted.

Similarly for another fixed $d_1$, another relation between $d_2$ and $(C_1 + C_2)$ can be plotted.

The procedure will be repeated several times, until relations between $d_2$ and $(C_1 + C_2)$ are plotted for all fixed $d_1$'s.

All these plots will be combined on a same graph and are called equi-capacitance contours. An example of equi-capacitance contours is shown in figure 5.6.

**An Example of Equi-Capacitance Contours**
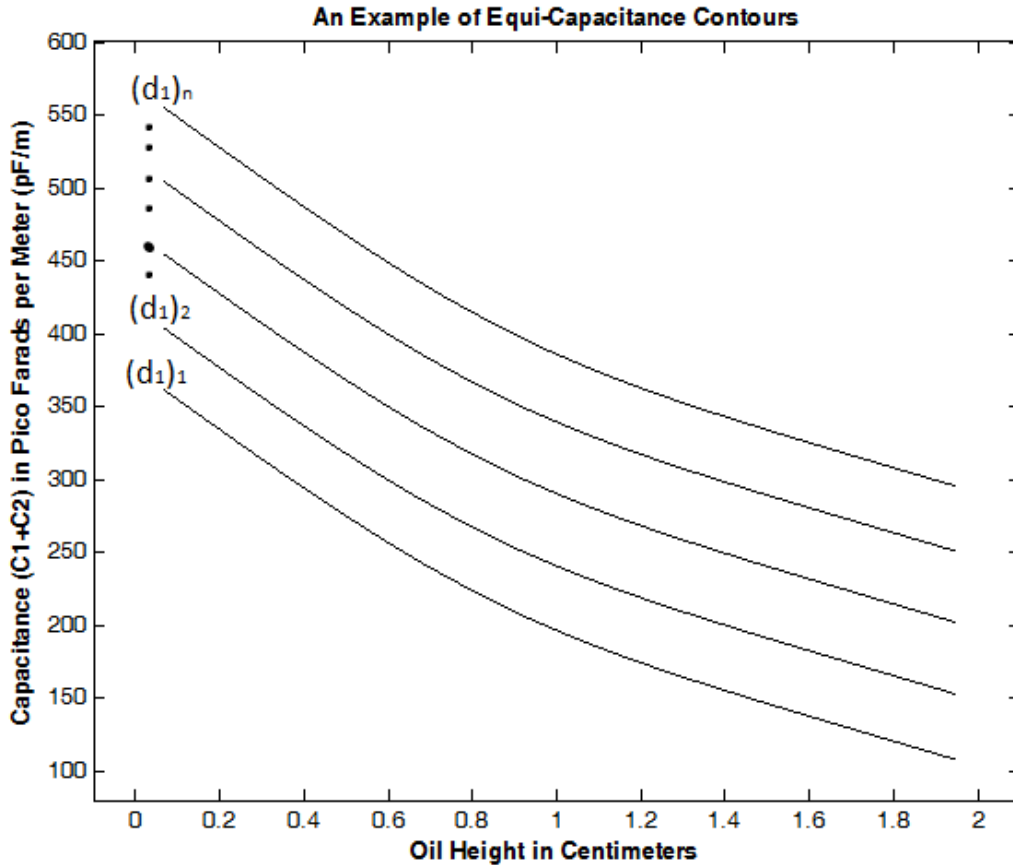
Figure 5.6: An example of equi-capacitance contours

The equi-capacitance contours will not intercept each other, and the knowledge of $(C_1 + C_2)$ and $d_2$ will determine $d_1$. And hence by using the graphs like figure 5.5 and 5.6 (actual graphs are given in chapter 6) we can estimate the height of each liquid inside an oil carrying pipeline, which can be easily translated to percentage of oil in the total volume of fluids flowing inside the pipeline.

68

# CHAPTER 6

# EXPERIMENTS AND RESULTS

In this chapter the different experiments and their results are discussed which are carried out to validate the theoretical and numerical work presented in previous chapters. Major experiments were measurement of dielectric constant of oil, capacitance measurement of an air filled waveguide, measurement of capacitance by placing the metal plates inside the tube, by considering two and three dielectrics (water-air and water-oil-air), measurement of conductivity of saline water, measurement of capacitance by putting the metal plates outside the tube and considering the one (air only), two (water and air) and three (water, oil and gas) dielectrics. Plexiglass tubes were fabricated locally for these experiments. To measure the conductivity of water, a plexiglass tube with a radius of 1.1 cm and length 20 cm was made having copper plates on both ends as shown in figure 6.1.
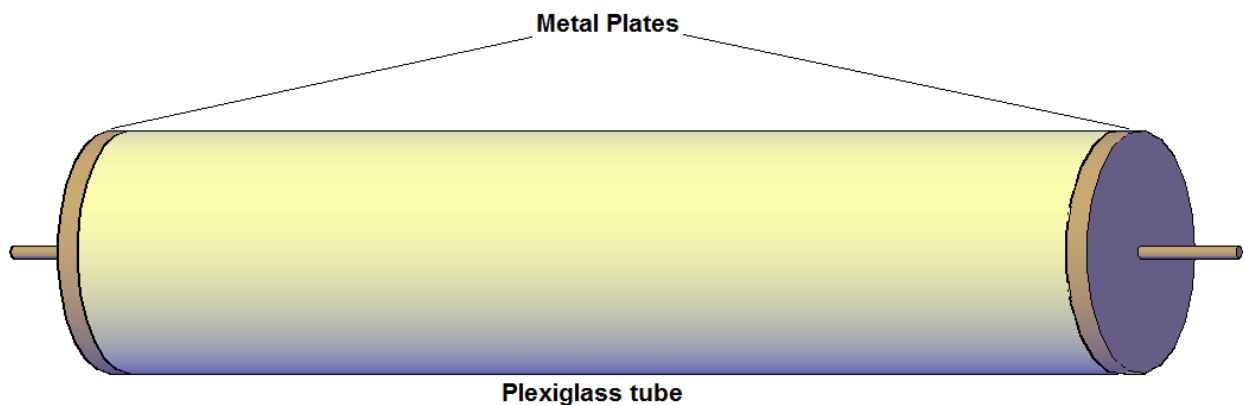


Fig.6.1: Model of plexiglass tube manufactured for measurement of water conductivity

For the measurement of dielectric constant of oil, plexiglass tube having a radius 4.375 cm and thickness of 0.5 cm was made. The tube was having a length of 30 cm, and two copper plates with a length of 20 cm each were put inside the tube. To measure the capacitance in a three phase flow, a plexiglass tube was made with similar dimensions, the only difference was, that this time the copper plates were placed outside the tube. The fabricated tube is shown in figure 6.2. All these experiments along with their results are discussed in the upcoming subsection.



Fig.6.2: Plexiglass tube with copper plates outside the tube

## 6.1    Experiment 1: Capacitance Measurement of an Air Filled Waveguide when Metal Plates Were Put Inside the Tube

The first experiment carried out was to find the capacitance of a circular waveguide when it was completely filled with air. A circular tube made of plexiglass was used as a waveguide. The metal plates were put inside the tube to neglect the effect of plexiglass. The length of tube was set to 30 cm and length of metal plates was 20 cm. The cross section of such tube is shown in figure 6.2. The capacitance of a structure can be measured by applying the voltage across it and then measuring the current. If a sinusoidal voltage of $V_{in}$ is applied at a frequency $f$ and the current $I$ is measured across the terminal of structure then the capacitance can be given by equation 6.1.
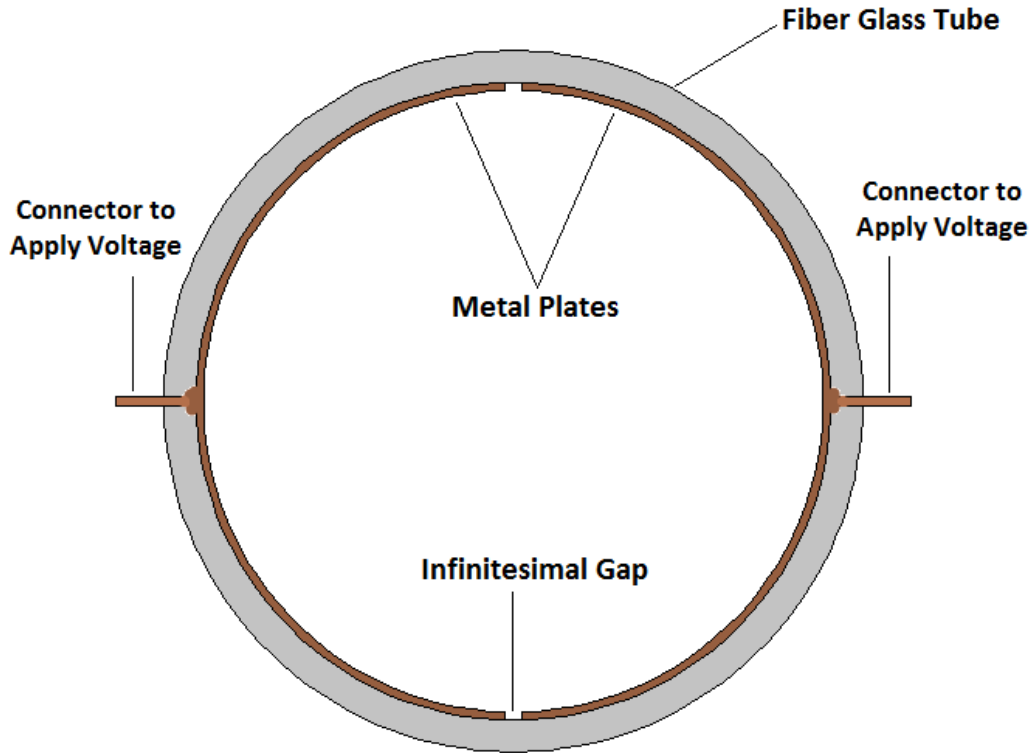
Figure 6.3: Cross Section of Plexiglass tube with metal plates inside

$$C = \frac{I}{2\pi fV}$$ (6.1)

Here *V and I* are voltage and current across the tube respectively.

As the cylindrical tube was completely empty so very less amount of current was flowing through it a low frequencies. In order to get a significant amount of current higher frequency was required. So a peak-to-peak voltage of 20 V at a frequency of 100 KHz is applied across the metal plates. To measure the current flowing through the tube, a series combination of a 1 KΩ resistor and tube is formed as shown in figure 6.4 and voltage across the 1 KΩ resistor is measured by using an oscilloscope. After measuring the voltage across 1 KΩ resistor the current flowing through the tube can be measured because current is

series circuit is always same. And then capacitance can be calculated by using equation (6.1).
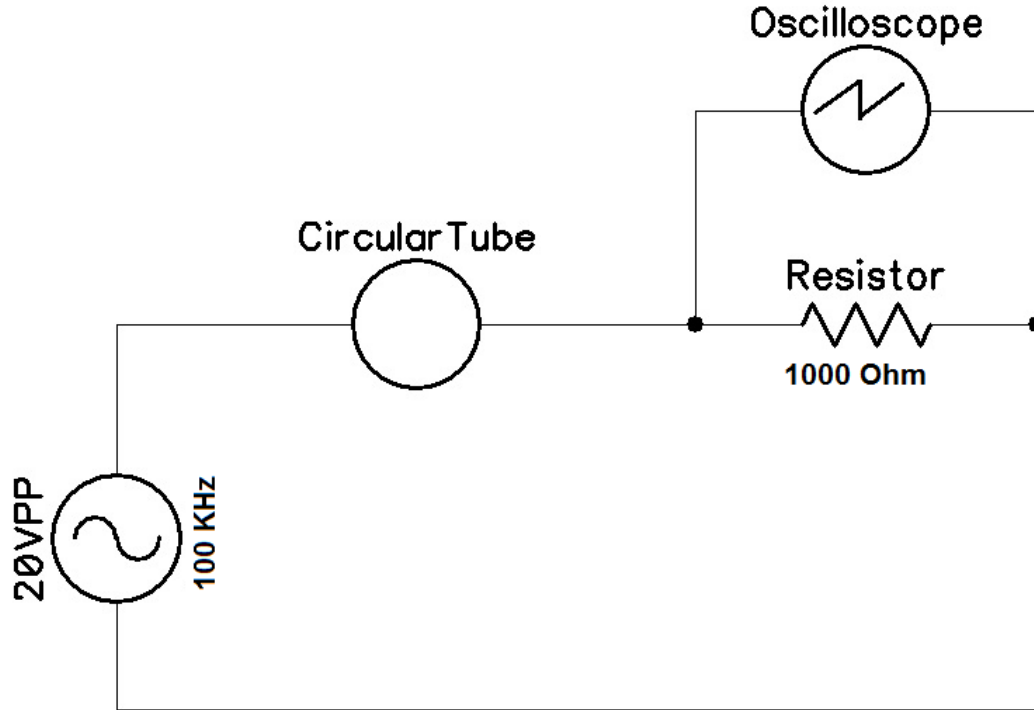


Figure 6.4: Series circuit formed for experiment 1

## Results and Discussion

Circuit shown in figure 6.4 was formed and a voltage of 260 mV peak to peak was obtained across the resistor, which corresponds to a current of 0.260 mA. By using equation (6.1) the value of capacitance found to be 20.6901 pF/cm. As the length of metal plates is 20 cm, so to convert the capacitance into standard units the obtained value is multiplied by 5, to get the capacitance in F/m. So the final value of capacitance obtained was 104.8107 pF/m. Table 6.1 is summarizing the values of capacitance obtained for an empty waveguide by theoretical, numerical and experimental methods.

| Theoretical | Finite Difference Method | Inclined Plate Capacitance Method | Experimental |
|---|---|---|---|
| 99.9621 pF/m | 103.4256 pF/m | 104.9481 pF/m | 104.8107 pF/m |

Table 6.1: Values of capacitance obtained for an empty circular waveguide when plates were put inside the tube

It can be seen clearly from the table that the results obtained from theoretical formulation, inclined plate capacitance method and finite difference method are very close to experimental results. So this experiment is a success and we conclude that inclined plate capacitance method and finite difference method can be used for multiphase flow as well.

## 6.2 Experiment 2: Capacitance Measurement of an Air Filled Waveguide when Metal Plates Were Put Outside the Tube

This experiment was same as experiment 1. The only difference was the position of metal plates. For this experiment the metal plates were put outside the tube as shown in figure below. To measure the capacitance similar procedure is applied and circuit shown in figure 6.4 is implemented and current flowing through circuit and voltage across the tube is measured. The results obtained are discussed below.
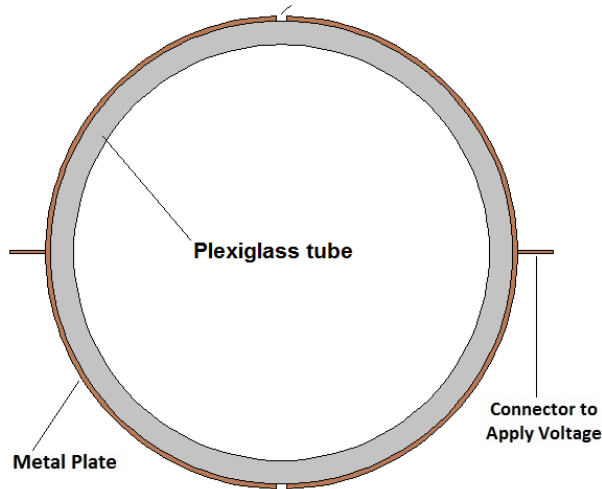
Figure 6.5: Cross Section of Plexiglass tube with metal plates outside

## Results and Discussion

Circuit shown in figure 6.4 was formed and a voltage of 290 mV peak to peak was obtained across the resistor, which corresponds to a current of 0.290 mA. By using equation (6.1) the value of capacitance found to be 23.4170 pF/cm. As the length of metal plates is 20 cm, so to convert the capacitance into standard units the obtained value is multiplied by 5, to get the capacitance in F/m. So the final value of capacitance obtained was 117.0850 pF/m. Table 6.2 is summarizing the values of capacitance obtained for an empty waveguide by theoretical, numerical and experimental methods.

| Theoretical | Finite Difference Method | Inclined Plate Capacitance Method | Experimental |
|---|---|---|---|
| 117.2963 pF/m | 116.4145 pF/m | 117.6923 pF/m | 117.0850 pF/m |

Table 6.2: Values of capacitance obtained for an empty circular waveguide when plates were put outside the tube

74

The value of capacitance obtained in this case is higher than the experiment 1, which was expected. As the plexiglass has a dielectric constant of around 3.2 and this higher value of dielectric constant is leading to higher value of capacitance. It is clear from table that, the values of capacitance obtained from different techniques are very close to experimental values.

## 6.3    Experiment 3: Measurement of Dielectric Constant of Lubricating Oil and Distilled Water

To measure the dielectric constant of lubricating oil, same tube is used which was used for experiment 1. As we know the capacitance of tube when it is completely empty and plates are put inside. So if we fill it completely with the lubricating oil or distilled water, then the capacitance will increase by a constant factor, that will be the dielectric constant of that that particular material which is inside the tube. By using this simple idea, the experiment is carried out, the tube was first completely filled with distilled water. The circuit shown in figure 6.4 was formed. An input voltage of 20 V peak to peak was applied and current and voltage across the tube is measured. Then removed all the water from tube, dried it completely and same procedure was repeated for lubricating oil. The results for this experiment are given on below.

### Results and Discussion

When the tube was completely filled with distilled water and 20 volt peak to peak voltage at 100 KHz was applied, the voltage across 1000 ohm resistor was measured to be 7.8 V peak to peak initially, but it increased gradually and stabled at 9.95 V peak to peak. By considering 10.14 volts peak to peak across the resistor the value of capacitance will be

8.1837 nF/m. As the capacitance of this empty tube was 104.8107 pF/m (as given in table 6.1) so by using these two values of capacitances the dielectric came out be 78.10, which is the normal value of distilled water at room temperature. Similarly when the tube was filled completely with lubricating oil, 610mV peak to peak voltage across the resistor was measured, which gives the value of capacitance around 250.3468 pF/m. Thus by using this value of capacitance we concluded that the dielectric constant of lubricating oil is around 2.39. The same values of dielectric constants for distilled water and lubricating oil are used in future calculations.

## 6.4    Experiment 4: Measurement of Conductivity of Saline Water

When oil is pumped from production wells, it contains saline water along with oil and gas, and saline water has some conductivity. So it is important to know the exact value of conductivity of saline water. For this purpose we designed a tube which is shown in figure 6.1. And measured the conductivity of different samples of water. These samples included distilled water, tap water and saline water. Salinity of water is increased by adding salt into it. If we have a tube length of $l$ cm, its area $A$, and resistance $R$, when it is filled with water. Then conductivity of water in Siemens per meter (S/m) is given as:

$$Conductivity = \frac{l}{R.A} \ S/m \qquad (6.2)$$

The tube was completely filled with the distilled water first, series circuit of tube and 1000 ohm resistor is formed and resistance of tube is measured by applying an input voltage. Then a sample of 300 ml of tap water was taken and repeated the experiment to measure the conductivity of tap water. The different amount of salt was added to same 300

ml of water and repeated the experiment several times to obtain the value of conductivity for each level of salinity.

### Results and Discussion

As we were using a circular with a length of 20 cm and radius of 1.1 cm. So in equation (6.2) $l = 0.2m$ and $A = \pi r^2 = \pi(0.011)^2 = 3.80 \times 10^{-4} m^2$. Then 300 ml of tap water was taken and 5, 10, 20, 30, 40 and 50 grams of salt added to it and conductivity for each case was obtained. The results are given in table below.

| Water Type | Amount of Salt added | Measured Resistance | Conductivity |
|---|---|---|---|
| Distilled Water | -- | 9.17 MΩ | 57.3618 µS/m |
| 300 ml of Tap Water | 0 g | 1233.3 Ω | 0.426 S/m |
| | 5 g | 387.81 Ω | 1.3595 S/m |
| | 10 g | 263.63 Ω | 1.9956 S/m |
| | 20 g | 194.11 Ω | 2.7103 S/m |
| | 30 g | 163.16 Ω | 3.2247 S/m |
| | 40 g | 150.00 Ω | 3.5057 S/m |
| | 50 g | 138.10 Ω | 3.8199 S/m |

Table 6.3: Conductivity of different types of water

It can be seen from results that conductivity of distilled water is very low. And as the salinity of water is increasing, the conductivity is increasing which was expected. For further experiments when the plates were put inside the tube distilled water was used and

when plates were put outside the tube, saline water with a conductivity of 3.82 S/m was used.

## 6.5 Experiment 5: Measurement of Capacitance When Plates Were Put Inside and Tube Was Partially Filled With Two Dielectrics

For this experiment a plexiglass tube with an inner radius of 4.375 cm and tube thickness of 0.5 cm was used. Two metal plates of length 20 cm each were put inside the tube, the gap between plates set to be 1mm, cross section of such a tube is shown in figure below. Distilled water and air were considered as two dielectrics. The circuit shown in figure 6.4 was implemented and capacitance is measured by changing the level of water. Then the values of capacitance are generated by finite difference method and inclined plates capacitance method for each case and experimental values are compared with numerical and theoretical values. The details of results are given below.

### Results and Discussion

The circuit shown in figure 6.4 was implemented and an input voltage of 20 volts peak to peak at 100 KHz was applied. Then capacitance was calculated by measuring the current flowing through circuit and voltage across the tube. The amount of water was increased from $5^0$ to $45^0$ with a step size of $5^0$ and capacitance was measured for each level of water. The dielectric constants for air and water were considered to be 1 and 78 respectively. The results obtained from this experiment are given below.
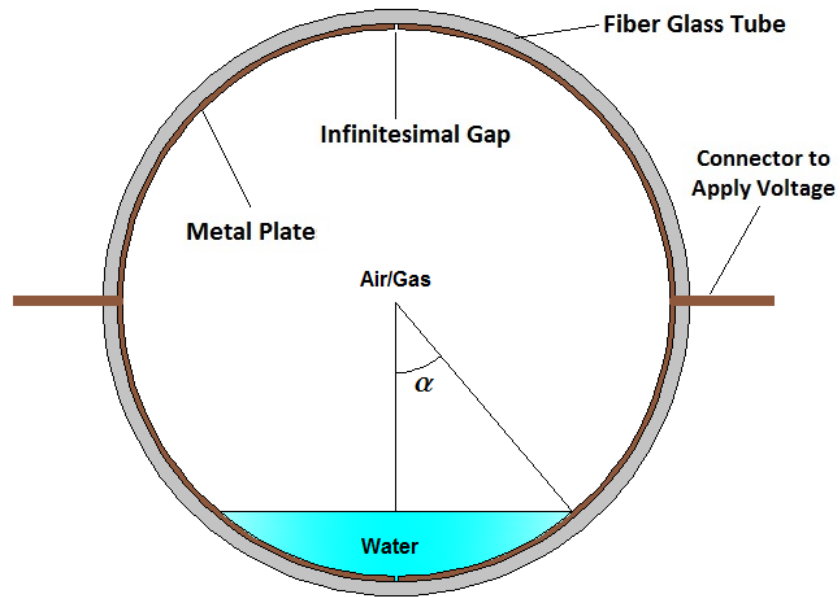
Figure 6.6: Cross section of plexiglass tube used for experiment 5

| Water Angle | Value of Capacitance | | |
| --- | --- | --- | --- |
| | Finite Difference Method pF/m | Inclined Plate Capacitance Method pF/m | Experimental Value pF/m |
| $0^0$ | 103.4256 | 104.9481 | 103.45 |
| $5^0$ | 392.4060 | 428.8905 | -- |
| $10^0$ | 598.1813 | 591.3443 | -- |
| $15^0$ | 679.8914 | 691.5962 | 720 |
| $20^0$ | 746.2875 | 766.4832 | 750 |
| $25^0$ | 804.9675 | 827.5606 | 780 |
| $30^0$ | 885.3698 | 879.9852 | 880 |
| $35^0$ | 910.9373 | 926.5170 | 908 |
| $40^0$ | 960.9389 | 968.8121 | 934 |
| $45^0$ | 999.9870 | 1001.9477 | 958 |

Table6.4: Comparison between capacitance values obtained from FDM, IPC and

experiments when tube was partially filled with two dielectric and plates were put inside
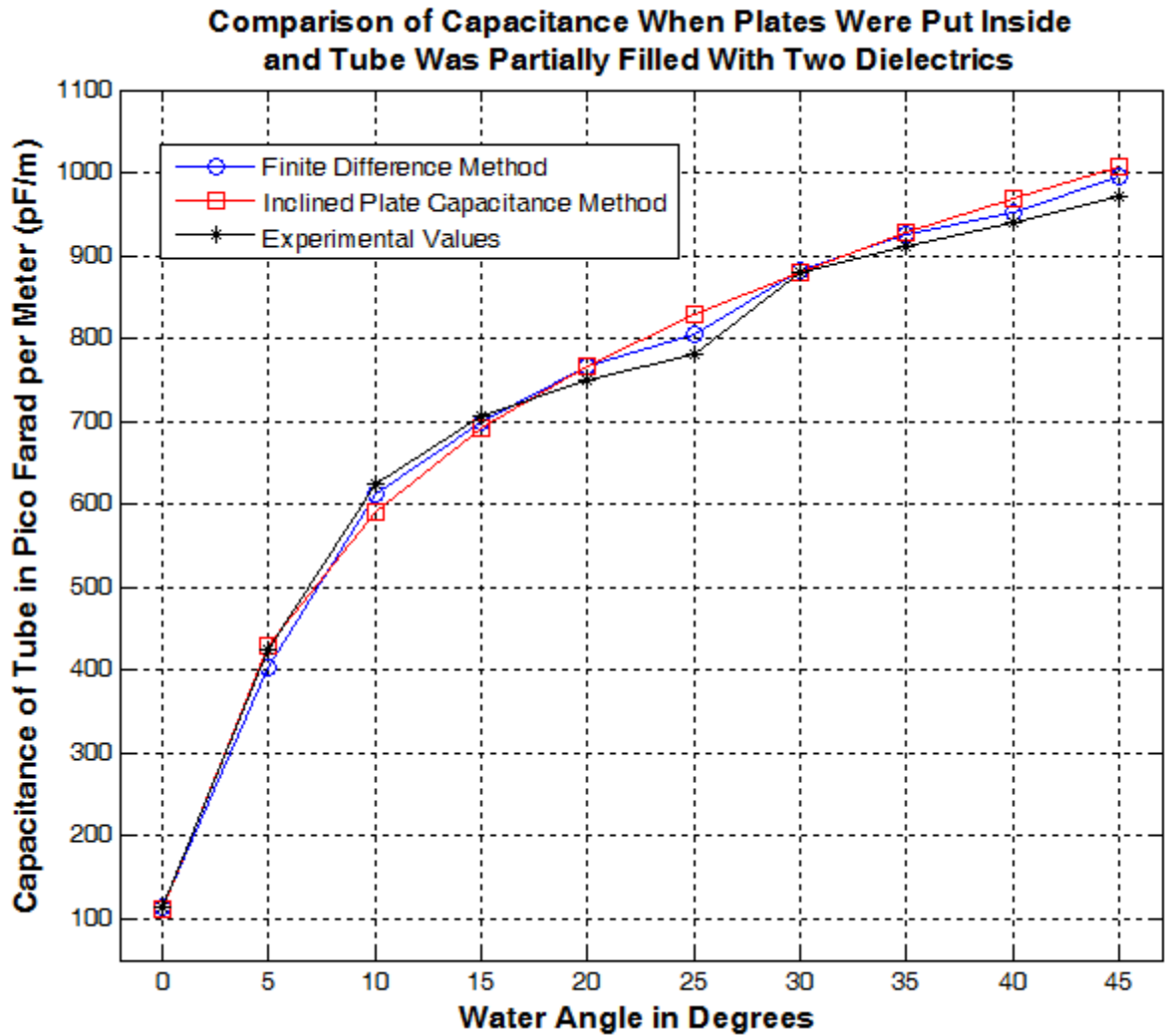
Figure 6.7: Comparison between capacitance values obtained from FDM, IPC and experiments, when tube was partially filled with two dielectric and plates were put inside

It is clear from table 6.4 and figure 6.7 that the experimental values are very close to values obtained by finite difference method and inclined plate capacitance method. We were unable to take the values at $5^0$ and $10^0$ of water, because at those angle of water, the amount of water was very less and hence accurate readings were not obtained. But the curve is extended up to $0^0$ of water and it is matching with the numerical and theoretical values.

## 6.6 Experiment 6: Measurement of Capacitance When Plates Were Put Inside and Tube Was Partially Filled With Three Dielectrics

This experiment was same as the experiment 5, the only difference was the number of dielectrics. For this case, water, oil and gas were considered as dielectrics. The dielectric constants for saline water, oil and gas were 78, 2.4 and 1 respectively. The cross section of a tube containing these three dielectrics is shown in figure below. To take the values for different levels of water and gas, the level of water was fixed and values were taken at different levels of gas. Then water level changed to another value and several values for gas level were taken. In this way water level was changed from $15^0$ to $45^0$ and for each level of water gas level changed from $15^0$ to $45^0$. In this way total 49 values of capacitance were measured. The results are given on next page.
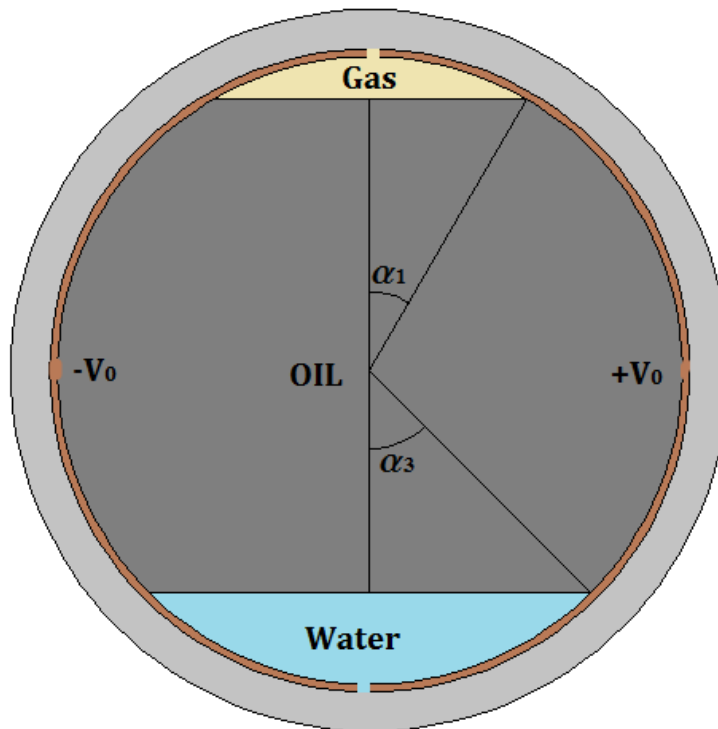


Figure 6.8: Cross section of plexiglass tube used for experiment 6

## Results and Discussion

The experiment was done with the same circuit as shown in figure 6.4. 20 volts peak to peak input voltage is applied and current through circuit and voltage across tube was measured. The experiment was repeated several times. Each time the angle of water was fixed and angle of gas changed from $15^0$ to $45^0$. The results obtained for each case are given below in the form of tables and graphs.

| Water Angle = $\alpha_3 = 5^0$ | | |
|---|---|---|
| **Gas Angle**<br>$\alpha_1$ | **Finite Difference Method**<br>**pF/m** | **Inclined Plate Capacitance Method**<br>**pF/m** |
| $5^0$ | 461.5534 | 464.7732 |
| $10^0$ | 459.1265 | 462.0305 |
| $15^0$ | 457.2278 | 460.3379 |
| $20^0$ | 456.0285 | 459.0736 |
| $25^0$ | 455.3641 | 458.0424 |
| $30^0$ | 454.7102 | 457.1573 |
| $35^0$ | 453.0247 | 456.3717 |
| $40^0$ | 452.1591 | 455.6576 |
| $45^0$ | 451.6985 | 454.9969 |

Table 6.5: Comparison between capacitance values obtained from FDM and IPC when tube was partially filled with three dielectrics and plates were put inside at $\alpha_3=5^0$

| Water Angle $\alpha_3$ | Gas Angle $\alpha_1$ | Finite Difference Method pF/m | Inclined Plate Capacitance Method pF/m | Experimental Value pF/m |
|---|---|---|---|---|
| $\alpha_3=10^0$ | $5^0$ | 620.8625 | 624.2732 | |
| | $10^0$ | 617.5206 | 621.5305 | |
| | $15^0$ | 616.3587 | 619.8379 | |
| | $20^0$ | 615.9182 | 618.5736 | |
| | $25^0$ | 614.1025 | 617.5424 | |
| | $30^0$ | 613.0256 | 616.6573 | |
| | $35^0$ | 612.1264 | 615.8717 | |
| | $40^0$ | 611.2510 | 615.1577 | |
| | $45^0$ | 610.3180 | 614.4969 | |
| $\alpha_3=15^0$ | $5^0$ | 720.0372 | 722.7023 | -- |
| | $10^0$ | 717.3550 | 719.9596 | -- |
| | $15^0$ | 715.7381 | 718.2671 | 720.28 |
| | $20^0$ | 714.1593 | 717.0027 | |
| | $25^0$ | 712.6527 | 715.9716 | 717.86 |
| | $30^0$ | 711.7360 | 715.0865 | |
| | $35^0$ | 710.0215 | 714.3009 | 715.67 |
| | $40^0$ | 709.1268 | 713.5868 | |
| | $45^0$ | 708.3504 | 712.9261 | 713.49 |

Table 6.6: Comparison between capacitance values obtained from FDM, IPC and experiments when tube was partially filled with three dielectrics and plates were put inside at $\alpha_3=10^0$ and $15^0$

| Water Angle $\alpha_3$ | Gas Angle $\alpha_1$ | Finite Difference Method pF/m | Inclined Plate Capacitance Method pF/m | Experimental Value pF/m |
|---|---|---|---|---|
| $\alpha_3=20^0$ | $5^0$ | 793.5541 | 796.2278 | -- |
| | $10^0$ | 790.3614 | 793.4851 | -- |
| | $15^0$ | 788.9654 | 791.7925 | |
| | $20^0$ | 787.3253 | 790.5282 | 791.80 |
| | $25^0$ | 786.2011 | 789.4970 | |
| | $30^0$ | 785.3580 | 788.6119 | 790.25 |
| | $35^0$ | 784.1011 | 787.8263 | 789.17 |
| | $40^0$ | 783.4236 | 787.1123 | |
| | $45^0$ | 782.1540 | 786.4515 | 787.03 |
| $\alpha_3=25^0$ | $5^0$ | 854.0147 | 856.1947 | -- |
| | $10^0$ | 851.3641 | 853.4520 | -- |
| | $15^0$ | 848.7598 | 851.7595 | |
| | $20^0$ | 847.1534 | 850.4951 | 853.06 |
| | $25^0$ | 846.0736 | 849.4640 | |
| | $30^0$ | 845.2581 | 848.5789 | 850.83 |
| | $35^0$ | 844.3645 | 847.7933 | |
| | $40^0$ | 843.5147 | 847.0792 | 848.68 |
| | $45^0$ | 842.6248 | 846.4185 | 847.16 |

Table 6.7: Comparison between capacitance values obtained from FDM, IPC and

experiments when tube was partially filled with three dielectrics and plates were put

inside at $\alpha_3=20^0$ and $25^0$

| Water Angle $\alpha_3$ | Gas Angle $\alpha_1$ | Finite Difference Method pF/m | Inclined Plate Capacitance Method pF/m | Experimental Value pF/m |
|---|---|---|---|---|
| $\alpha_3=30^0$ | $5^0$ | 906.1835 | 907.6662 | -- |
| | $10^0$ | 903.5647 | 904.9235 | -- |
| | $15^0$ | 901.8670 | 903.2309 | 903.89 |
| | $20^0$ | 899.5725 | 901.9666 | |
| | $25^0$ | 898.6864 | 900.9354 | 898.96 |
| | $30^0$ | 896.9964 | 900.0503 | |
| | $35^0$ | 896.0143 | 899.2647 | 896.99 |
| | $40^0$ | 895.3172 | 898.5506 | |
| | $45^0$ | 894.5201 | 897.8899 | 895.78 |
| $\alpha_3=35^0$ | $5^0$ | 952.6512 | 953.3519 | -- |
| | $10^0$ | 949.4501 | 950.6092 | -- |
| | $15^0$ | 947.0072 | 948.9166 | 947.65 |
| | $20^0$ | 946.2563 | 947.6523 | |
| | $25^0$ | 945.5428 | 946.6211 | 948.92 |
| | $30^0$ | 944.8614 | 945.7360 | 944.39 |
| | $35^0$ | 943.6257 | 944.9504 | |
| | $40^0$ | 942.8314 | 944.2363 | 942.71 |
| | $45^0$ | 941.9108 | 943.5756 | 941.35 |

Table 6.8: Comparison between capacitance values obtained from FDM, IPC and experiments when tube was partially filled with three dielectrics and plates were put inside at $\alpha_3=30^0$ and $35^0$

| Water Angle $\alpha_3$ | Gas Angle $\alpha_1$ | Finite Difference Method pF/m | Inclined Plate Capacitance Method pF/m | Experimental Value pF/m |
|---|---|---|---|---|
| $\alpha_3=40^0$ | $5^0$ | 992.7858 | 994.8780 | -- |
| | $10^0$ | 990.6541 | 992.1353 | -- |
| | $15^0$ | 988.8512 | 990.4427 | 992.47 |
| | $20^0$ | 987.4516 | 989.1784 | |
| | $25^0$ | 986.3569 | 988.1472 | 989.37 |
| | $30^0$ | 985.4521 | 987.2621 | |
| | $35^0$ | 984.1235 | 986.4765 | 987.77 |
| | $40^0$ | 983.5234 | 985.7625 | |
| | $45^0$ | 982.6412 | 985.1017 | 984.49 |
| $\alpha_3=45^0$ | $5^0$ | 1031.1891 | 1033.3021 | -- |
| | $10^0$ | 1029.6541 | 1030.5593 | -- |
| | $15^0$ | 1026.9974 | 1028.8668 | 1030.56 |
| | $20^0$ | 1025.8615 | 1027.6024 | |
| | $25^0$ | 1025.6657 | 1026.5713 | 1027.81 |
| | $30^0$ | 1024.4569 | 1025.6862 | |
| | $35^0$ | 1023.2189 | 1024.9006 | 1025.67 |
| | $40^0$ | 1022.1189 | 1024.1865 | |
| | $45^0$ | 1021.6487 | 1023.5258 | 1024.15 |

Table 6.9: Comparison between capacitance values obtained from FDM, IPC and experiments when tube was partially filled with three dielectrics and plates were put inside at $\alpha_3=40^0$ and $45^0$
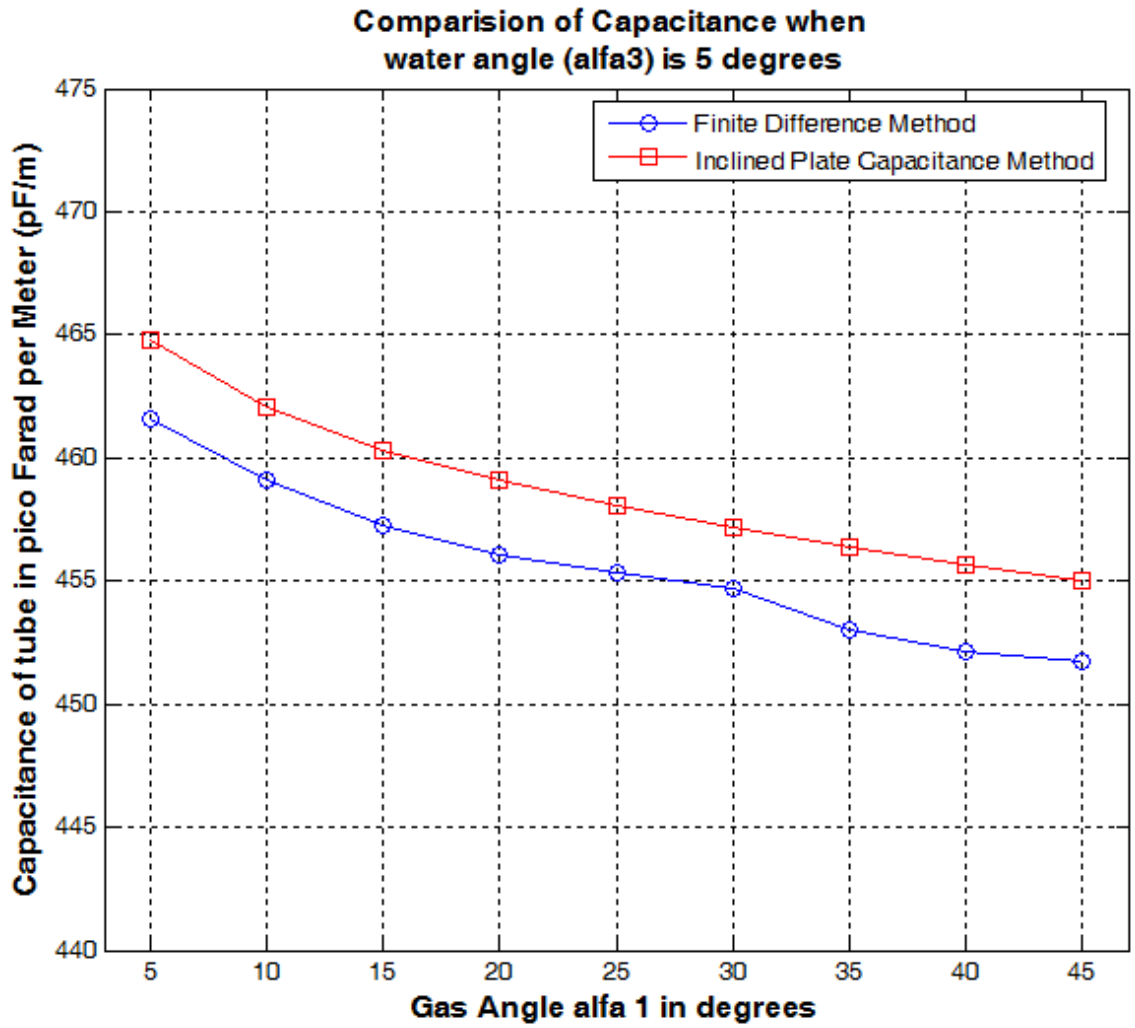
Figure 6.9: Comparison between capacitance values obtained from FDM and IPC when tube was partially filled with three dielectric and plates were put inside at $\alpha_3 = 5^0$
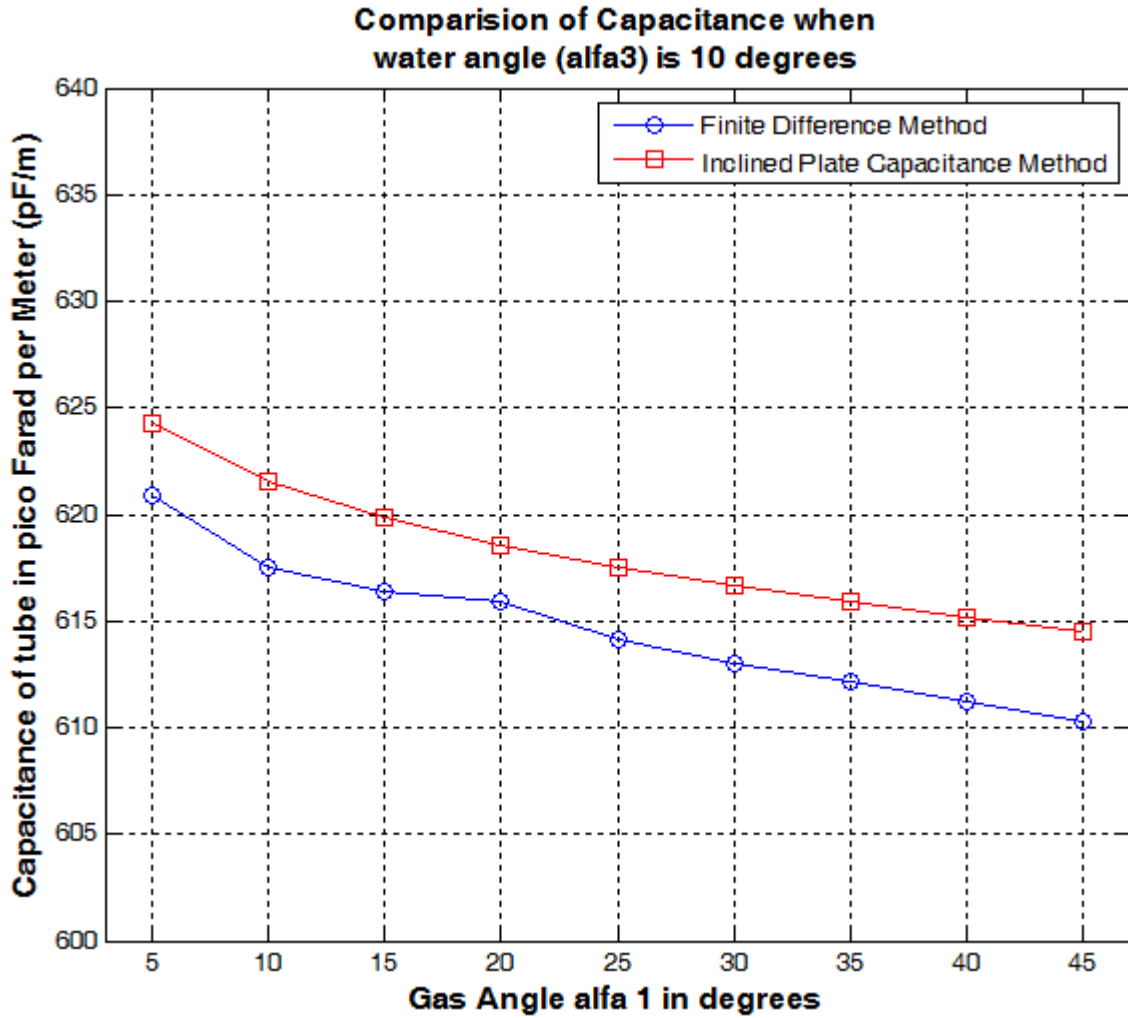
Figure 6.10: Comparison between capacitance values obtained from FDM and IPC when

tube was partially filled with three dielectric and plates were put inside at $\alpha_3=10^0$
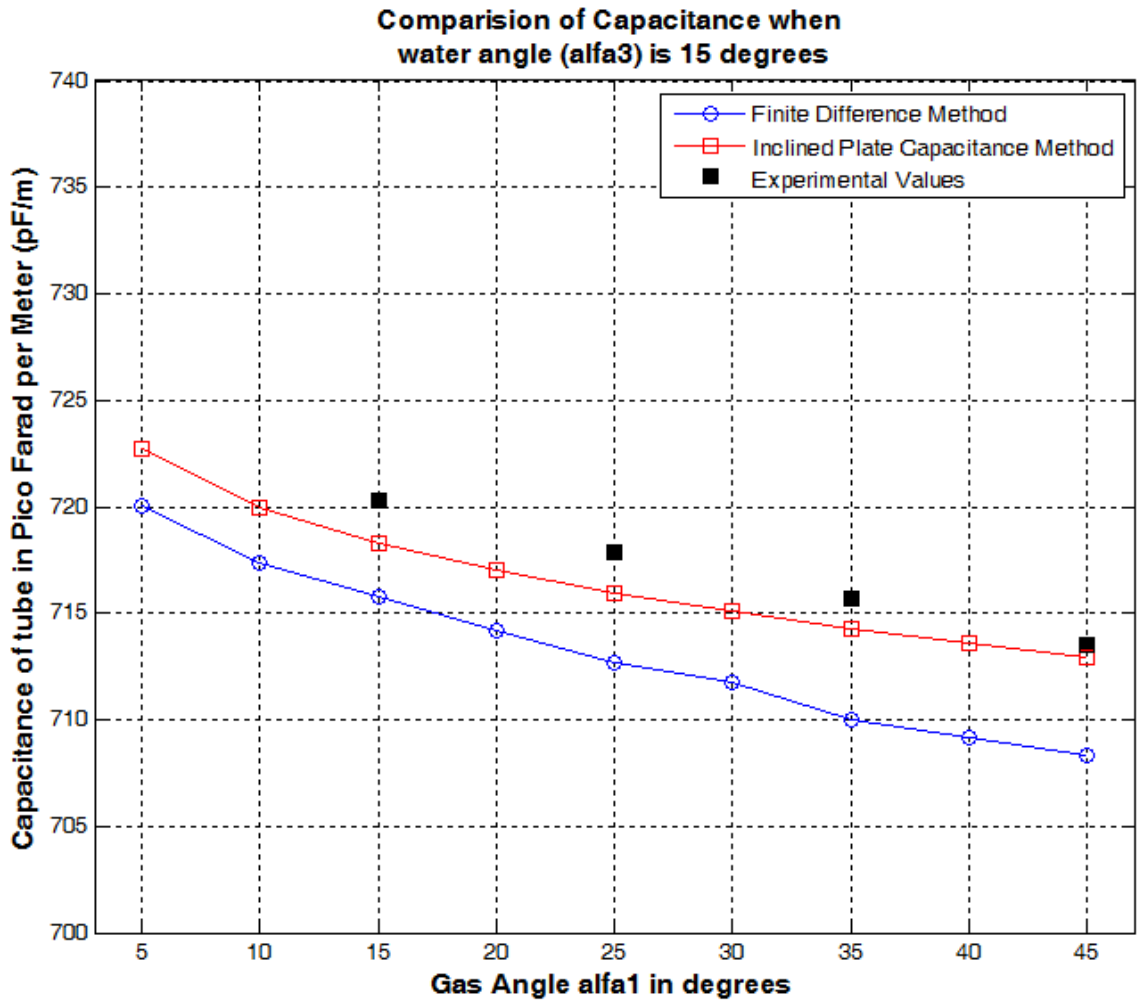
Figure 6.11: Comparison between capacitance values obtained from FDM, IPC and Experiments when tube was partially filled with three dielectric and plates were put inside at $\alpha_3=15^0$
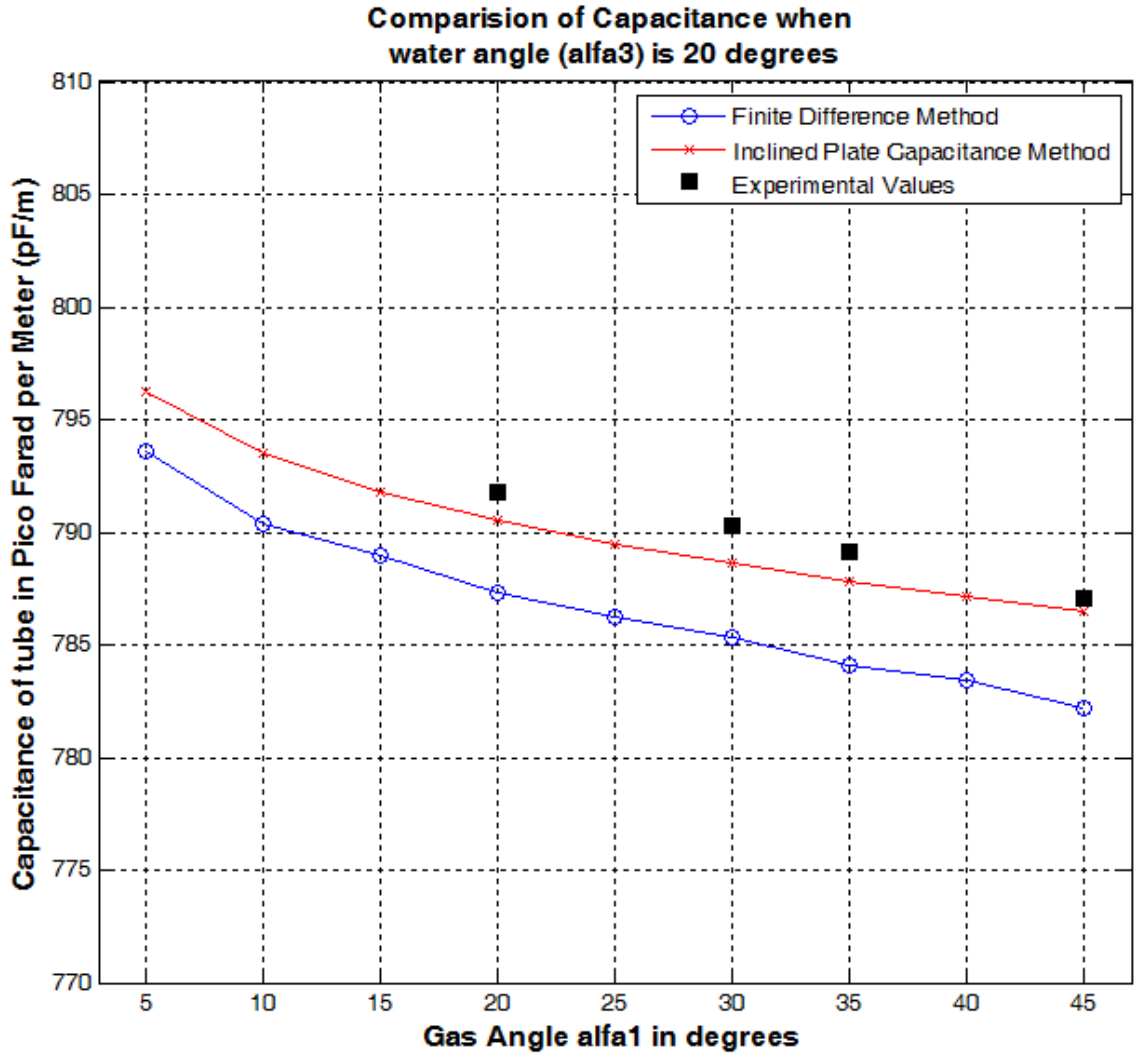
Figure 6.12: Comparison between capacitance values obtained from FDM, IPC and

Experiments when tube was partially filled with three dielectric and plates were put
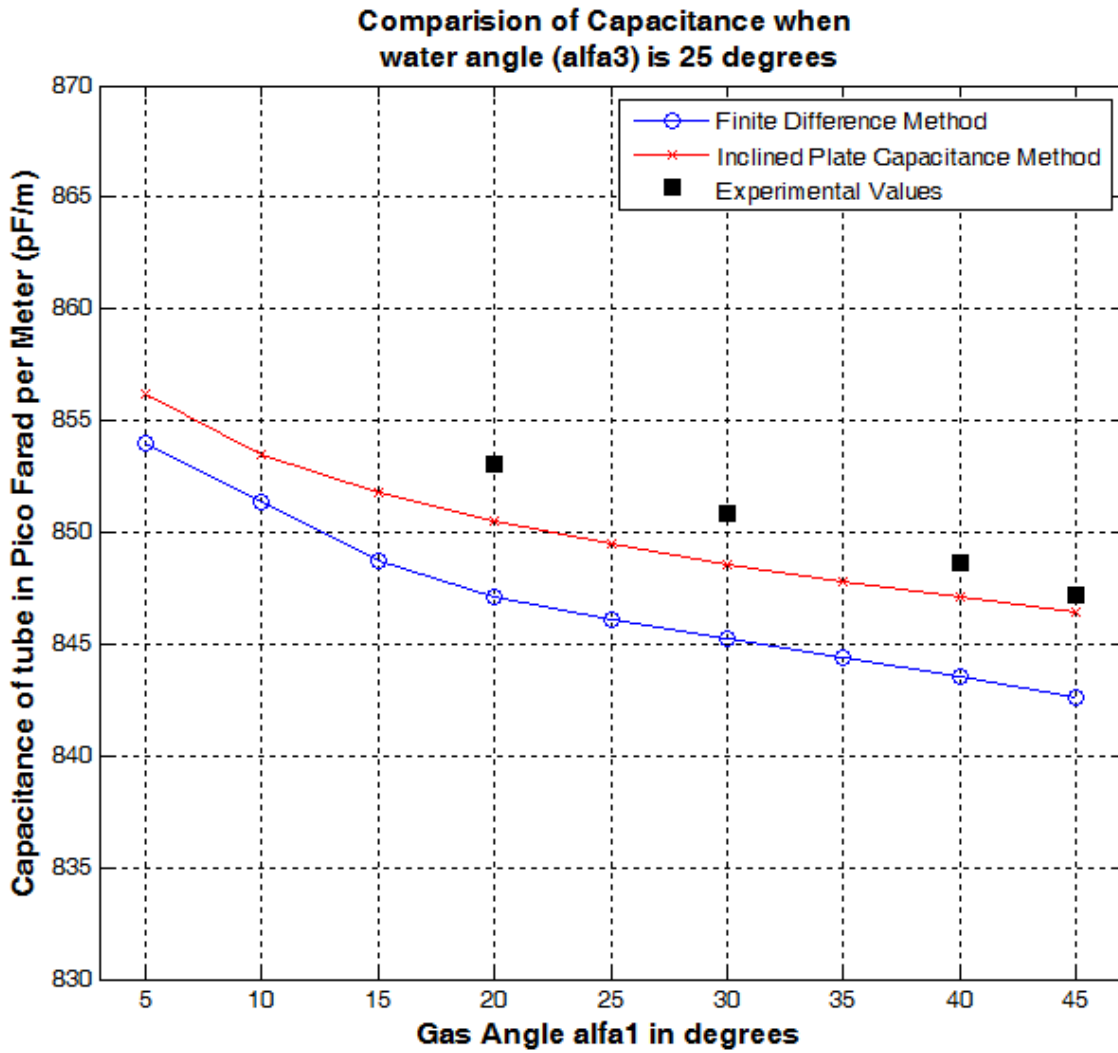
inside at $\alpha_3 = 20^0$

Figure 6.13: Comparison between capacitance values obtained from FDM, IPC and Experiments when tube was partially filled with three dielectric and plates were put inside at $\alpha_3 = 25^0$
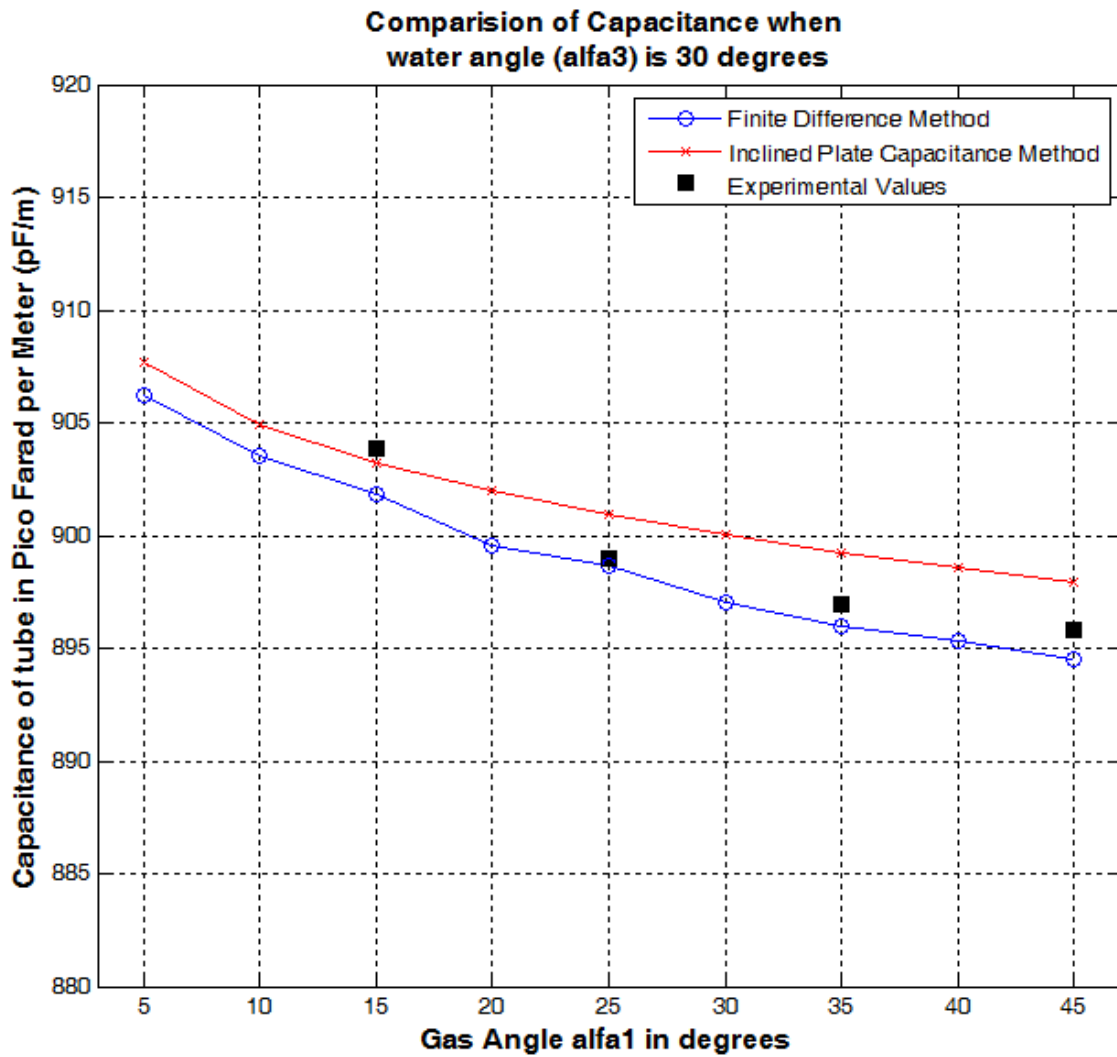
Figure 6.14: Comparison between capacitance values obtained from FDM, IPC and Experiments when tube was partially filled with three dielectric and plates were put inside at $\alpha_3=30^0$
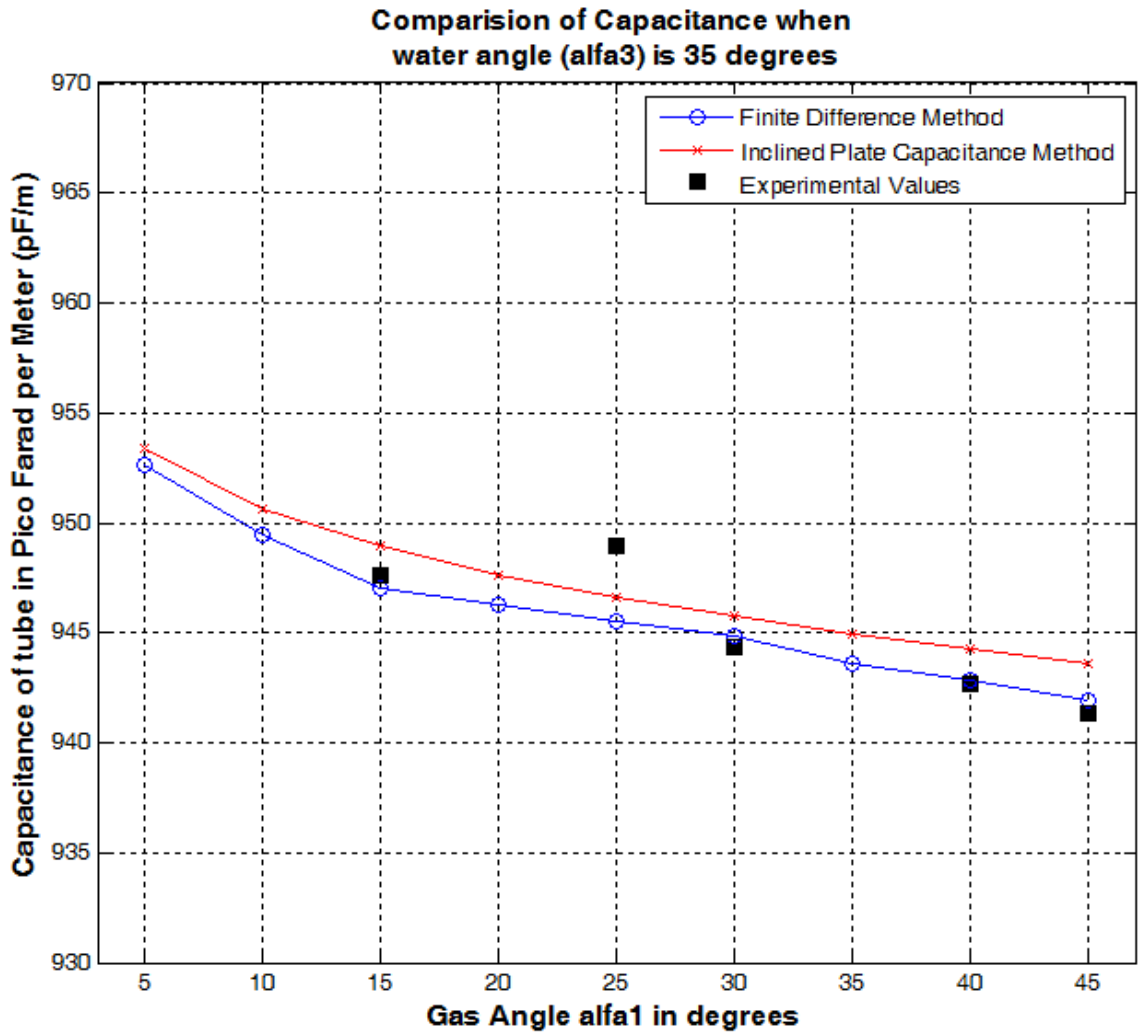
Figure 6.15: Comparison between capacitance values obtained from FDM, IPC and Experiments when tube was partially filled with three dielectric and plates were put inside at $\alpha_3=35^0$
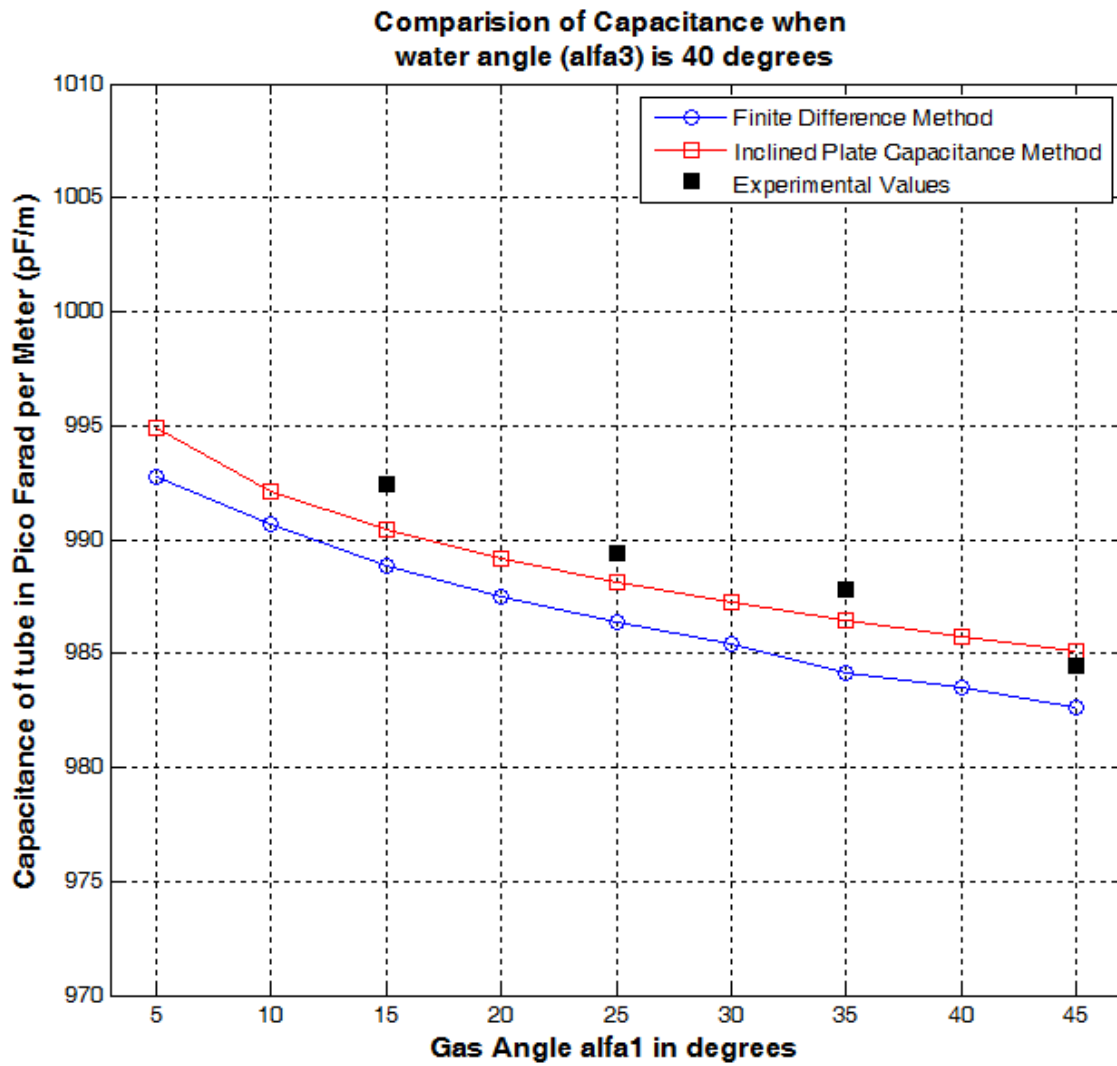
Figure 6.16: Comparison between capacitance values obtained from FDM, IPC and

Experiments when tube was partially filled with three dielectric and plates were put

inside at $\alpha_3=40^0$

Figure 6.17: Comparison between capacitance values obtained from FDM, IPC and Experiments when tube was partially filled with three dielectric and plates were put inside at $\alpha_3 = 45^0$

It is clear from the tables and graphs that for each pair of $\alpha_1$ and $\alpha_3$ a unique value of capacitance exists. So by measuring the capacitance of tube one can easily tell that what the heights of individual substances in the tube are. For example if the capacitance is measured and it came out to be 945 pF/m, then from table and graph we can tell that in this case the angles $\alpha_1$ and $\alpha_3$ are $30^0$ and $35^0$ respectively. Which means that in this case the tube is carrying 92.6 % oil, 4.48 % saline water and 2.92 % gas.

## 6.7    Experiment 7: Measurement of Capacitance When Plates Were Put Outside and Tube Was Partially Filled With Two Dielectrics

This experiment was similar to experiment 5. The only difference was position of plates. In this case the plates were put outside the tube. The tube used in this case had a radius of 4.375 cm and tube thickness of 0.5 cm. The length of each metal plate was 20 cm and those plates were separated by a distance of 1 mm. The cross section of such a tube is shown in figure below.
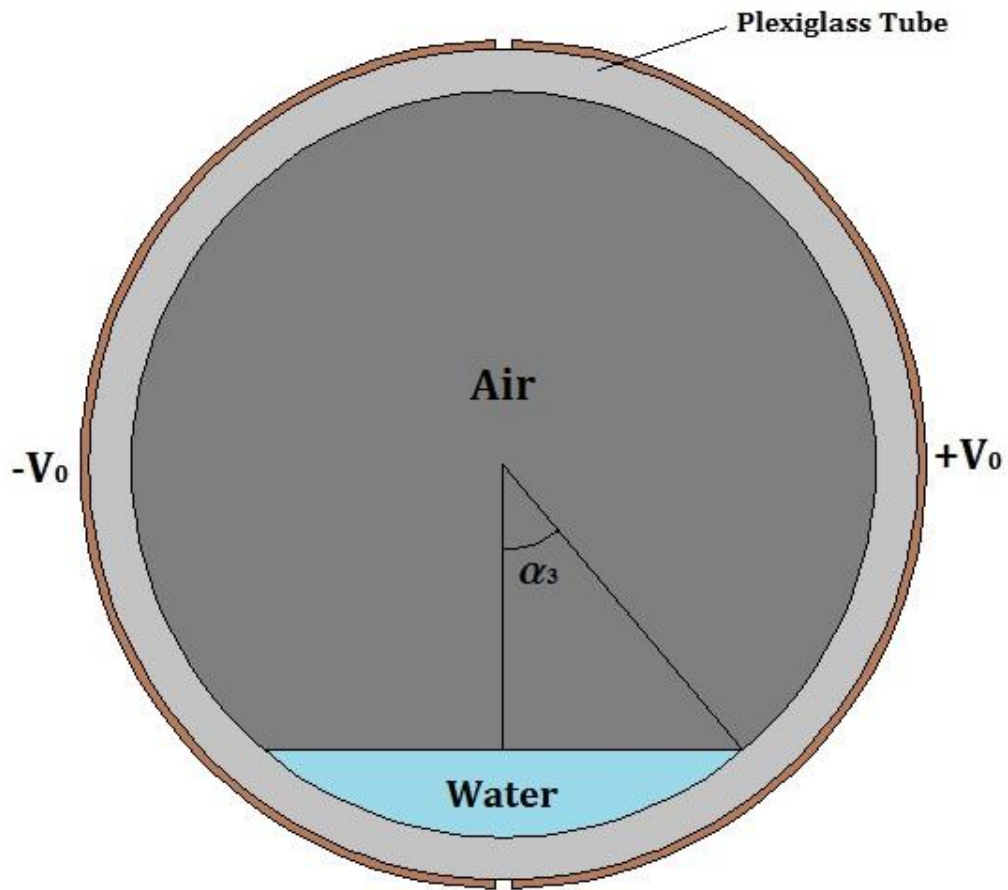


Figure 6.18: Cross section of tube used in experiment 7

The experiment was conducted by putting different levels of saline water, and capacitance was measured for each level of water. The results are given below.

## Results and Discussion

The experimental setup for this case is shown in figure below. A 20 volts peak to peak signal at a frequency of 100 KHz was applied through a function generator. And series circuit is formed as shown in figure 6.4. Then the current flowing through circuit and voltage across the tube was measured by using an oscilloscope. Dielectric constants of saline water and plexiglass were taken 78 and 3.2 respectively. Like experiment 5, in this case the water angle varied from $15^0$ to $45^0$. Because at $5^0$ and $10^0$ the amount of water is too small and an accurate reading was not obtained. The result are given below in the form of table and graph.
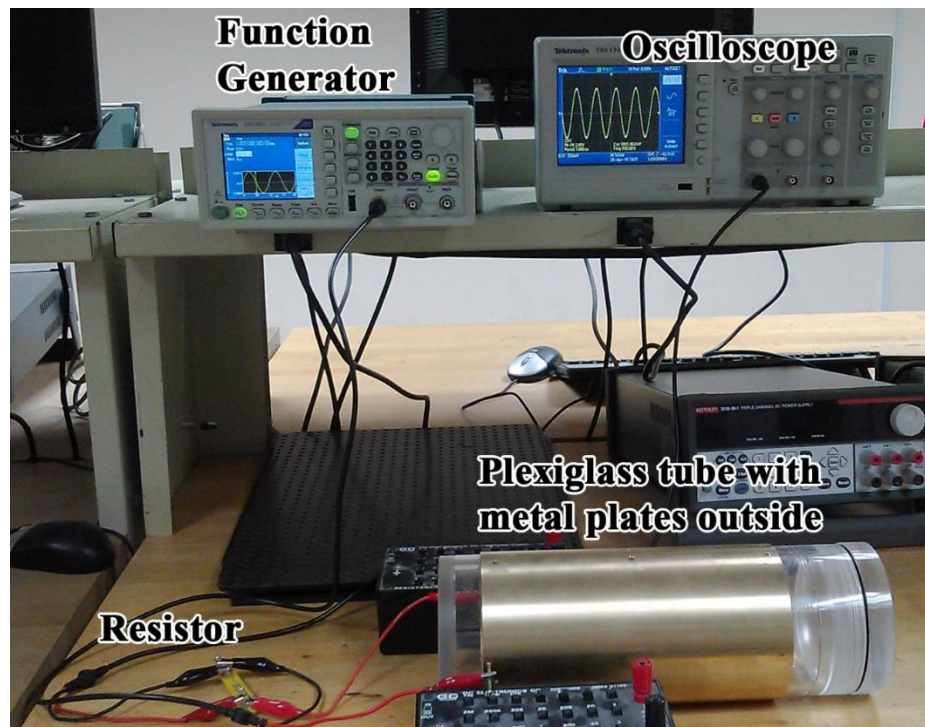


Figure 6.19: Experimental setup for experiment 7

| Water Angle | Value of Capacitance | | |
|---|---|---|---|
| | Finite Difference Method | Inclined Plate Capacitance Method | Experimental Value |
| $0^0$ | 117.26 | 116.32 | 117.68 |
| $5^0$ | 134.62 | 135.48 | - |
| $10^0$ | 142.21 | 144.18 | - |
| $15^0$ | 154.44 | 156.47 | 159.10 |
| $20^0$ | 168.29 | 166.86 | 170.69 |
| $25^0$ | 180.28 | 176.81 | 181.89 |
| $30^0$ | 190.02 | 185.54 | 189.83 |
| $35^0$ | 198.62 | 194.76 | 196.51 |
| $40^0$ | 205.38 | 203.81 | 205.72 |
| $45^0$ | 214.75 | 212.71 | 215.78 |

Table 6.10: Comparison between capacitance values obtained from FDM, IPC and experiments when tube was partially filled with two dielectrics and plates were put outside
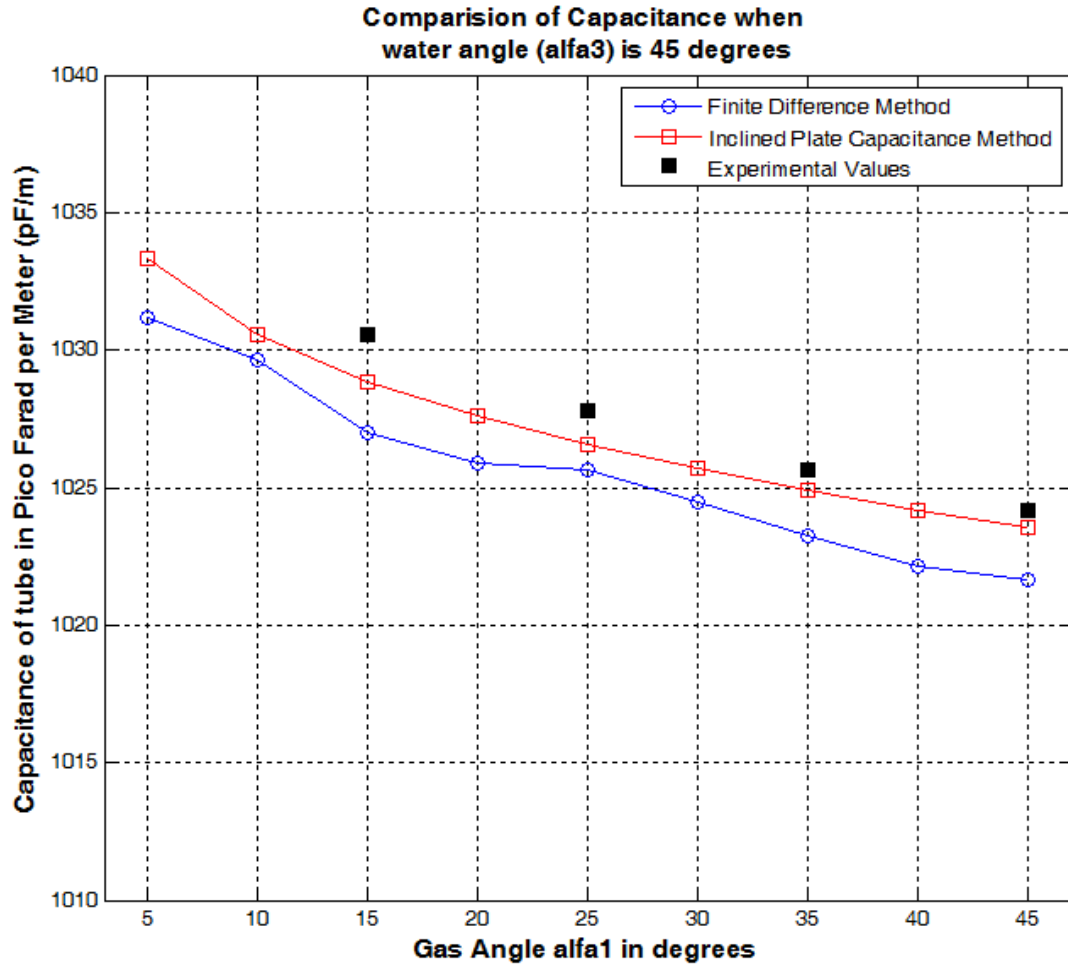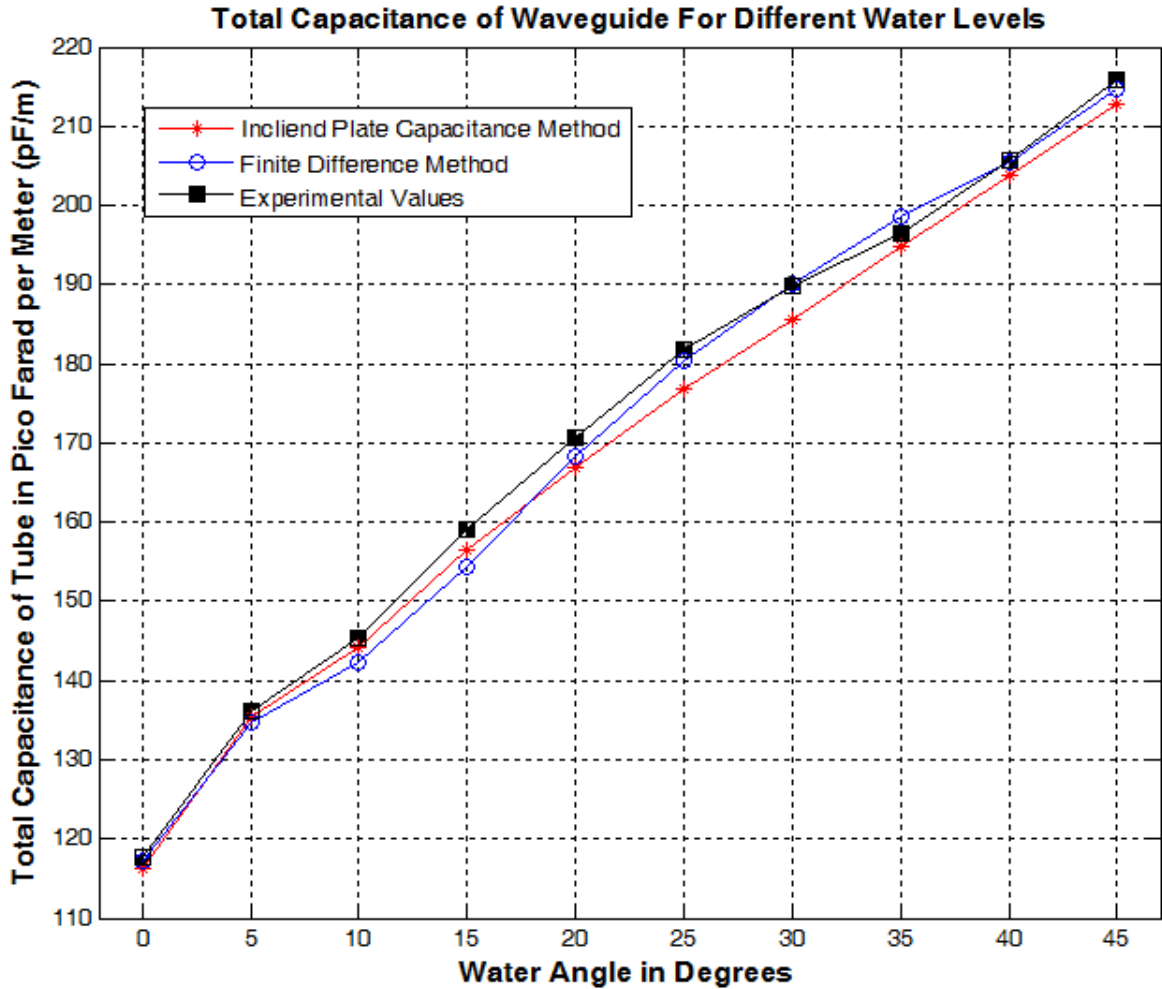
Figure 6.20: Comparison between capacitance values obtained from FDM, IPC and experiments, when tube was partially filled with two dielectric and plates were put outside

In this case the change in capacitance is much lower different than experiment 5. And this result was expected, because the plexiglass tube also has a capacitance which is combining in series with the total capacitance of tube, thus overall change in capacitance due to increase in water level will not be large. Moreover the values generated by finite difference method and inclined plate capacitance method are also very close to experimental results, which indicate the success of experiment.

## 6.8 Experiment 8: Measurement of Capacitance When Plates Were Put Outside and Tube Was Partially Filled With Three Dielectrics

This experiment was same as the experiment 6. The only difference was the position of copper plates. In this experiment the metal plates were put outside the tube. For this case, saline-water, oil and gas were considered as dielectrics. The dielectric constants for saline water, oil and gas were 78, 2.4 and 1 respectively. The cross section of a tube containing these three dielectrics is shown in figure below. To take the values for different levels of water and gas, the same procedure is followed as experiment 6. The results are given on next page.
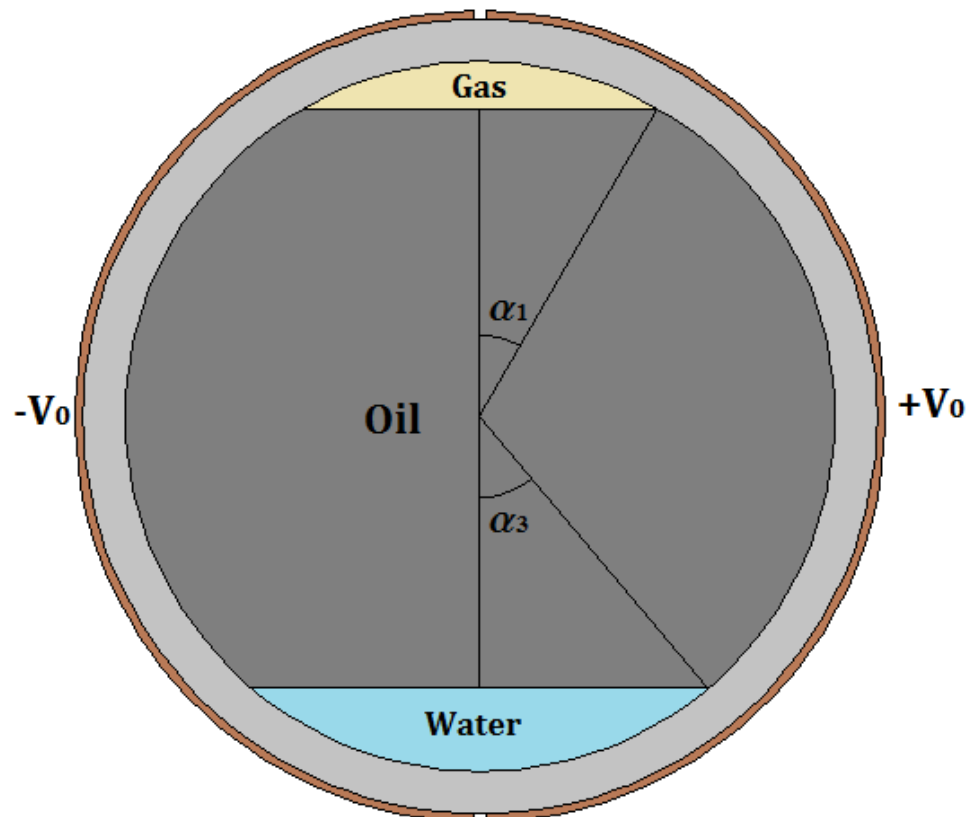


Figure 6.21: Cross section of plexiglass tube used for experiment 8

### Results and Discussion

The experiment was done with the same circuit as shown in figure 6.4. 20 volts peak to peak input voltage is applied and current through circuit and voltage across tube was measured. The experiment was repeated several times. Each time the angle of water was fixed and angle of gas changed from $15^0$ to $45^0$. The results obtained for each case are given below in the form of tables and graphs.

| Water Angle = $\alpha_3 = 5^0$ | | |
|---|---|---|
| **Gas Angle $\alpha_1$** | **Finite Difference Method pF/m** | **Inclined Plate Capacitance Method pF/m** |
| $5^0$ | 161.23 | 159.10 |
| $10^0$ | 160.10 | 158.36 |
| $15^0$ | 159.25 | 157.97 |
| $20^0$ | 158.42 | 157.16 |
| $25^0$ | 157.16 | 156.46 |
| $30^0$ | 156.52 | 155.65 |
| $35^0$ | 155.76 | 154.67 |
| $40^0$ | 154.29 | 153.40 |
| $45^0$ | 152.77 | 151.48 |

Table 6.11: Comparison between capacitance values obtained from FDM and IPC when tube was partially filled with three dielectrics and plates were put outside at $\alpha_3=5^0$

| Water Angle $\alpha_3$ | Gas Angle $\alpha_1$ | Finite Difference Method pF/m | Inclined Plate Capacitance Method pF/m | Experimental Value pF/m |
|---|---|---|---|---|
| $\alpha_3=10^0$ | $5^0$ | 168.22 | 166.11 | |
| | $10^0$ | 167.51 | 165.58 | |
| | $15^0$ | 166.86 | 164.92 | |
| | $20^0$ | 165.99 | 164.17 | |
| | $25^0$ | 165.01 | 163.67 | |
| | $30^0$ | 164.24 | 162.82 | |
| | $35^0$ | 163.08 | 161.88 | |
| | $40^0$ | 162.11 | 160.61 | |
| | $45^0$ | 161.47 | 159.69 | |
| $\alpha_3=15^0$ | $5^0$ | 175.88 | 173.96 | -- |
| | $10^0$ | 174.96 | 173.41 | -- |
| | $15^0$ | 174.04 | 172.85 | 172.35 |
| | $20^0$ | 173.47 | 172.22 | 171.52 |
| | $25^0$ | 172.61 | 171.52 | 170.69 |
| | $30^0$ | 171.29 | 170.71 | 169.04 |
| | $35^0$ | 170.23 | 169.73 | 168.37 |
| | $40^0$ | 169.07 | 168.61 | 166.72 |
| | $45^0$ | 168.61 | 166.54 | 165.06 |

Table 6.12: Comparison between capacitance values obtained from FDM, IPC and experiments when tube was partially filled with three dielectrics and plates were put outside at $\alpha_3=10^0$ and $15^0$

| Water Angle $\alpha_3$ | Gas Angle $\alpha_1$ | Finite Difference Method pF/m | Inclined Plate Capacitance Method pF/m | Experimental Value pF/m |
|---|---|---|---|---|
| $\alpha_3=20^0$ | $5^0$ | 184.21 | 181.98 | -- |
| | $10^0$ | 183.62 | 181.34 | -- |
| | $15^0$ | 182.79 | 180.87 | 184.00 |
| | $20^0$ | 181.66 | 180.24 | 183.17 |
| | $25^0$ | 180.57 | 179.54 | 182.33 |
| | $30^0$ | 179.62 | 178.73 | 180.67 |
| | $35^0$ | 178.45 | 177.75 | 179.00 |
| | $40^0$ | 177.55 | 176.48 | 177.36 |
| | $45^0$ | 176.02 | 174.56 | 174.85 |
| $\alpha_3=25^0$ | $5^0$ | 194.66 | 192.32 | -- |
| | $10^0$ | 193.87 | 191.78 | -- |
| | $15^0$ | 193.01 | 191.20 | 194.01 |
| | $20^0$ | 192.57 | 190.58 | 193.17 |
| | $25^0$ | 191.36 | 189.88 | 192.34 |
| | $30^0$ | 190.15 | 189.06 | 191.51 |
| | $35^0$ | 188.87 | 188.09 | 189.84 |
| | $40^0$ | 187.61 | 186.81 | 188.17 |
| | $45^0$ | 185.36 | 184.89 | 186.50 |

Table 6.13: Comparison between capacitance values obtained from FDM, IPC and experiments when tube was partially filled with three dielectrics and plates were put outside at $\alpha_3=20^0$ and $25^0$

| Water Angle $\alpha_3$ | Gas Angle $\alpha_1$ | Finite Difference Method pF/m | Inclined Plate Capacitance Method pF/m | Experimental Value pF/m |
|---|---|---|---|---|
| $\alpha_3=30^0$ | $5^0$ | 204.13 | 202.61 | -- |
| | $10^0$ | 203.67 | 202.07 | -- |
| | $15^0$ | 202.46 | 201.50 | 204.04 |
| | $20^0$ | 201.97 | 200.88 | 203.21 |
| | $25^0$ | 201.06 | 200.17 | 202.37 |
| | $30^0$ | 200.23 | 199.36 | 201.53 |
| | $35^0$ | 198.99 | 198.38 | 199.86 |
| | $40^0$ | 197.81 | 197.11 | 198.19 |
| | $45^0$ | 195.87 | 195.19 | 196.52 |
| $\alpha_3=35^0$ | $5^0$ | 215.14 | 212.84 | -- |
| | $10^0$ | 214.66 | 212.30 | -- |
| | $15^0$ | 213.51 | 211.73 | 214.10 |
| | $20^0$ | 212.63 | 211.01 | 213.26 |
| | $25^0$ | 211.52 | 210.40 | 212.42 |
| | $30^0$ | 210.37 | 209.59 | 211.59 |
| | $35^0$ | 209.02 | 208.61 | 209.91 |
| | $40^0$ | 207.83 | 207.34 | 208.23 |
| | $45^0$ | 206.37 | 205.42 | 206.55 |

Table 6.14: Comparison between capacitance values obtained from FDM, IPC and

experiments when tube was partially filled with three dielectrics and plates were put

outside at $\alpha_3=30^0$ and $35^0$

| Water Angle $\alpha_3$ | Gas Angle $\alpha_1$ | Finite Difference Method pF/m | Inclined Plate Capacitance Method pF/m | Experimental Value pF/m |
|---|---|---|---|---|
| $\alpha_3=40^0$ | $5^0$ | 225.27 | 223.00 | -- |
| | $10^0$ | 224.54 | 222.46 | -- |
| | $15^0$ | 223.75 | 221.89 | 223.34 |
| | $20^0$ | 222.65 | 221.02 | 222.50 |
| | $25^0$ | 221.47 | 220.56 | 221.66 |
| | $30^0$ | 220.61 | 219.75 | 220.82 |
| | $35^0$ | 219.23 | 218.77 | 219.14 |
| | $40^0$ | 218.15 | 217.50 | 217.46 |
| | $45^0$ | 216.66 | 215.58 | 215.78 |
| $\alpha_3=45^0$ | $5^0$ | 237.67 | 235.38 | -- |
| | $10^0$ | 236.97 | 234.84 | -- |
| | $15^0$ | 235.69 | 234.17 | 235.14 |
| | $20^0$ | 234.31 | 233.64 | 234.29 |
| | $25^0$ | 233.15 | 232.94 | 233.45 |
| | $30^0$ | 232.74 | 232.10 | 232.61 |
| | $35^0$ | 231.85 | 231.15 | 230.92 |
| | $40^0$ | 230.65 | 229.88 | 229.24 |
| | $45^0$ | 229.12 | 227.96 | 227.55 |

Table 6.15: Comparison between capacitance values obtained from FDM, IPC and experiments when tube was partially filled with three dielectrics and plates were put outside at $\alpha_3=40^0$ and $45^0$

Figure 6.22: Comparison between capacitance values obtained from FDM and IPC when tube was partially filled with three dielectric and plates were put outside at $\alpha_3 = 5^0$

Figure 6.23: Comparison between capacitance values obtained from FDM and IPC when

tube was partially filled with three dielectric and plates were put outside at $\alpha_3 = 10^0$
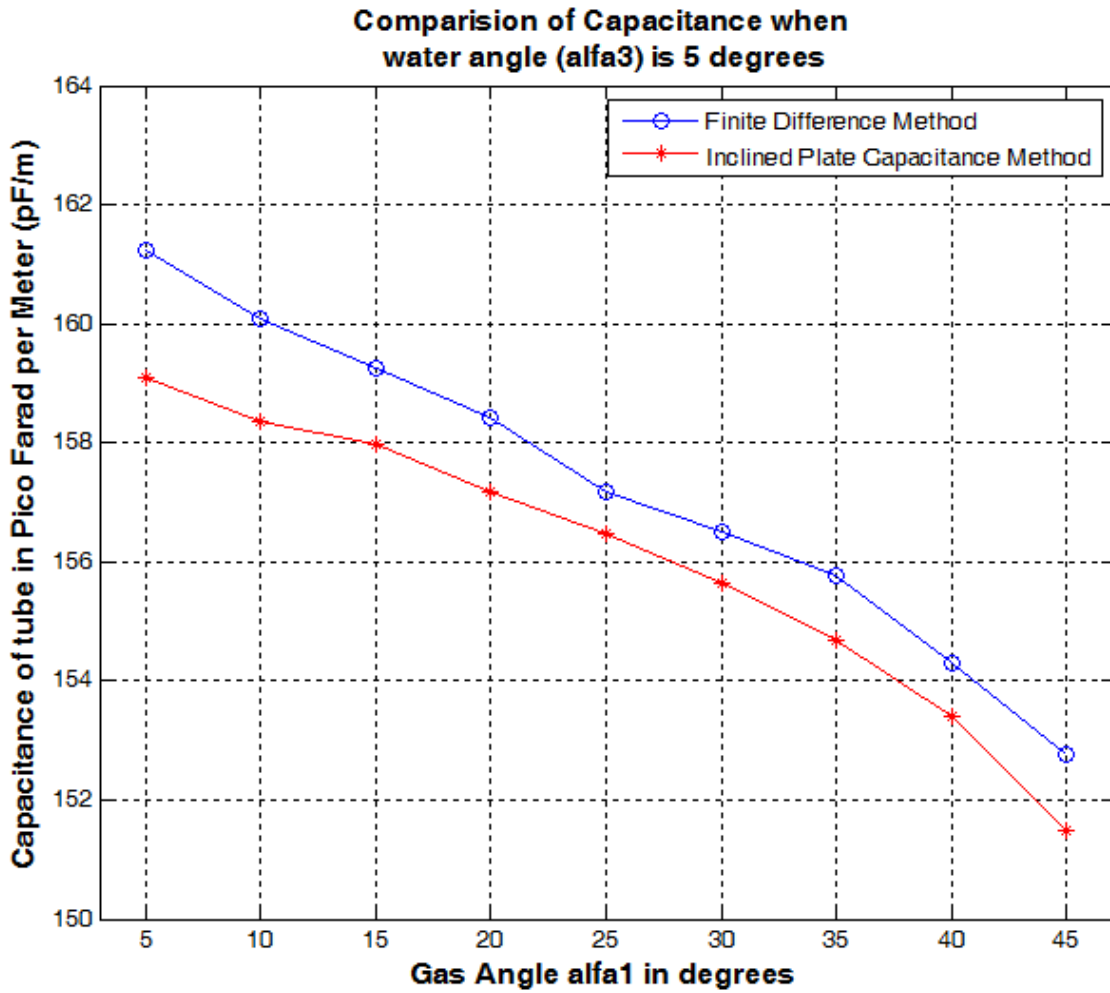
Figure 6.24: Comparison between capacitance values obtained from FDM and IPC when

tube was partially filled with three dielectric and plates were put outside at $\alpha_3=15^0$

Figure 6.25: Comparison between capacitance values obtained from FDM, IPC and experiments when tube was partially filled with three dielectric and plates were put outside at $\alpha_3 = 20^0$

Figure 6.26: Comparison between capacitance values obtained from FDM, IPC and experiments when tube was partially filled with three dielectric and plates were put outside at $\alpha_3 = 25^0$

Figure 6.27: Comparison between capacitance values obtained from FDM, IPC and experiments when tube was partially filled with three dielectric and plates were put outside at $\alpha_3 = 30^0$
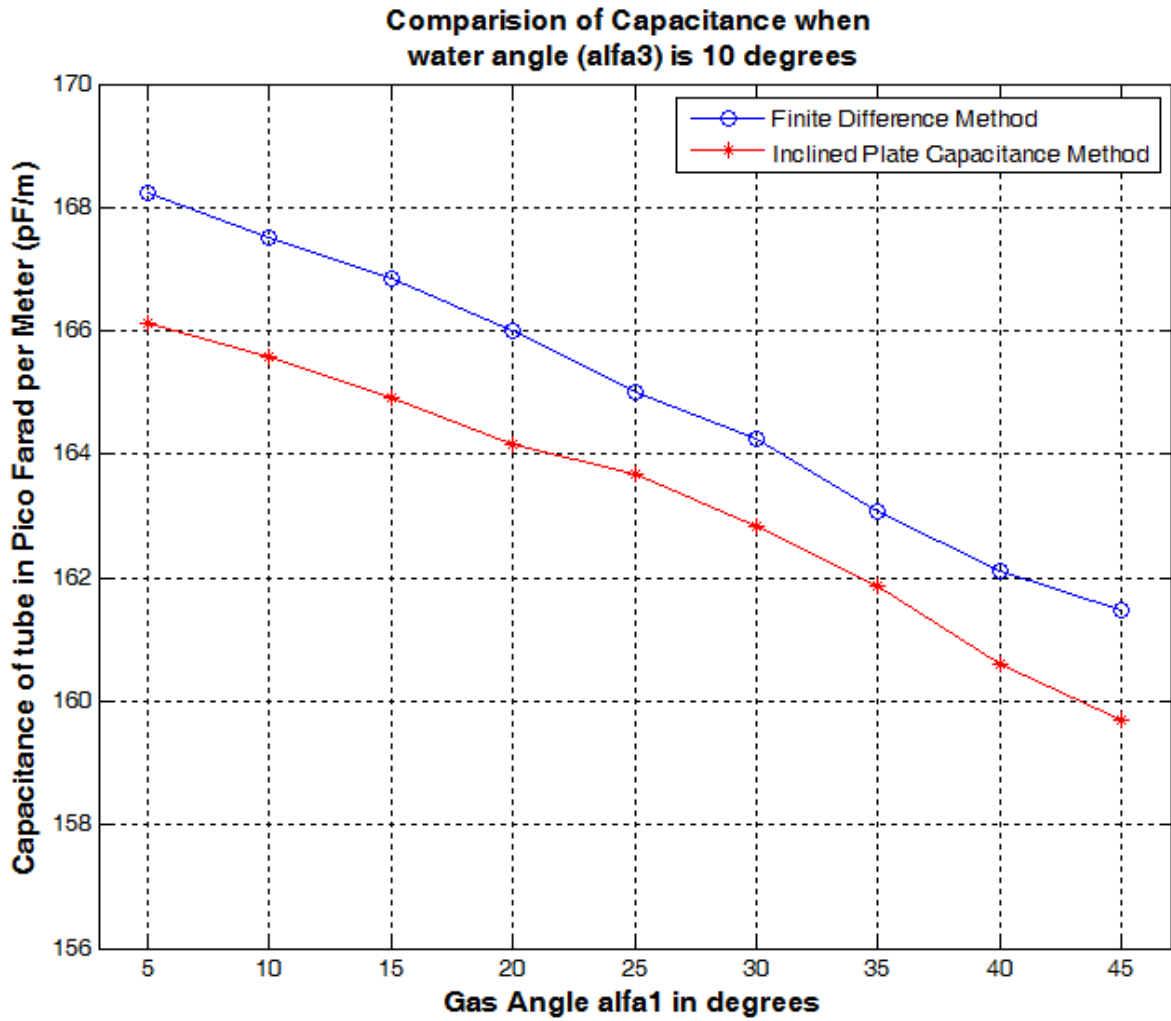
Figure 6.28: Comparison between capacitance values obtained from FDM, IPC and experiments when tube was partially filled with three dielectric and plates were put outside at $\alpha_3 = 35^0$
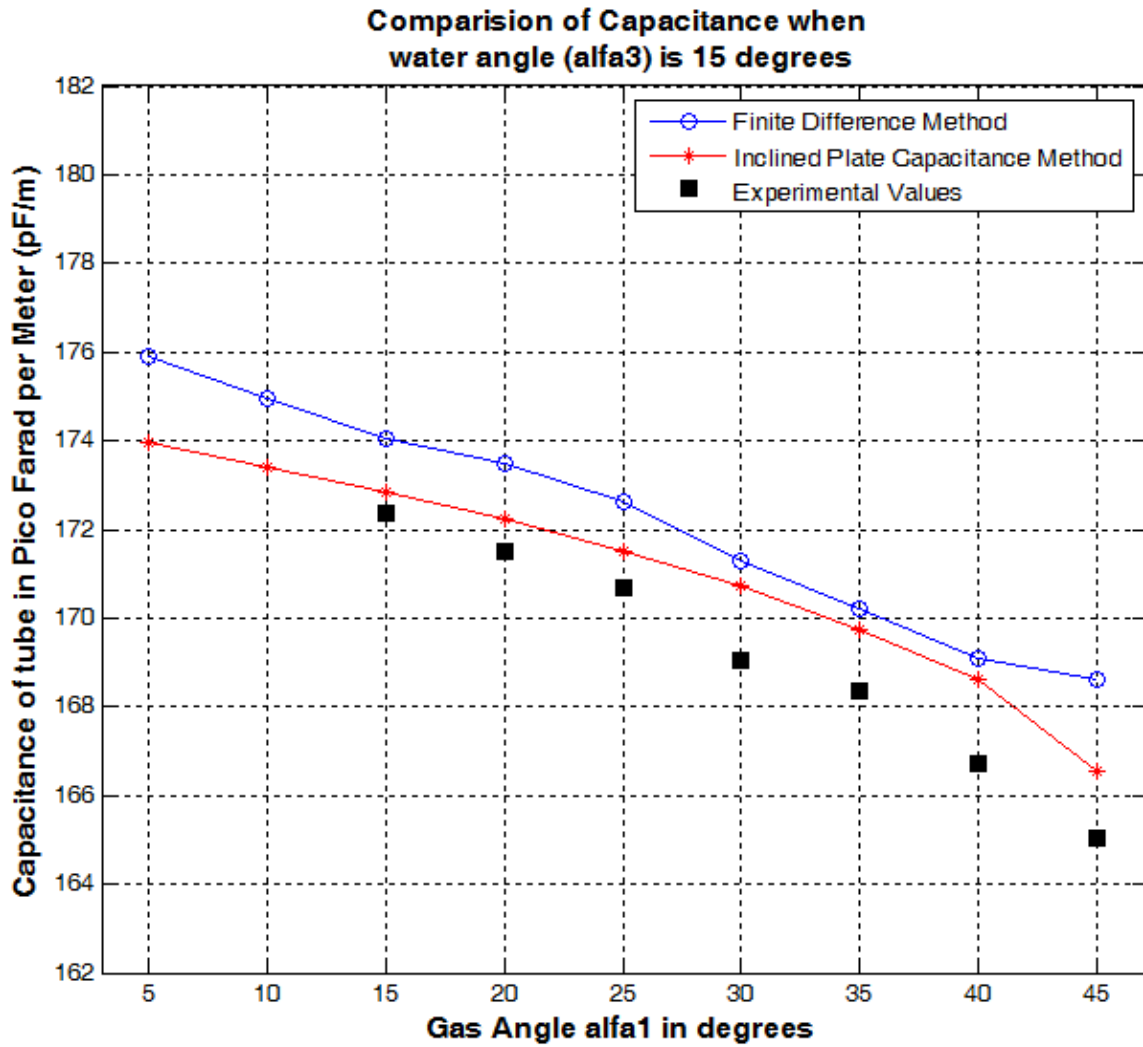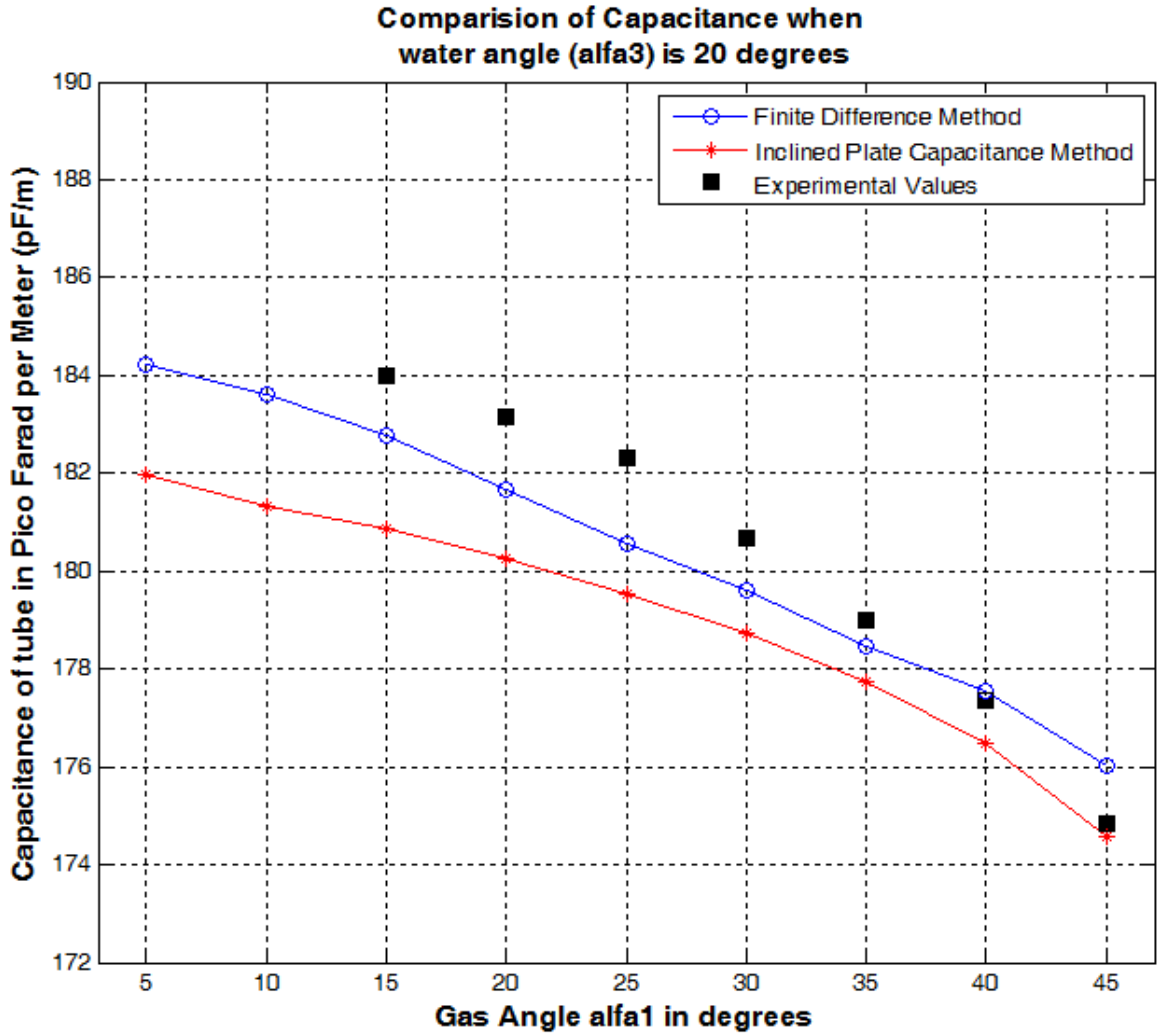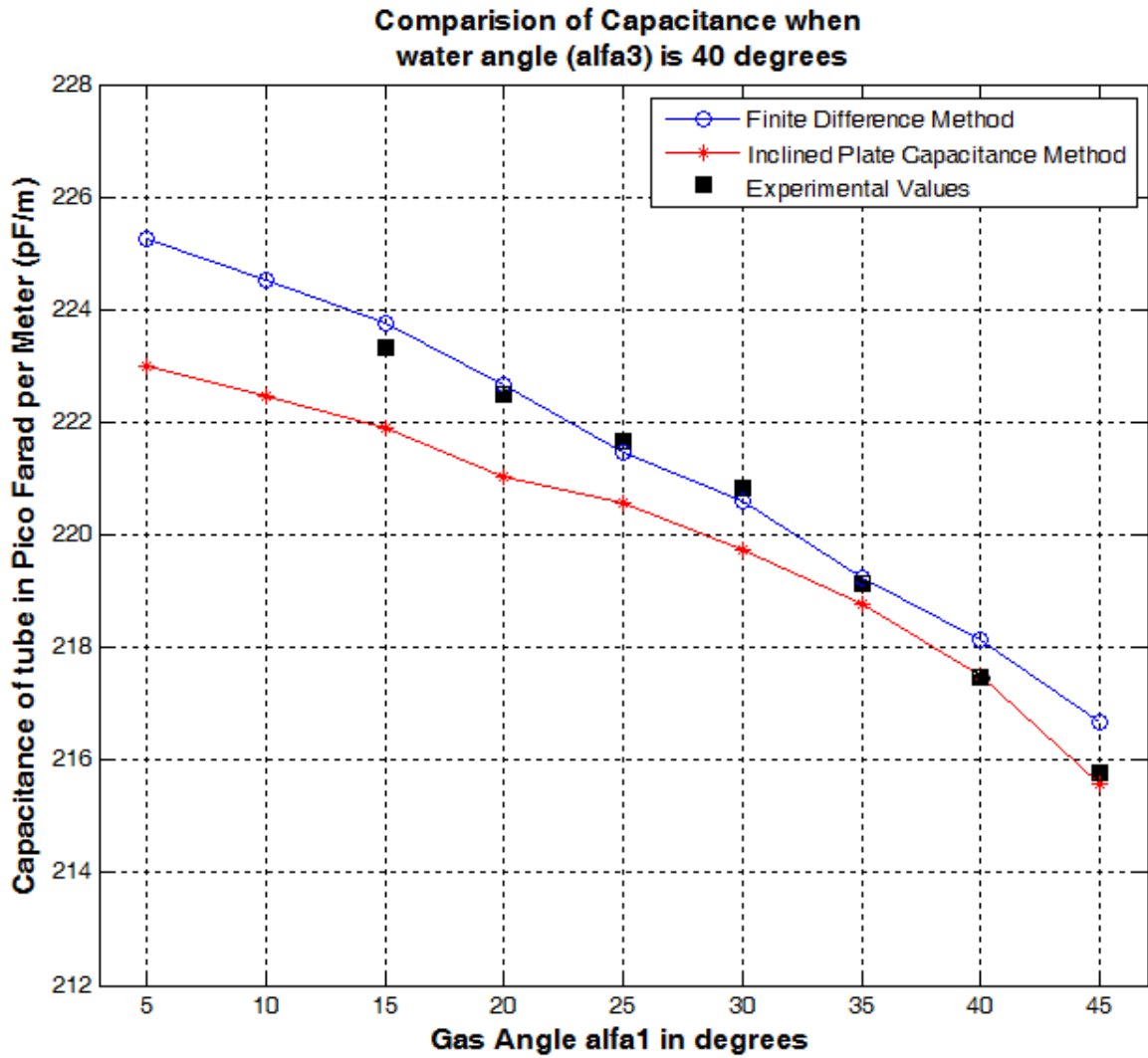
Figure 6.29: Comparison between capacitance values obtained from FDM, IPC and experiments when tube was partially filled with three dielectric and plates were put outside at $\alpha_3=40^0$
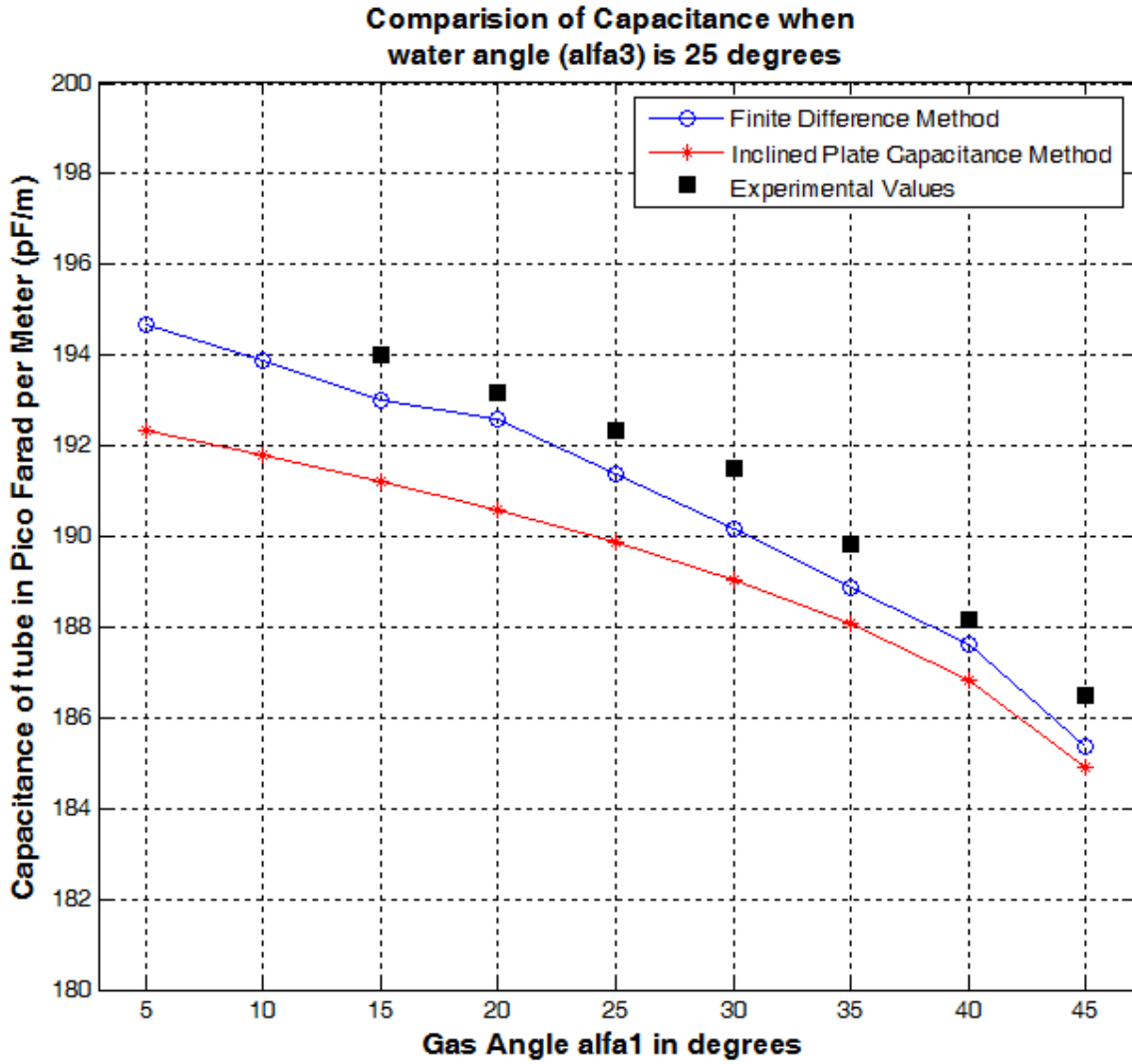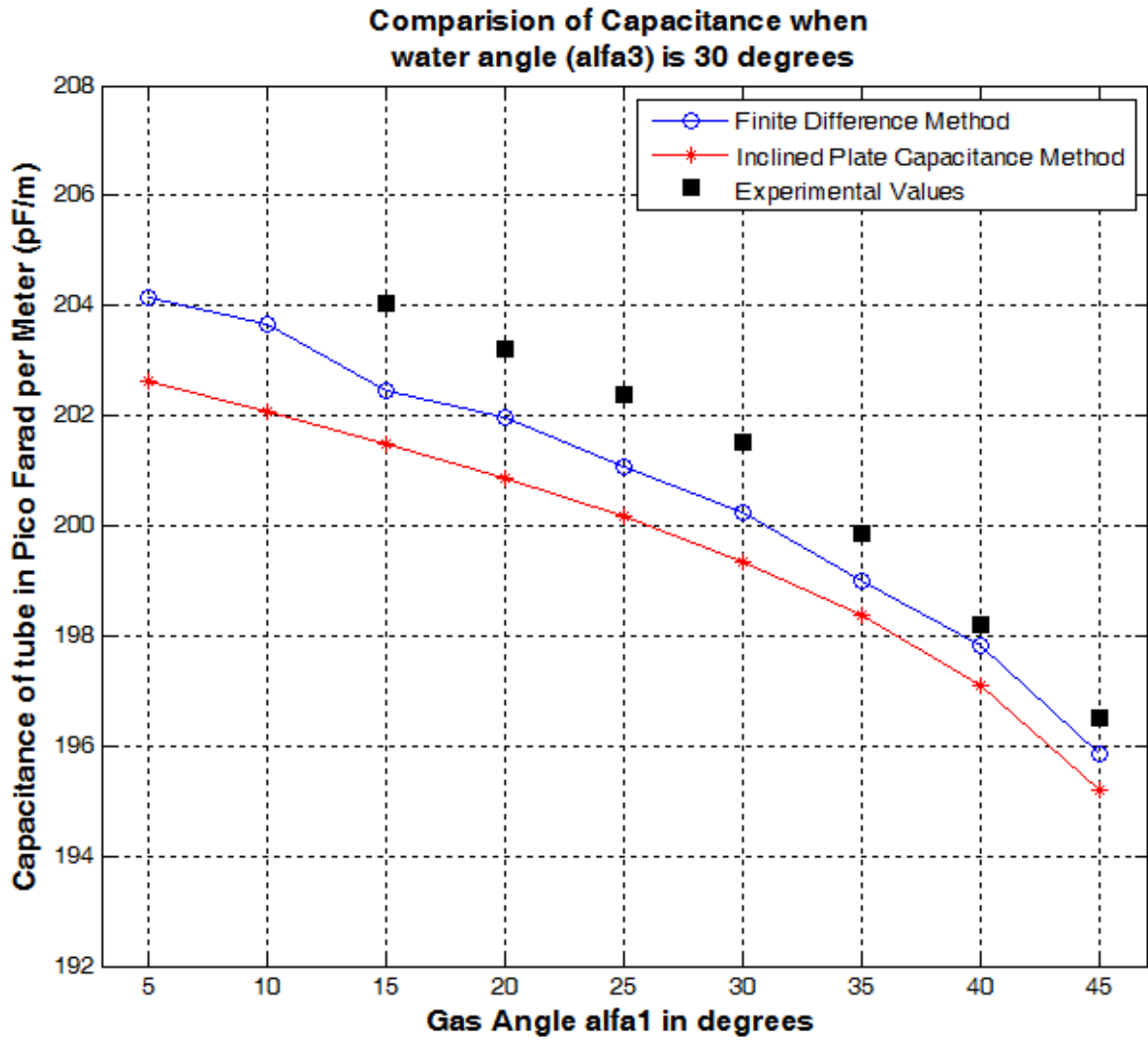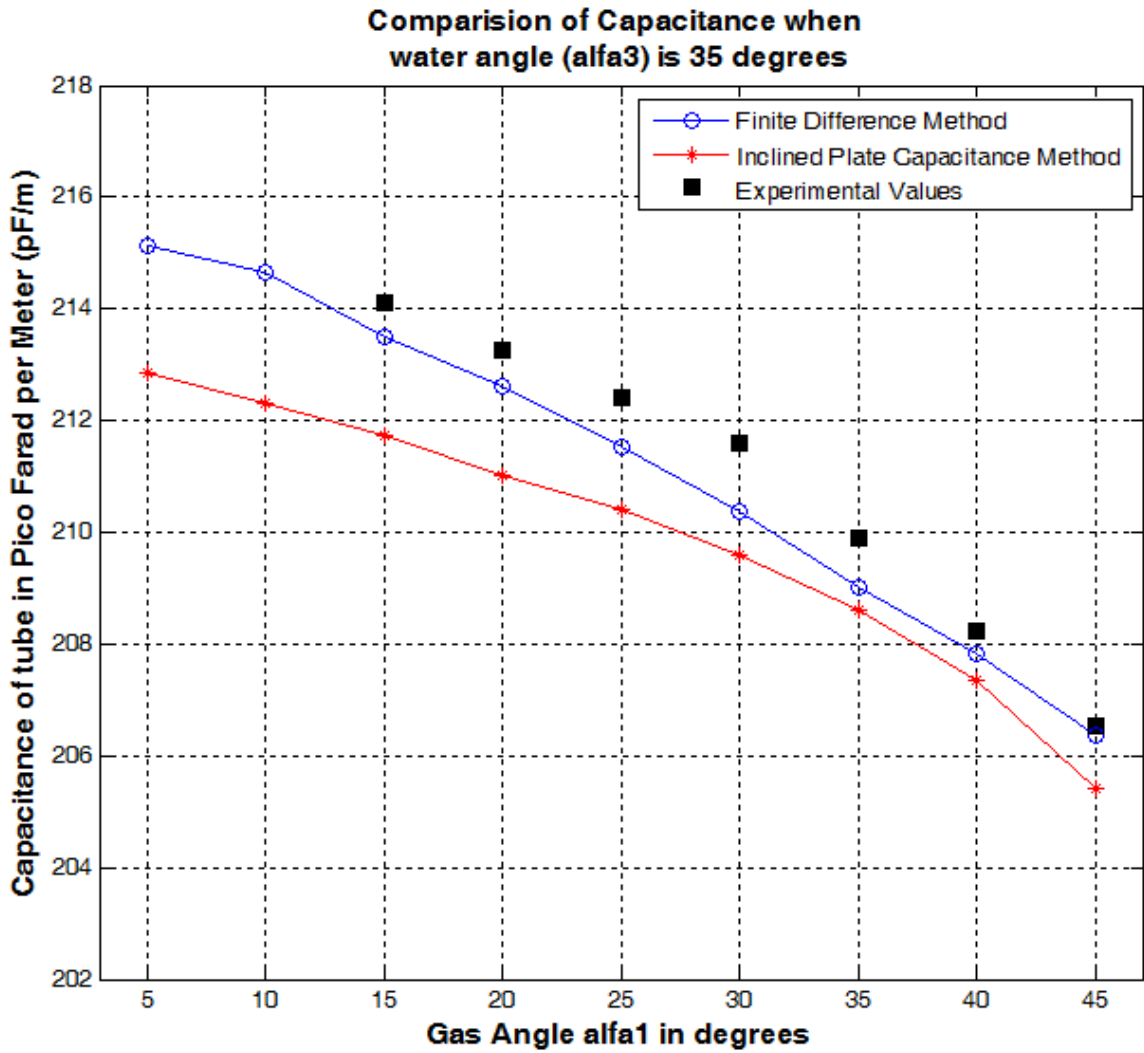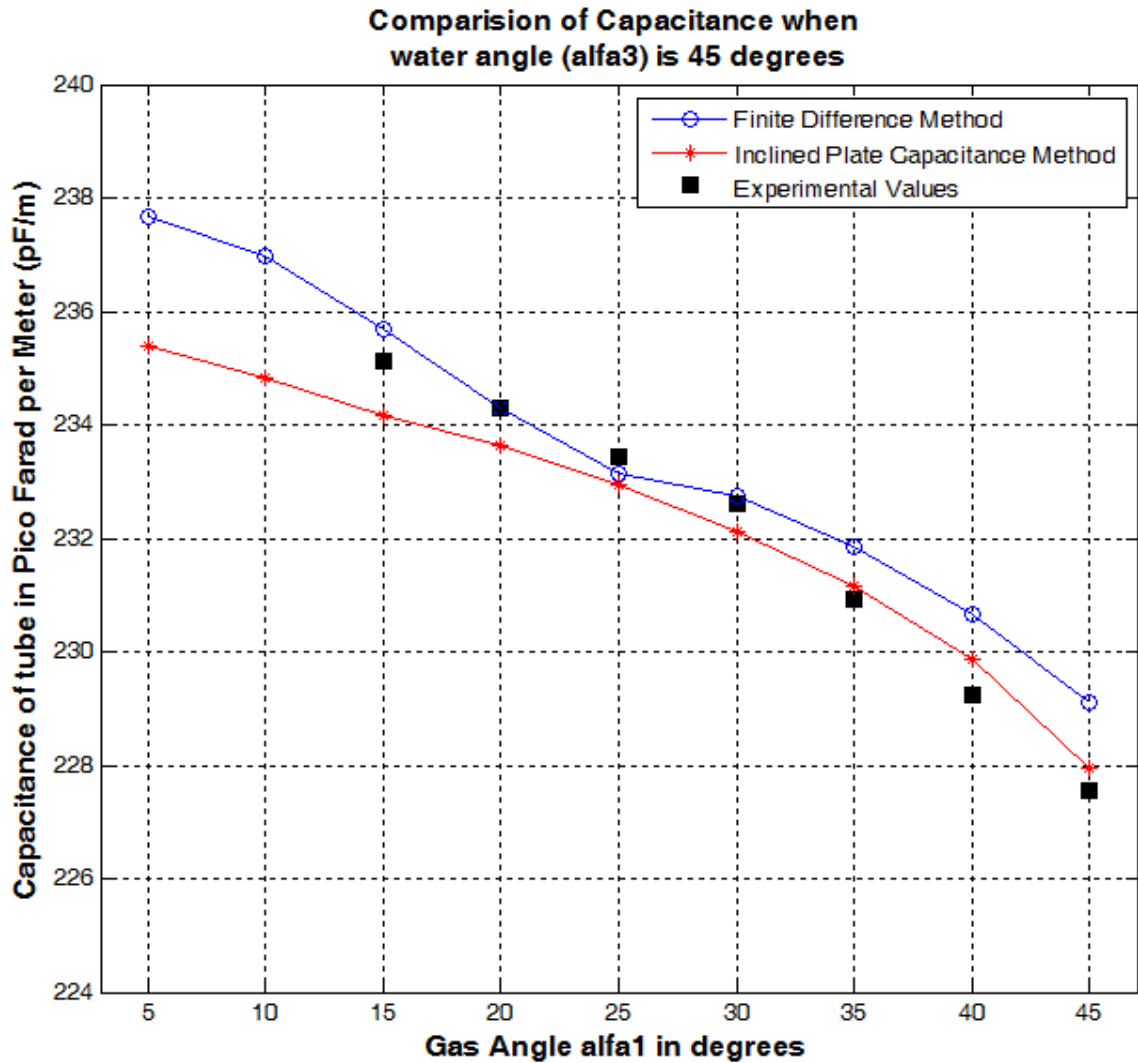
Figure 6.30: Comparison between capacitance values obtained from FDM, IPC and experiments when tube was partially filled with three dielectric and plates were put outside at $\alpha_3=45^0$

It is clear from the tables and graphs that for each pair of $\alpha_1$ and $\alpha_3$ a unique value of capacitance exists. So by measuring the capacitance of tube one can easily tell that what the heights of individual substances in the tube. For example if the capacitance is measured and it came out to be 198 pF/m, then from table and graph we can tell that in this case the angles $\alpha_1$ and $\alpha_3$ are $40^0$ and $30^0$ respectively. Which means that in this case the tube is carrying 90.5 % oil, 2.95 % saline water and 6.55 % gas.

We are glad to say that all the experimental results are very close to theoretical and numerical results. And on the basis of above listed experiments one can easily estimate the height of individual substance by externally measuring the capacitance of an oil carrying pipeline under the steady flow conditions at a high degree of accuracy.

# CHAPTER 7

# CONCLUSION

## 7.1    Main Contribution

After all this work we are able to say that during this research a novel metering system for the three phase flow in horizontal oil pipes under steady flow is designed. The proposed system is non-intrusive and less expensive as compared to other techniques available in open literature. The proposed solution has used for the first time the static electric field of a longitudinally partially filled circular waveguide to relate the value of capacitance to liquid heights. A proper theory is formulated for this problem and results are generated theoretically and numerically. A new method for finding the capacitance of a partially filled circular waveguide is also explained. The new method for finding the capacitance called "Inclined Plate Capacitance (IPC) Method" is producing accurate results as other numerical techniques. The main advantage of this new proposed method for capacitance calculation is the time taken by computer to calculate different values of capacitance for different heights of dielectrics. If we compare the time taken by Finite Difference Method (FDM) with inclined plate capacitance method, then IPC is far better than FDM in terms of time taken. IPC takes 4-6 seconds to generate the values of capacitance for 81 different combinations of $\alpha_1$ and $\alpha_3$. Whereas FDM takes around 7 minutes to generate one value of capacitance. So we conclude that IPC method is more efficient than FDM in terms of time. It is also shown in results and discussion section that values of capacitance generated by IPC are comparable to FDM and experimental values.

116

In short we conclude that the problem of finding the percentage of oil in three phase flow is solved by relating the capacitance of partially filled circular waveguide to the height of individual substance. Capacitance is found theoretically, numerically and experimentally and it is found that the experimental, numerical and theoretical results are within 2% of each other, which indicate the higher order of accuracy of proposed technique.

## 7.2   Limitations

Although the proposed technique is working fine but there are some limitations also. First limitation is that currently the solution is limited to steady flow only. All these calculations and experiments are carried out by considering electrostatic fields and good results are obtained. Second limitation is that when the amount of water or gas is too small (less than 0.2% of total volume), then we are unable to detect this small amount of water or gas.

## 7.3   Future Work

As far as the future work is concerned, the technique can be enhanced for turbulent flows as well. For turbulent flow, the electrical filed will become sinusoidal instead of static. In that case the problem will become very complex to apply finite difference method. But it still can be solved by using inclined plate capacitance method that is also producing very accurate results. In order to guard against the turbulent flow, the values of capacitance can be measured over a period of time and then average value of capacitance can be used to plot the equi-capacitance contours. Currently no information is given about flow rate, so in order to complete the analysis, the velocity of flow must be determined. This can be done by using the simple technique. Two capacitances $C_1$ and $C_2$ can be measured at two different locations separated by distance $Z$, over a same period of time $T$. These two

capacitances will be function of time $t$. Then the time $\tau_m$ the fluid takes to cover the distance $Z$ can be obtained from $\tau$ that maximizes the cross correlation integral given by:

$$R(\tau) = \int_0^T C_1(t - \tau)C_2(t)dt$$

Then the velocity of flow can be easily calculated by using the equation:

$$v = \frac{Z}{\tau_m}$$

Above equation will give the amount of flow per second, flow rate can be given by the oil cross section area multiplied by flow velocity ($v$), which will enhance the accuracy of the analysis.

# References

[1]    X.Chen and L.Chen, "Crude Oil/Natural gas/Water Three Phase Flow meter," SPE, 63rd annual technical conference and exhibition of the society of petroleum Engineers, Houston, Texas, Oct 2-5,1988.

[2]    R. Oliemans, "Oil-Water Liquid Flow Rate Determined from Measured Pressure Drop and Water Held-up in Horizontal Pipes," Journal of the Brazilian Society of Mech. Sci. and Eng., Special Issue 2011, Vol. XXXIII, pp.259-264.

[3]    P. Spedding, G. Donnelly and E. Benard, "Three Phase Oil-Water and Gas horizontal co-current flow Part II. Hold up measurement and prediction," Asia Pacific Journal of Chemical Engineering, 2007-2, pp. 130-136.

[4]    G. Xue and Y.Shen, "Study on measurement of oil gas water three phase flow with conductance correlative flow meter," Proceedings of IEEE, International Conference on Automation and Logistics, Qingado, China, Sept.2008, pp.1295-1297.

[5]    M.R.Taherian, T. M. Habashy, "Microwave Device and Method for Measuring Multiphase Flow," US Patent No.5, 485,743, Date: Jan 23 1996.

[6]    O. Isaksen, "Three Phase Pipe Flow Imaging Using a Capacitance Tomography System," IEEE Colloquim on Advances in Sensors for Fluid Flow Measurements, 1996, pp 11/1-11/6.

[7]    A.C. Sheila et al, "Multi Phase Flow Metering with Patch Antenna," US Patent No. 20110196625, Date: 11-08-2011.

[8]   T. J. Hanratty, T. Theofanous, J. M. Delhaye, J. Eaton and J. Mclaughlin, "Workshop on Scientific Issues in Multiphse Flow", Held at ILLINOIS, May 7-9, 2002, pp.2-8.

[9]   Ove Bratland, "Pipe Flow 2: Multi-phase Flow Assurance," 2009, pp.5-10.

[10]  M. N. O. Sadiku, "Elements of Electromagnetics," Oxford University Press Inc, August 2000, pp.669-682.

[11]  J.M. Bueno, S. César, S. Catalan-Izquierdo1, F. C.Sesé, "Capacitance Evaluation on Perpendicular Plate Capacitors By Means Of Finite Element Analysis," International Conference on Renewable Energies and Power Quality (ICREPQ'09), Valencia (Spain), April 15-17, 2009.

[12]  Y. Xiang, "The electrostatic capacitance of an inclined plate capacitor", Journal of Electrostatics 64 (1) (2006), pp.29-34.

[13]  B. R. Patla, "Small Angle Approximation for non-parallel plate capacitors with Applications in Experimental Gravitation," arXiv: 1208.2984v3 [gr-qc] 16 May 2013.

[14]  S. L. Ceccio and D. L. George "A review of electrical impedance techniques for the measurement of multiphase flows, "Journal Fluids Engineering, vol. 118. pp. 391-399, 1996.

[15]  E. A. Hammer, G. A. Johansen, T. Dyakowski, E. P. L. Roberts, J. C. Cullivans, R. A. Willians, Y. A. Hassan, and C. S. Claiborn, "Advanced experimental techniques." 2006.

[16]  C. Kak and M. Slaney, Principles of Computerized Tomographic Imaging, New York: IEEE Press., 1988.

[17]  T. Dyakowski, "Process tomography applied to multi-phase flow measurement," Measurement Science and Technology, vol. 7, p. 343-353, 1996.

[18]  J. Chaouki, F. Larachi and M. P. Dudukovic, "Non-invasive tomographic and velocimetric monitoring of multiphase flows," Industrial and Engineering Chemistry Research, vol. 36, pp. 4476-4503, 1997.

[19]  R. A. Williams and X. Jia, "Tomographic imaging of particulate systems," Advanced Powder Technology, vol. 14, pp. 1-16, 2003.

[20]  H. M. Prasser, "Novel experimental measuring techniques required to provide data for CFD validation," Nuclear Engineering and Design, vol. 238, pp. 744-770, 2008.

[21]  R. A, Williams and M. S. Beck (eds.), Process Tomography: Principles, Techniques and Applications, Oxford, UK: Butterworth-Heinemann, 1995.

[22]  H. McCann, D. M. Scott (eds.), Process Imaging For Automatic Control, Boca Raton, FL: CRC Press, 2005.

[23]  D. M. Scott and R. A. Williams (Eds), Frontiers in Industrial Process Tomography, New York: AIChE & Engineering Foundation, 1995.

[24]  Kwun Ho Ngan, Karolina Ioannou, Lee D. Rhyne, Panagiota Angeli, "Effect of glycerol addition on phase inversion in horizontal dispersed oil—water pipe flows," Experimental Thermal and Fluid Science, 2011.

[25]  E Bonder de la Bernardie, O Dubrunfaut, J C Badot, A Fourrier-Lamer, E Villard, P Y David, B Jannier, N Grosjean and M Lance, "Low (10-800 MHz) and high (40 GHz) frequency probes applied to petroleum multiphase flow characterization." Meas. Sci. Technology, vol. 19, 2008.

[26] M J Da Silva. E Schleicher and U Hampel, "Capacitance wire-mesh sensor for fast measurement of phase fraction distributions." Meas. Sci. Technol., vol. 18, p. 2245-2251. 2007.

[27] S R Wylie. A Shaw and A I Al-Shamma'a, "RF sensor for multiphase flow measurement through an oil pipeline." Meas. Sci. Technol,. pp. 2141-2149, 2006.

[28] Sheikh S. I, Alqurashi K, Ragheb H and Babelli I, "Simple Microwave Method For Detecting Water Holdup," Microwave and Optical Technology Letters (MOTL). vol. 50. No. 2, February 2008.

[29] Andreas Penirschke. Aleksandar Angelovski and Rolf Jakoby, "Moisture Insensitive Microwave Mass Flow Detector for Particulate Solids," in Instrumentation and measurement technology Conference (12MTC), IEEE, Austin, TX., 2010.

[30] Andreas Penirschke and Rolf Jakoby, "Microwave Mass Flow Detector for Particulate Solids Based on Spatial Filtering Velocimetry," IEEE transactions on microwave theory and techniques vol. 56, no. 12, pp. 3193-3199, December 2005.

[31] Andreas Penirschke. Aleksandar Ancelovski and Rolfiakoby, "Helix-shaped CRLH-mass flow detector for the cross-sectional detection of inhomogeneous distributed pneumatic conveyed pulverized solids." in Instrumentation and measurement Technology Conference (12MTC) Graz, Austria. 10-12 May 2011.

[32] Aleksandar Anijelovski, Andreas Penirschke and Rolf Jakoby, "Helix-shaped CRLH-TL sensor for inhomogeneties detection for pneumatic conveyed

pulverized solids," in proceedings of 6th German Microwave Conference, Darmstadt, Germany, 14-16 March 2011.

[33] H. Yeung, "Multiphase flow measurement - the holy grail." in Sensor Conference 2007 Proceedings I, Nurnberg, Germany, May 2007.

[34] L. N. Dworsky, "Introduction to Numerical Electrostatics Using MATLAB," First Edition, John Wiley & Sons, Inc.2014, pp.183-198.

# Vitae

| | |
|---|---|
| Name | Muhammad Sajid Iqbal |
| Nationality | Pakistani |
| Date of Birth | 03 November 1988 |
| Email | sajid_iqbal18@hotmail.com |
| Address | Chak # 54/2L near Govt. Boys High School Okara, Pakistan |
| Academic Background | Master of Sciences in Electrical Engineering, King Fahd University of Petroleum and Mineral, Dhahran, Saudi Arabia, May 2015. |
| | Bachelor of Science in Telecommunication Engineering, National University of Computer and Emerging Sciences, Karachi, Pakistan. |
| Work Experience | Lab Engineer, Electrical Engineering Department, National University of Computer and Emerging Sciences, Karachi, Pakistan. |
| Research Interests | Electromagnetic waves propagation and scattering |
| | Microwave antenna designs |
| | Fiber Optic Communication |
| | Optical Fiber Sensors |